STUDY OF SEISMICITY AND ITS IMPLICATIONS ON SNOW AVALANCHE OCCURRENCES IN NUBRA-SHYOK REGION, NW HIMALAYA, INDIA

By

RAJINDER PARSHAD
(SAP ID - 500024923)

SCHOOL OF ENGINEERING

DEPARTMENT OF PETROLEUM ENGINEERING AND EARTH SCIENCES

Submitted

IN PARTIAL FULLFILMENT OF THE REQUIREMENT OF THE DEGREE OF

DOCTORATE OF PHILOSOPHY

TO

UNIVERSITY OF PETROLEUM AND ENERGY STUDIES
DEHRADUN, INDIA

AUGUST, 2018

Under the Guidance of

Dr. Pankaj Kumar Srivastava
Associate Professor
Department of Petroleum Engineering and Earth Sciences
University of Petroleum and Energy Studies, Dehradun, India

Dr. Snehmani
Scientist 'F', and Joint Director
Snow and Avalanche Study Establishment
Defence Research & Development Organization, Chandigarh, India

DEDICATED TO
MY FAMILY,
MY FRIENDS
AND
THE ALMIGHTY

ACKNOWLEDGMENTS

I would like to express my gratitude to Dr. Snehmani, Sc. 'F' & Joint Director, Snow and Avalanche Study Establishment, DRDO, Chandigarh for his supervision, advice, and guidance from the very early stage of this research as well as giving me extraordinary experiences throughout the work. Above all and the most needed, he provided me unflinching encouragement and support in various ways.

I express my sincere gratitude to Dr. Pankaj Kumar Srivastva, Associate Professor, University of Petroleum and Energy Studies, Dehradun for his supervision and encouragement throughout the Ph.D. work.

I would like to extend my special thanks to my friend Dr. Parveen Kumar, Scientist 'B' Wadia Institute of Himalayan Geology, Dehradun, his help proves the real source of inspiration and guidance to complete this research work.

I am thankful to the administration and staff of Snow and Avalanche Study Establishment, DRDO, Chandigarh for extending all the help required to carry out field work in inhospitable and remote areas.

I am grateful to the Additional Director General & Head of the Department, Geological Survey of India, Northern Region, Lucknow and the Dy. Director General, Geological Survey of India, Faridabad for permitting me to carry out this research work.

I am thankful to my friends Mr Anil Kumar and Mr Mahavir Mann, Sr. Geophysicist, ONGC, Dehradun, Dr. Anil Kumar Scientist 'C' Wadia Institute of

Himalayan Geology, Dehradun, Dr Somdutt, Scientist 'C' Wadia Institute of Himalayan Geology, Dehradun for their encouragement and making my stay pleasant at Dehradun.

I would like to thank Indian Metrological Department, Delhi for providing the earthquake hypocentral data and Ministry of Earth Scineces, Govt. of India, Delhi for providing the fund vide grant no. MoES/P.O(Seismo)/1(83)/2010, dated 10.08.2010.

I would like to thank my elder brother Mr. Ramniwas Sharma, my sister-in-law, Dr. Anita Sharma, for their love and constant support. I sincerely acknowledge the unconditional love affection, care patience, understanding and constant personal support of my wife Mrs. Usha Rani. I wish to thank my nephew Mr. Shiven and my daughter Ms. Nityashree for their love and patience.

Finally, I wish to thank all those whose names have not figured above but have helped me directly or indirectly during the course of my research work. Really this thesis would not have been written without any of you.

(RAJINDER PARSHAD)

DECLARATION

I hereby declare that this submission is my own work and that, to the best of my knowledge and belief, it contains no material previously published or written by another person nor material which has been accepted for the award of any other degree or diploma of the university or other institute of higher learning, except where due acknowledgment has been made in the text.

(RAJINDER PARSHAD)
SAP ID: 500024923
Ph.D. Research Scholar
Date: 25.07.2018
Department Of Petroleum Engineering
and Earth Sciences
University of Petroleum and Energy Studies
Dehradun-248007, India

UPES

www.upes.ac.in

THESIS COMPLETION CERTIFICATE

This is to certify that the thesis on **"STUDY OF SEISMICITY AND ITS IMPLICATIONS ON SNOW AVALANCHE OCCURRENCES IN NUBRA-SHYOK REGION, NW HIMALAYA, INDIA"** by **Rajinder Parshad (SAP ID: 500024923)** in partial completion of the requirements for the award of the Degree of Doctor of Philosophy (Earth Sciences) is an original work carried out by him under our joint supervision and guidance.

It is certified that the work has not been submitted anywhere else for the award of any other diploma or degree of this or any other University.

Pankaj Kr Srivastava

Dr. Pankaj Kumar Srivastava
Associate Professor
Department of Petroleum Engineering & Earth Sciences
School of Engineering, University of Petroleum & Energy Studies (UPES)
Vill & P.O-Bidholi, Via-Prem Nagar
Dehradun - 248007
Email: pksrivastava@ddn.upes.ac.in
Date: 4-8-18

Tel : 0172-2699804-06
Fax: 0172-2699802/2699970
Mail: snehmani@sase.drdo.in

Govt of India
Ministry of Defence
Snow & Avalanche Study Estt (SASE)
Research & Development Centre (RDC)
Him Parisar, Plot No 1, Sector 37-A
Chandigarh - 160 036 (UT)

THESIS COMPLETION CERTIFICATE

This is to certify that the thesis on "STUDY OF SEISMICITY AND ITS IMPLICATIONS ON SNOW AVALANCHE OCCURRENCES IN NUBRA-SHYOK REGION, NW HIMALAYA, INDIA" by RAJINDER PARSHAD (SAP ID: 500024923) in Partial completion of the requirements for the award of the Degree of Doctor of Philosophy (Earth Sciences) is an original work carried out by him under our joint supervision and guidance.

It is certified that the work has not been submitted anywhere else for the award of any other diploma or degree of this or any other University.

25/7/18

(Dr. Snehmani)
Sc. 'F' & Joint Director
SASE RDC, DRDO
Chandigarh (UT)-India

डॉ स्नेहमणि
वैज्ञानिक 'एफ' एवं निदेशक
सासे आर डी सी
डी आर डी ओ, रक्षा मंत्रालय,
हिम परिसर, सेक्टर 37-ए,
चंडीगढ़-160 036 (यू.टी.)

ABSTRACT

Earthquakes are the most destructive among the natural calamities. The implications of earthquakes are more dangerous in the mountainous region, which are prone to slope failure. About 3.1 % area of the earth land surface is prone to earthquake triggered snow avalanche (Podolskiy et al., 2010a). In the snow bound mountainous region earthquake triggered snow avalanches can be a significant collateral hazard associated with earthquakes. The Nubra-Shyok region, North-West, Himalaya, India is highly mountainous snow bound region with steep slopes and higher seismicity. In this study, the local seismological studies comprising of coda Q estimation, source parameters estimation and local seismicity carried out to know the effect of seismicity on avalanche occurrences and the avalanche potential of the region has been mapped using remote sensing and GIS technique.

Coda wave quality factor (Q_c) has been determined for this virgin region by using the single backscattering method. A total of thirty earthquakes recorded in this region, which fall in the epicentral distance range of 3 to 115km have been used for the present work. A 30 sec window length of coda waves at different central frequencies 1.5, 3.0, 6.0, 9.0, 12.0, 18.0 and 24.0 Hz have been studied to determine Q_c at four recording stations. The frequency dependent coda wave quality factor regional relationships using four Broad Band Seismograph data, have been computed of the form $Q_c(f) = (121\pm7.2)f^{(1.0\pm0.04)}$. The present regional relation developed for Nubra-Shyok region indicates heterogeneous and tectonically active region.

The source parameters of local earthquakes have been estimated from the waveform data of 17 local earthquake events, following Brune (1971) circular earthquake source model. The seismic moment is found between 2.1 x 10^{20} dyne-cm to 3.34 x 10^{23} dyne-cm and their moment magnitude ranges between 2.7 to 5.0. The source dimension in terms of the radius of circular fault varies from 532.3 m to 1.296 Km. The stress drops of these earthquakes ranges between 0.1 to 61.7 bars and found in agreement with the other regions of Himalaya.

The pattern of local seismicity has been studied using the hypocentral parameters of local earthquakes recorded by four BBS during 2010-2012. It is found that most of the earthquake events are confined in the upper crust. The middle part of the crust (17 - 40 km) is found aseismic in the Nubra-Shyok, region. This aseismic layer (17 - 40 km) is sandwiched between two seismically active layers and depicts a good spatial correlation with the observations of low resistivity reported from earlier magnetotelluric studies.

Expert based AHP model considering avalanche contributory factors (aspect, elevation, slope, curvature and land cover) was used to map the avalanche potential zones in the area. The calculated weight values of the slope factor is 0.47, which is found most significant, while the elevation with weight value 0.25, were also found to be significant factor. The weight value of Land cover was 0.05 and creates a least importance. The curvature and aspect weight values were 0.12 and 0.11 respectively, and produce intermediate degree of importance. The avalanche susceptibility map of the Nubra-Shyok region was divided into five zones: - (i) Very High (ii) Moderate-to-High (iii) Moderate (iv) Low (v) Very

Low, and covers 27.5% , 28.0% 19.0%, 20.0%, and 4.8%, of the total area respectively. Receiver operator characteristics- Area under the Curve technique was applied to verify the study results. The value of Area under the curve (0.911) shows that results of the present study are acceptable and 91.1% avalanche pixels are properly categorized.

The affect of earthquake occurred in the area around 600 km radius from study area on snow avalanches in the study area for a decade (i.e. year 2002-2012), reveal that out of 1448 natural avalanche, 347 avalanches was triggered in relation to the earthquake events during this period. The geo-spatial analysis of avalanche susceptibity map of the area and locations of reported avalanche sites shows that only 1.66% of reported snow avalanches falls in very low susceptibility zone, while very high susceptible zone accounts for 32.78 % . The avalanches triggered due to natural seismicity during the period of 2002-2012 related with earthquakes of magnitude $1.7 \leq M_w \leq 6.0$ and distance of induced snow avalanche from epicenter of earthquakes lies in the range of 4-594 km. Relation between earthquake magnitude and distance of induced snow avalanche from epicenter reveal that an earthquake of magnitude 1.4 (M_w) can trigger a snow avalanche as distance approaches to zero from earthquake epicenter.

Keywords: Coda Q, Moment Magnitude, Seismogenic Avalanches, Karakoram Fault, Nubra, Shyok, Moment Magnitude, Source Parameters, Avalanche Susceptibilty.

TABLE OF CONTENTS

LIST OF FIGURES

LIST OF TABLES

ABBREVIATIONS AND SYMBOLS

AHP	Analytical Hierarchy Process
AUC	Area Under Curve
ASTER	Advanced Spaceborne Thermal Emission and Reflection Radiometer
ASI	Avalanche Susceptibility Index
BBS	Broad Band Seismograph
BIS	Bureau of Indian Standard
CI	Consistency Index
CR	Consistency Ratio
DEM	Digital Elevation Model
GDEM	Global Digital Elevation Model
KDG	Khardungla
IMD	Indian Metrological Department, Delhi
TKS	Taksha
ITSZ	Indus Tsangpo Suture Zone
KF	Karakoram Fault
FFT	Fast Fourier Transform
SE	South-East
MCT	Main Central Thrust
MBT	Main Boundary Thrust
GIS	Geographical Information System
SAC	Space Application Center
SASE	Snow and Avalanche Study Establishment
ROC	Receiver Operator Characteristics
NRSC	National Remote Sensing Centre, Hyderabad

USGS	United State Geological Survey
KSZ	Karakoram Shear Zone
SSZ	Shyok Suture Zone
KBC	Karakoram Batholith Complex
HNL	Hanley
Q_c	Coda Q
P	Primary Seismic Wave
S	Secondary Seismic Wave
f_c	Corner Frequency
r	Source Radius
M_0	Seismic Moment
V	Velocity
ρ	Average Density
$R_{\theta\Phi}$	Average Radiation Pattern
M_w	Moment Magnitude
$\Delta\sigma$	Stress Drop
m.w.e.a $^{-1}$	Melt Water Equivalent per Annum
R_i	Ratings of each class of factor
X	Distance of induced avalanche site from epicenter
W_i	Weight value of each factor
Y_{max}	Principal Eigen Value

CHAPTER 1

INTRODUCTION

1.1 Introduction

Earthquake is one of the most destructive forces among the natural calamities in terms of casualties and destruction to property. The earthquake has catastrophic effects in hilly region and ruinous effects on areas prone to slope failure. The secondary effects of earthquake such as Mass movements and Tsunamis are responsible for 21.5% of total fatalities by the earthquake (Marano et al., 2010). Around 6.2% area of the earth land surface is prone to snow avalanches (Glazoversuskaya et al., 1992), and nearly half area is prone to earthquake triggered snow avalanche (Podolskiy et al., 2010a). Earthquake triggered snow avalanches can be a significant collateral hazard associated with earthquakes. This is generally happening in the region having steep snow covered mountains and higher seismicity. The systematic study of geographical distribution of earthquakes (seismicity), earthquake process/ causes and the secondary effects of earthquakes may help in planning to reduce the loss of property and life.

The snow avalanche is a moving snow mass down the slope which can be so small to be harmless to man and material or large enough to wipe out entire forest and villages (Maggioni , 2004). The snow avalanche can entraps the rock, ice, trees, etc. coming in its way. Snow avalanches are a significant natural hazard that impact structures, roads, and threaten human lives in mountainous area. Snow avalanches occur due to the interaction of the

snowpack with terrain and weather. The general avalanche occurrence conditions are as follows: the terrain must have the characteristics necessary for the avalanche to start, the weather conditions must be proper to create snowpack instability, and a triggering factor to initiate the avalanche.

The snow avalanches are natural geophysical phenomena in the snow bound alpine regions and accurate prediction of snow avalanches is very complex process in space and time. Which includes dynamic meteorological factors *viz.* temperature, snowfall, wind speed, precipitation and its intensity and static terrain factors such as slope, elevation, aspect, curvature and land cover (McClung and Scheweizer, 1993). The temporal and spatial variation of snow pack instability cannot be known accurately (McClung and Schweizer, 1999). The effect of external triggering factors such as earthquake is not known precisely on avalanche occurrences in snow bound regions as the regular monitoring and recording of natural seismic events is very complex in the snow bound regions. An avalanche susceptibility map proves very useful tool for the evaluation of danger and planning for safe travel activities in snow covered regions. Geographical Information System (GIS) has proved its usage in the assessment of natural hazards in snow covered regions. The major advantage of GIS in natural hazard evaluation is its capability of integration of large heterogeneous datasets, their management and analysis.

Strong ground motion produced by the earthquakes can cause a number of disastrous geological processes including (Hewitt et al., 2008) slope failure phenomena such as Landslide, rock fall, rockslide, debris flow, etc. Huge Life and property loss may occur, when an unstable snowpack is

disturbed by an earthquake, resulting catastrophic avalanches (LaChapelle, 1968). In the past number of earthquake induced snow avalanches were happened all around the globe (Chernous et al, 2004, Podoloskiy et al. 2010a, Fah et al., 2012, Guileen, 2016). The Huascaran snow, ice and rock avalanche in Peru, in 1970, is the most devastating example of an earthquake-induced avalanche. This earthquake triggered avalanche buried the towns of Yungay and Ranrahirc resulting in death of thousands people (Chernous et al., 2002). The avalanche triggered by the Nepal earthquake occurred on 25 April, 2015 with moment magnitude 7.8 (USGS, 2015) buried the Langtang village completely. The 300 peoples present in the village engulfed by this avalanche; only few peoples survive (Dave, 2015). Another avalanche triggered by Nepal earthquake hit the Mount Everest Base camp violently and killed 22 peoples and injured 61 (Ghosh, 2015). Many avalanches are also triggered by aftershock of this earthquake in and around Mount Everest region.

Earthquake source parameters *viz.* seismic moment, stress drop, source radius and moment magnitude are imperative parameters which are needed to quantify the size of an earthquake and to know about the tectonics and seismicity of the region. The seismic moment is a measure of the size of an earthquake and is often used to compare the size of different earthquakes. The stress drop is defined as the average difference between the stresses on a fault before an earthquake to the stress after the earthquake (Keilis- Borok 1959). The rupture plane is assumed to be circular in shape (Brune, 1970), thus source radius is defined as the radius of circular rupture plane. Attenuation characteristics of medium decide the decay of the amplitude of

ground motion at various sites. Seismic energy released from earthquake attenuates while it travels through earth medium. Attenuation relation is one of the simple relations to describe decay rate of ground motion for an earthquake. The seismological parameters used in the attenuation relation characterize the path of seismic wave between the source and the observation point (Campbell, 2001). Attenuation property of earth medium is also quantitatively defined by a dimensionless quantity know as quality factor 'Q' given by Knopoff (1964). The quality factor 'Q' is defined as the fractional loss of energy per cycle (Knopoff, 1964). It is also defined as a ratio of stored energy to dissipated energy during one cycle of the wave (Johnston and Toksoz, 1981). The attenuation characteristics of a region can provide essential information regarding earthquake hazard of that region.

The study area for the present research work is one of the highly glacerized outside the polar regions. The steep slopes of the region give rise to the natural mass movements. Snow avalanche is a significant natural hazard in the present study region. This region is situated in the colliding zone of Indian plate and Eurasian plate, which is still going on and the region is tectonically and seismically active. The continuous passive seismic data observed by local seismic network of this region is available. Avalanches has threatened to the peoples of this region in past by devastating the structure and killing the peoples. Hence this region is suitable to study the seismogenic avalanches

1.2 Study Area

The study area is situated in Ladkah district of Jammu and Kashmir, India (Figure 1.1). This is highly mountainous region of North-West (NW)

Himalaya. The altitude in the study region varies from 2468m to 7709m (Figure 1.1). This region is accessible through Khardungla pass (altitude 18380 ft), the highest motor able road in the world for a limited period in the year. This region is of strategic importance to the nation as due to its location in the border areas. Thousands of personnel are present in this region all over the year to safe guard our borders.

This region is heavily glacerized, approximately 37% area of Nubra basin and 20% of Shyok basin are glacerized. The Siachen glacier, largest glacier of Karakoram Himalaya and second largest outside the polar region, with length of about 74 Km, is the main glacier system in the study area. South Terong, North Terong, Termashehr Lolofond and Gyongla are the prominent tributary glaciers of the Siachen glacier. South-Easterly flowing Nubra River, meets the Shyok river after flowing around 76 Km. Siachen glacier system covers about 700Km^2 area and 1.3-3.2 Km wide. Westlries are the prominent source of precipitation in the study region. This region receives the precipitation mainly in solid form (snow fall) due to its high altitude, however sometimes liquid precipitation mainly in the form of drizzles received during peak summer. Snehmani et al., (2016) reported a shift of 1.5 km in the position of snout of Siachen glacier from 1978 to 2013 using Landsat satellite imageries.

The region is characterized by cold temperatures. The daily average winter temperature in the region is extremely low (up to -50^0 C), the daily average temperature up to 27^0 C is reported during peak summers (Bhutiyani et al., 2010, Dimri and Dash., 2010). The average annual winter snow fall

around 1000 Cm received by the region (Bhutiyani et al., 2010, Shekhar et al., 2012). Owing to high relief and steep valley slopes, this region has experienced large number of slope failure of huge magnitude (Dortch et al., 2009). Changing climatic condition in the last three decades in the NW Himalayas has increased the incidences of cloud bursts, flash floods, landslides and avalanches (Bhutiyani et al., 2013).

The study region is tectonically disturbed (Rai, 1983). The prominent tectonic feature of this region is, approximately 800 Km, dextral strike slip Karakoram fault. The Karakoram fault separates rocks of the Karakoram and Ladakh terrains and it runs almost parallel to the main body of Siachen glacier. The activity along the Karakoram fault is an ongoing process which continued through late Holocene (Imsong et al., 2017). The Karakoram Fault is seismically active in Ladakh region and Karakoram region (Kana et al., 2018, Hazarika et al., 2017, Rajinder et al., 2016). The other major tectonic features of this region are Karakoram shear zone, Shyok Suture zone and Khalsar thrust.

Numerous snow covered steep slopes present in the seismically active Nubra-shyok region posed a potential threat to the infrastructure and movement of personals in the region. The local seismicity of this northern most part of Indian plate is not studied and the avalanche potential of this region is also not mapped. The effect of seismicity on avalanche occurrence is not explored in the region.

The study region is seismically active and more or less unexplored region as no local seismic study and avalanche susceptible studies have been carried out before this study. The local seismicity of this region is also studied

first time and also the effect of NW Himalaya seismicity on the avalanche occurrence in Nubra Region was studied first time.

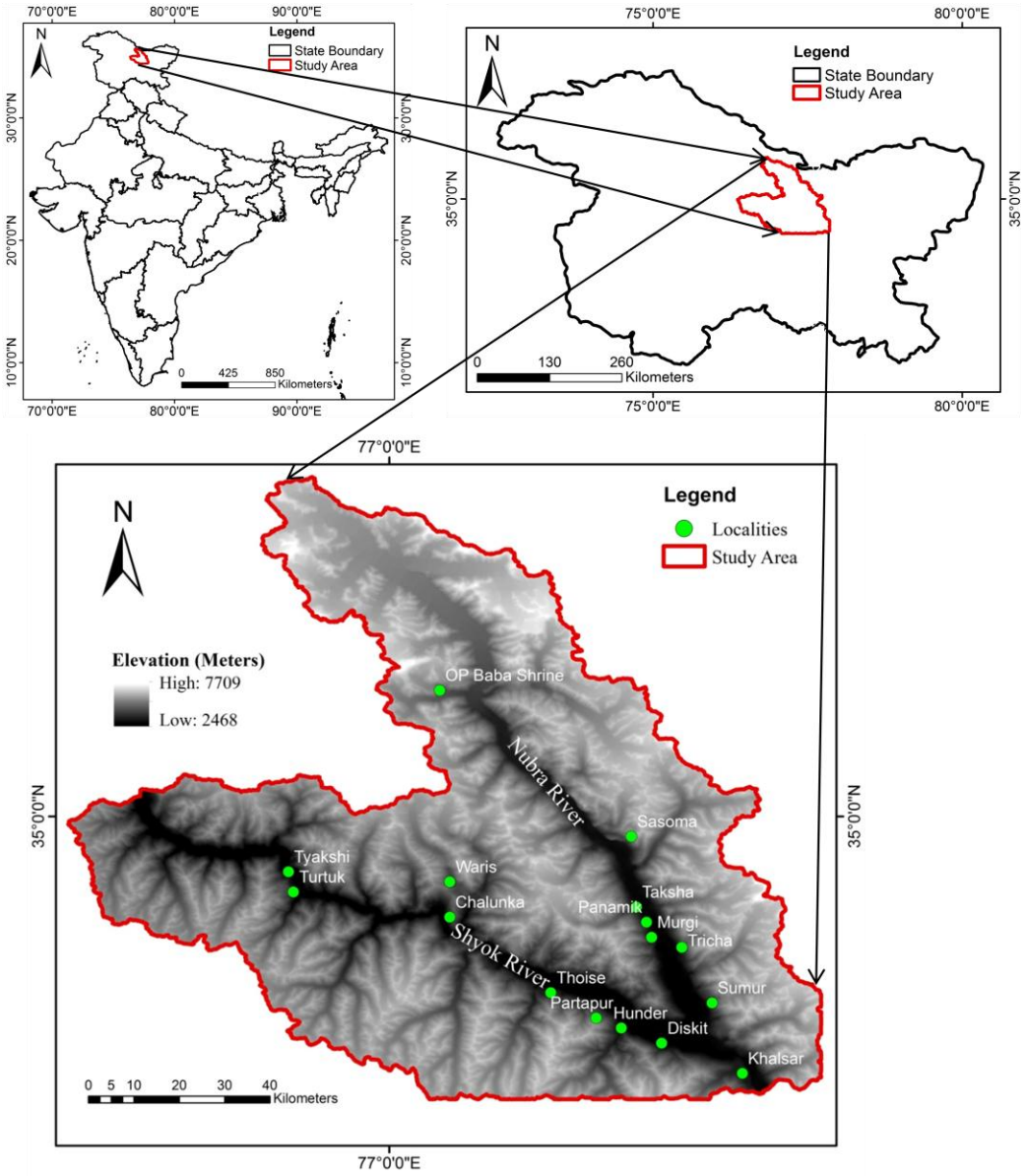

Figure 1.1: Location map of study area

1.3 Literature Review

This chapter discussed the literature survey related to seismogenic avalanches worldwide, avalanche studies in Himalaya cryosphere, usage of AHP method in avalanche studies and the seismicity studies in and around the present study area. Which leads to find the research gap and objective of this

study. In the first sub section of literature survey available literature worldwide about the effects of active and passive seismic activity on avalanche occurrences were discussed. In the second sub section of literature survey the avalanche studies carried in the Himalayan cryosphere and the suitability of Analytical Hierarchy Process (AHP) method for avalanche potential mapping in the complex snow bound terrains have been discussed. The third sub section of literature survey discussed the seismicity studies carried out in and around the present study area using regional and teleseismic data.

1.3.1. Seismicity Studies in the region

This region falls in the zone IV of the seismic zoning map of India (IS: 1893–2002 (Part l) General Provisions and Buildings), and seismotectonic atlas of India and its enviors (Dassgupta et al., 2000). The geophysical seismicity studies carried out in the region are given below

Wittlinger et al. (2004) carried out deep seismic imaging of subducting lithosphere beween Karakoram Fault and Tarim Basin using radial receiver function and it is reported that the crust thickness is continuously increasing towards Bangong Suture in the north of the Karakoram Fault up to the where the crust is around 80 km thick. It is also observed a step like increase of around 10 Km in Moho depth and crust thickness around 90 km.

Kumar et al. (2005) carried out S receiver function analysis in Tien Shan-Karakoram, region of Himalaya. The considerable S-to-P converted wave energy from the crust-mantle and lithosphere-asthenosphere boundaries,

respectively in and around Karakoram orogenic belt have been observed and used for the estimation of the crust thickness and the mantle lithosphere.

Rai et al. (2006) used the seismogram recorded at 17 seismic stations along a traverse length of approximately 700 Km in NW Himalaya India started from Delhi (NDI) to Taksha (TKS) in Nubra-Shyok region along Karakoram fault, to map the Mohorovicnic discontinuity. The Rayleigh wave (15-60 secs) group velocities inverted with telesiesmic receiver function jointly. The crust beneath Delhi station (NDI) is mapped approximately 40 km thick, with a relatively transparent structure, this result is almost similar to Indian Shield (Rai et al. 2003). The crust thickens approximately 50 km depth beneath the foothills and to 60–65 km depth below the highest part of the Himalaya. The Moho depth from 70 to 75 km below the surface mapped from south of the Indus Zangpo Suture (IZS) to the Karakoram Fault. The crustal thickness approximately 75 Km beneath the Taksha (TKS) seismic station was mapped. Among these 17 seismic station, Taksha is the only seismic station in Nubra region, which lies in extreme SE part of Nubra Valley. Rest of the Nubra-Shyok region is almost virgin from local seismological observation point of view.

Oreshin et al. (2008), carried out an integrated study of teleseismic body wave recorded by the 16 broadband seismographs deployed in an linear array from Delhi (NDI) in Indo gangetic plain to Taksha (TKS) in Ladakh Himalaya. The P and S receiver functions, teleseismic P and S residuals and observations of shear wave splitting in SKS was used to understand the deep structure of western Tibet, Ladakh and Western Himalaya. The P-wave velocity and S-wave velocity was modelled for the crust and mantle using

teleseismic body waves. Any significant crustal low velocity layer under the seismic stations south of the Tethyan Himalaya was not observed, but a mid-crustal low velocity layer under four seismic stations in the ITSZ was reported (HNL and MTH and, less clearly, HMS and RTS). It was reported a lower-crustal low velocity layer under the Khardung (KDG) seismic station North of the ITSZ, in Ladakh. The results of this study does not show crustal low velocity layer under two northern most seismic stations i.e. TKS and TGS in Ladakh.

Caldwell et al. (2009) used the data of 12 months recoded during 2002-2003, by same network as used by Oreshin et al. (2008). The 36 earthquake events happened in the source-reciver distance of approximately 300-900 Km was used. The group velocity dispersion of Rayleigh waves was calculated and inverted the average dispersion curve of five regions viz. the Indus Tsangpo suture zone, Ladakh arc complex, Tibetan plateau, Tethyan Himalaya, and Himalayan thrust belt to get one-dimensional shear-wave velocity model. In contrast to Oreshin et al. (2008), a continuous low-velocity layer with 7–17% velocity reduction centered at ~30 km depth was observed. It is also found that this low velocity layer shows a good spatial correlation with the high resistivity layer reported by Arora et al. (2007) with the help of magneto telluric studies. The most like reason for low resistivity and low velocity layer is presence of aqueous fluid or melt or both in the upper-middle part of crust.

Rai et al. (2009), uses the Lg wave recorded by these 17 seismic stations to estimate the seismic attenuation and found that the SE part of Nubra region is characterized by high attenuation (Q_0~70). The presence of aqueous

fluid/partially molten crust was found responsible for the high attenuation in this region.

Paul et al. (2011) studies the fault mechanism of local earthquakes to understand the seismic activity around Karakoram fault and to study the seismic hazard scenario around the Indian plate, NW Himalaya, with the help of an integrated analysis of seismic events recordings from an array of 4 broad band seismographs deployed in Nubra-Shyok region, NW Himalaya, India. The composite fault plane solutions for 35 earthquake events were determined from the study of first P-wave motion. These events are mainly reported from the focal depth in shallow crust < 15 km and intermediate deep crust (40-63 km) and mantle events > 90 km is not uniform. The events can be grouped for depth < 15 and in depth range 40-63 km in intermediate crust. The two faults mechanism solutions in the western and eastern segments of Karakoram fault (KF) shows major thrust faults with small strike slip component. The strikes of the fault planes of thrust faulting earthquakes are almost in NW-SE direction based on the analyses of the stereonet diagrams of fault plane solutions. Thus two retrieved fault plane solutions agree with the geometrical trend of known surface faults across the Karakoram fault. The seismicity plot suggests that the activity is more pronounced in a narrow range cutting across Karakoram fault.

(Mridula et al., 2016) carried out a study in western Himalaya to identify the seismically susceptible areas between latitude 29^0–36^0N and longitude 73^0–80^0E. The pattern recognition technique was used. In this technique the feature were identified, subsequently feature was selected and finally feature was extracted from the available seismotectonic data of the region. The discriminant analysis were applied to these features and the study area were

classified into three classes such as Area A: most susceptible area, Area B: moderately susceptible area, and Area C: least susceptible area. The Nubra-Shyok region was kept in class 'B' i.e. seismically moderately susceptible.

Hazarika et al. (2017) studied the seismotectonic scenario of the northwest part of the India-Asia collision zone lies in the south-eastern part of area selected for study in the present work. The seismic data recorded by 14 broadband seismographs consists of 10 stations established by the Wadia Institute of Himalayan Geology (WIHG), Dehradun in the eastern part of the Ladakh-Karakoram zone for passive seismological study, and four broaband stations of the Kinnaur network (Kumar et al., 2014) was analysed for local earthquake studies and calculated the focal mechanism solution of 13 earthquake events. The cluster of seismicity in the Karakoram Fault zone and strike slip faulting was oberved. The two cluster of microseismicity at a depth range of 5-20Kms and the south-eastern and north-western fringes of the Tso Morari gneiss dome were also found.

Kana et al. (2018) used the seismic data recorded by 16 Broadband seismographs (as used by Rai et al., 2006, 2009 and Caldwell et al., 2009) during June 2002 to December 2003 to study the micro-seismicity and seismotectonics in Ladakh-Karakoram region and Western Himalaya. The hypocenteral parameters of 206 earthquakes in the magnitude range of 1.5 to 4.9 and fault plane solutions of 19 earthquake events were estimated. It was found that earthquakes in Ladakh-Karakoram region are mainly confined to crustal depths, whereas in Himalayan region earthquakes are distributed in Crust as well as in Upper Mantle. The fault plane solutions of earthquakes reported in Ladakh-Karakoram region exhibit the right lateral strike slip

faulting, which is also in the consonance of the reported geology of the region (Jain and Singh, 2009). The seismically active nature of Karakoram fault was also reported in this study.

The literature survey reveal that the region is tectonically and seismically active and Indian plate are under thrusting the Eurassioan plate in this region, but the local wave form data of Nubra-Shyok, region was not available, hence local seismicity of the region was not mapped. In this thesis the local seismic data of Nubra-Shyok, region is analysed to decipher the local seismicity of the region.

1.3.2 Snow Avalanche Studies

Bhutiyani (1992) studied the effect of avalanches in Nubra Valley, NW, Himalaya, India and found that avalanches are the great enemy for the peoples of this region. The avalanche had caused loss of life of peoples and damage to the properties. Most of the casualties happened due to avalanche, when the peoples are on travel.

Sharma and Ganju, (2000), presents the complexities of Avalanche forecasting in Western Himalaya. The Western Himalaya region was divided the in to three climatic zones Lower, Middle and Upper Himalaya. The Nubra-Shyok region is an part of Upper Himalaya zone and the climatic conditions of this region are close to continental snow conditions up to some extent; being different in altitudes, unstable terrain, and absence of vegetation.

Singh and Ganju (2002) presents a study about the effect of earthquakes on avalanche occurrence in Western Himalaya, it is found that earthquake has direct bearing on avalanche occurrence in Western Himalaya. It was suggested

that as the seismic activity is increasing in Himalaya, hence the seismic tremors should be considered as an indicator of likely avalanching in the Himalaya and this will help towards the better forecasting of avalanches. The results of this study were discussed by Podolskiy et al. (2010a), it was felt that this region with high seismicity and high avalanche potential needs more such studies considering the rising population of India and infrastructure development in the snow bound regions of Himalaya. The issues related to the avalanche triggered by earthquake shall be considered in detail in Himalayas.

Ganju et al. (2002) have presented the characteristics of avalanche accidents in Western Himalaya, India. It is observed that the main reason behind the triggering of avalanches is unprecedented weather condition. The total 2344 people have been caught in avalanche accidents and about 1452 peoples have been killed. Around 62% of people got killed by avalanches when they are travelling. Around 63% of avalanches were triggered by natural means (except ground shaking), however, the cause of triggering of around 33% of avalanches is not known. The significant decrease in avalanche accidents of local civilians was observed and the general awareness of people for this decline is found responsible. It was suggested that basic research and general awareness can play a key role towards mitigation of this mountainous hazard.

Ganju and Dimri (2004), have presented the cause of avalanches, the magnitude of their destruction power and the methods used in Western Himalaya by India for mitigating avalanche disasters. It was felt that an integrated approach for mitigating the avalanche disasters should be set up at national level, involving all stake holders such as defense forces and local authorities.

Podolskiy et al. (2009) have presented the data for the period 1995 to 2006 for selected Asian countries, excluding Nepal. During this period maximum casualties (565) were reported in India followed by other Asian countries such as Afghanistan (209), Pakistan (291), Tajikistan (151) and China (80). This data contains the casualties of villagers and travellers in the valley bottom.

Mcclung (2016) have studied the avalanche character and fatalities in the high mountains of Asia during 1895-2014. He pointed out that avalanche risk to the mountaineers may affect the economy of alpine regions. It was observed that the people in villages, on roads, the general movement of people, and army patroling are the biggest source of fatalities caused by avalanches in mountainous region of Asia.

Snehmani et al. (2014) used the remote sensing and AHP technique to map the avalanche hazard of Gangotri glacier basin using the slope, curvature, land cover, elevation and aspect as input parameters. The accuracy assessment carried out with comparing the existing avalanche sites identified from the ground surveys shows more than 93% of avalanche affected areas covered under the high hazard and moderate hazard zones. Similarly the AHP model has been effectively used for delineation of avalanche prone zones (Seluck, 2013, Mohammed et al., 2015, Yilmaz 2016).

Literature survey reveal that avalanche potential mapping of Nubra-Shyok, region is not taken up. It is also revealed that AHP and remote sensing techniques are very effective in the mapping of potential avalanche zones in the snow bound region.

1.3.3 Seismogenic avalanche

Ragle et al. (1965) studied the field photographs and oblique black-and-white photographs taken after the Alaska earthquake of 27 March 1964, occurred with moment magnitude 9.2 (second largest instrumentally recorded earthquake), to know the affects of this great earthquake on glacier and related features. It was found that several avalanches comprising of snow, ice and rock had been caused by this great earthquake. The nine avalanches with large run out distances had been observed as a result of this earthquake.

Fedorenko et al. (2002) described that explosion made for mining activities in the Khibini mountain in Arctic Northwest of Russia, triggers the snow avalanches. It was observed that around 225 snow avalanches were triggered by the mining explosion during 1959-1995, by correlating the avalanche day with explosion activity.

Woerd et al. (2004) reported that several large avalanches were induced by the ground shaking produced by the Kokoxili earthquake occurred on 14 November 2001 at Kunlun fault with moment magnitude 7.9. The Ikonos high resolution and ASTER satellite imagery acquired soon after the Kokoxili earthquake was used to identify and map the area of surface rupture, but while examining these imageries six large avalanches was found. Two of these avalanches were formed by the glacier collapse at the edge of ice cap and four were formed by the steep sides of ice cap, these avalanches runs 2-3Kms beyond the snout of contemporary glacier. It was pointed towards the likely increase of glacier hazard in the high seismicity snow bound regions.

Chernous et al. (2006) studies the influence of seismicity caused by technological explosions at mines in the Khibini Mountains on snow stability and avalanche releases. The influence of seismicity on snow stability on a slope was quantified and found that these are statistically significantly correlated. It was observed that two factors caused by ground shaking one increase of downhill force and decrease of friction (Inertia) and decrease of snow strength on the slope are mainly responsible for decrease in snow stability.

Podolskiy et al. (2010a) compiled the inventory of seismogenic snow avalanche triggered by natural seismicity and/or artificial seismicity. Twenty two cases of seismogenic avalanches were identified for the period 1899-2010, with moment magnitude $1.9 \leq Mw \leq 9.2$ and epicentral distance in the range ~0.2-640 kms. Around 2000 large scale avalanches associated with seismicity in extreme conditions were observed. The lower limit of earthquake magnitude that can trigger the snow avalanches determined is 1.9. It is found that the maximum distance of the reported avalanche site from the earthquake epicentre increasing with earthquake magnitude. It was reported that this result is in line with the upper limit of earthquake induced landslides proposed by Keefer (1984).

Schaer M. (2012) presented the significance of seismogenic snow avalanches in the context of the overall earthquake hazard. The known cases of earthquake induced snow avalanche worldwide were also presented including the earthquake induced snow avalanches in Indian Himalaya reported by Singh and Ganju (2002). The avalanche triggered by earthquake were also characterize and classified into three categories such as 1). Surface slab layer

avalanche 2) Full depth avalanche and 3) Mixed avalanche of snow ice and rock.

Guillen et al. (2014) analysed an earthquake occurred on December 06, 2010 near to VDLS test site in the Alps mountain of Switzerland and showed that an avalanche is likely triggered by this earthquake. The three component seismic signal and infrasound data was used to decipher that the avalanche starts after the arrival time of earthquake and this is supported by the GEODAR radar data. The avalanche starting time determined by the seismic signal analysis of recorded data by nearby seismic stations and by analysing Radar data, this suggest that December 06, 2010 earthquake was the most likely triggering factor for this avalanche. The snow stability data was analysed on various earthquake days including the December 06, 2010, and observed that the triggering of avalanche by earthquake depends on snow stability also.

Kargel et al. (2015) with the help of remote sensing data post to the Nepal's 2015 Gorkha earthquake happened with moment magnitude 7.8 on 25 April, 2015, found that snow/ ice avalanches and rockfalls triggered by this great earthquake was the main reason of destruction in Langtang Valley, Nepal that killed around 350 people.

Literature survey of seismogenic avalanches reveals that workers has either carried out the study of effect of active seismic activity on avalanche occurrences or the effect of any particular earthquake on avalanche occurrences. Few of the studies considered the effect of earthquakes recorded at regional network and/or teleseismic network on avalanche occurrences.

1.4 Research Gap

The literature survey revealed that the Nubra-Shyok region, is seismically active and prone to snow avalanches. But the local seismicity of the region is not studied and avalanche potential zones is not mapped in the region. The implications of earthquake activities on avalanche occurrences is also not taken up by any researcher.

The available literature of Nubra-Shyok region, India shows that the local waveform seismic data of this region was not available, hence seismological studies, which requires waveform data was not carried out for this region. The attenuation characteristics of seismic waves, earthquake source parameters of local earthquakes, and seismicity of this region are not known properly.

Avalanche had killed several people and damaged properties in the Nubra-shyok region, but the avalanche potential of this region was not mapped. Literature survey revealed that study region is tectonically and seismically active and prone to avalanches as well but the effects of seismic activities on avalanche occurrence is not studied in the region except one study carried by Singh and Ganju (2002) for NW, Himalaya.

The available literature on the seismogenic avalanches studies carried out worldwide reveals that either the effect of explosion or a particular earthquake have been studied on avalanche occurrences. The available seismogenic avalanche inventories across the globe reveals that hardly data of local seismic network of avalanche prone areas were available and analysed

for this purpose. It has been found that none of the study on earthquake induced avalanches was taken up in any part of the globe using continious data of earthquakes recorded by local seismic network in the avalanche prone region.

1.5 Statement of the problem

This region falls in the zone IV of the seismic zoning map of India (BIS, 2002) as well as highly glacerized mountainous region. Thousands of peoples have lost their lives in Nubra-Shyok region, three-fourth of the deaths were caused by avalanches and harsh climatic conditions. The casualties on the Pakistan side are even more (Pandit and Mishra, 2014, Pandit, 2016). The avalanches are the most dangerous enemies for the people of Nubra region (Bhutiyani, 1992). Moreover, no systematic studies have been carried to map the avalanche potential in the region except few marked as registered avalanche sites along the popular routes based on field surveys. The footfall of peoples are increasing in Nubra-Shyok region and this region is also of strategic importance for our country, but being the remote and unexplored area limited knowledge is available about this region. Hence, the concern about the natural hazards in Nubra region has increased many folds.

1.6 Objectives

Based upon the research gap identified with the help of literature survey and statement of the problem, the work presented in this thesis is divided into three parts, the first part deals with the seismological study of the

region, in the second part avalanche potential of the region is presented and in the third part effect of seismicity on avalanche occurrence is discussed.

The research work presented in this thesis is targeted with the following objectives

1) To study the attenuation characteristics of seismic waves in Nubra-Shyok, region.
2) Estimation of earthquake source parameters in Nubra-Shyok region.
3) To study the pattern of local seismicity in Nubra-Shyok region.
4) Avalanche Susceptibility mapping of Nubra-Shyok, region.
5) To study the effect of local seismicity on the occurrence of snow avalanches in Nubra-Shyok, region.

1.7 Methodology

The methodology adopted for the research work presented in this thesis is given in, Figure 1.2. The details of every method used in this thesis is given in the concerned Chapter.

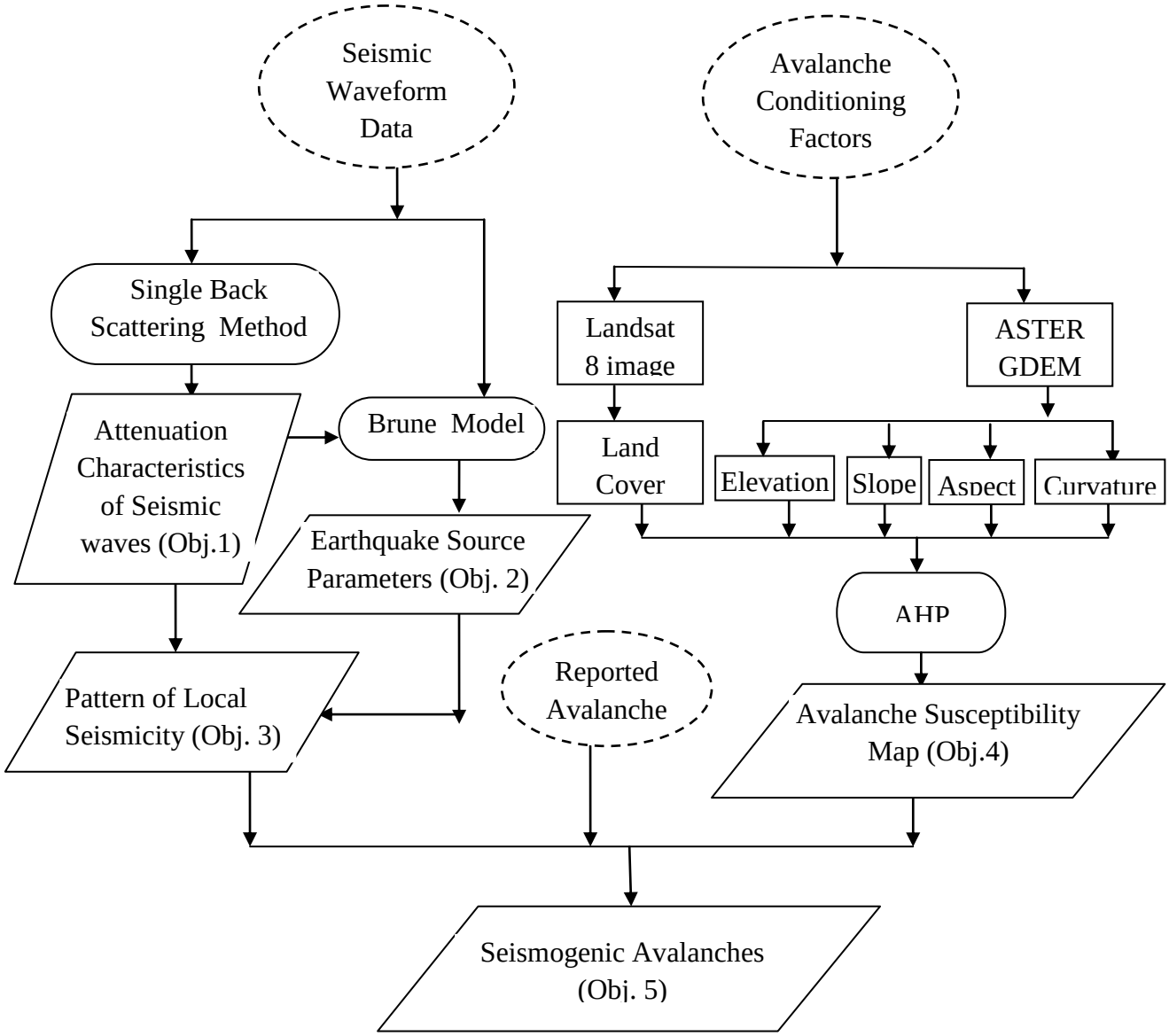

Figure 1.2: Methodology flow chart.

1.8 Data Used

The following data was used for the research work presented in this thesis.

1. Waveform seismic data recorded by a network of digital broadband seismograph equipped with 3-component digital Trillium 120P seismometer installed in Nubra-Shyok, region.
2. Hypocentral data of earthquakes reported by Indian Metrological Department (IMD), Delhi
3. Avalanche occurrence data of Nubra-Shyok region, India.
4. Landsat 8 imagery (dated 15.02.2015), ASTER GDEM and various ancillary data.

1.9 Thesis Outline

This thesis comprises of seven chapters. Literature survey and literature review about the seismogenic avalanches, avalanche studies and AHP and seismicity studies in the region is presented in Chapter 1. The various kind of seimogenic avalanche related studies carried out in various parts of the world are described in this chapter. The various research gaps identified based upon literature review are listed in this chapter. The objective of this thesis are also discussed in this chapter. The general features and importance of study region are presented in this chapter.

The attenuation studies of seismic waves recorded by local seismic network are presented in Chapter 2. This region is virgin for attenuation studies, Coda wave have been used for this purpose because the coda waves sample the large portion of subsurface medium in comparison to other seismic waves. Single back scattering method (Aki and Chouet, 1975) have been used for attenuation studies. Comparison of seismic wave attenuation studies with other parts of Himalaya are also presented in this chapter.

Source parameters of local earthquakes recorded by local seismic network have been presented in Chapter 3. Brune's earthquake source model (1970) used for earthquake source parameter is also described in this chapter. Various earthquake source parameters such as moment magnitude, source radius and seismic moment estimated for this region and their comparison with the other part of Himalaya are given in this chapter.

Chapter 4 describes about the local seismicity and pattern of local seismicity. The methodology used for seismicity study is also given in this chapter. The comparison of inferences drawn from the local seismicity study of the region with other subsurface studies of the region are presented in this chapter.

The avalanche potential of Nubra-Shyok region mapped using remote sensing and GIS technology is given in Chapter 5. The parameters used for this study and detailed methodology are also presented in this chapter. The validity of avalanche susceptibilty mapping results are also given in Chapter 5.

The implications of seismicity on avalanche occurrence of Nubra-Shyok region are discussed in Chapter 6. The distance magnitude relationship estimated for reported seismogenic avalanches of Nubra-Shyok region is presented in this chapter. Comparison of magnitude distance relation of seismogenic avalanches with earthquake triggered landslide and earthquake triggered avalanches is presented in this chapter.

The conclusion of this thesis are given in Chapter 7. Summary of research work carried out for this thesis and conclusions are also presented in this chapter.

CHAPTER 2

ATTENUATION STUDIES OF SEISMIC WAVES

2.1. Introduction

The collision of Indian plate with Eurasian plate started around 55 Ma ago (Yin and Harrison, 2000), resulting in the formation of Himalaya and this collision is still going on in present time (Wang et al., 2001). The collision has also resulted into large scale thrusting and the same is progressed southward forming the Main Central Thrust (MCT) and Main Boundary Thrust (MBT). The Indus-Tsangpo Suture Zone (ITSZ) located about 250 km, North of MCT marks the pre-collision boundary along which the Indian plate subducted below the Eurasian plate and the subduction ended in Eocene times (Gansser, 1964). The Higher Himalaya over-thrusted the Lesser Himalaya along the MCT and Lesser Himalaya thrusted over the Siwalik along MBT. The Nubra-Shyok region is situated in the alpine terrain of higher Himalaya. This region is considered as virgin region as, till now no study has been made regarding the attenuation characteristics of seismic waves in this area. Attenuation characteristics of medium decide the decay of the amplitude of ground motion at various sites. The attenuation characteristics of a region can provide essential information, regarding earthquake hazard of that region. Various methods have been developed to know about the attenuation characteristic of seismic waves, which uses the different phases of the seismogram (e.g., Aki, 1969; Aki and Chouet, 1975; Hermann, 1980; Mitchell, 1995). Quantitatively attenuation characteristics have been studied by using quality factor. The quality factor ‘Q’ is defined as the fractional loss of energy per cycle

(Knopoff, 1964). In the present work, single back scattering method proposed by Aki and Chouet (1975) has been used to determine the coda wave quality factor (Q_c) for Nubra-Shyok region, India. In this method coda portion of seismogram have been utilized to calculate the quality factor.

Ground motion in the locality of earthquakes often dies away gradually leaving a coda wave following the direct body waves and surface waves because of inhomogeneity in the Earth. These seismic coda waves are backscattering waves from numerous randomly distributed heterogeneities in the earth (Aki, 1969; Aki and Chouet, 1975; Rautian, 1976; Rautian and Khalturin, 1976). The single backscattering method given by Aki and Chouet (1975) have been used for the estimation of Coda Q for Nubra-Shyok, region, India.

2 .2 Tectonic Setting and Data

The modern Karakoram range is presumably a result of collision between the Indian and Asian continental lithospheres (Gansser 1964; Molnar and Tapponnier, 1975). The Karakoram range lies on the western end of the Tibetan Plateau, between the Kunlun mountains on the north and the Himalayas on the south. The nearly 3 km wide Karakoram fault zone is a major dextral strike-slip fault system that separates the Indian Himalaya and Ladakh batholith from the Qiangtang terranes of Tibet to the north (Leech 2008). The estimates for the initial timing of slip on the Karakoram fault range between early Miocene and Pliocene time and fault has been active since at least 21 Ma (Valli et al. 2007). Because this time frame is concurrent with activity on the MCT and South Tibetan Detachment (STD) (Godin et al. 2006), it raises the prospect that the Karakoram fault could have been involved

in conveying crustal melts to shallow melts level. Surficial geology indicates that active deformation in the Karakoram is accompanied by right-lateral strike slip and thrust faulting Guangwei and Ni, 1989; Stocklin 1977; Molnar and Tapponier, 1978). The northern end of the Karakoram fault opens into a series of faults and merges with the Pamir thrust fault zone. Although its present motion is strike slip, it may originally have been the suture between various crustal blocks comprising the southern margin of Asia (Sharma 1987). The geological and geophysical data indicate that the Indian lithosphere is actively under-thrusting the Himalaya (Gansser, 1980; Ni and Barazangi, 1984), and the Tarim Basin continues to under-thrust southward beneath the western Kunlun mountains (Molnar, 1988). Therefore, crustal shortening occurs on both the north and south edges of the Karakoram range. Convergence of the sub crustal portions of the Indian and Asian lithosphere appears to be responsible for the intermediate-depth events as well as for other measurable geophysical anomalies. The gravity anomalies across the Karakoram show a marked symmetrical pattern with a narrow band of approximately -60 mGals isostatic gravity anomalies centered over the Karakoram (Marussi, 1964). First motion fault plane solutions reported by Chen and Molnar (1983), indicate thrust and strike-slip faulting in the upper crust and normal and strike-slip faulting in the uppermost mantle. The fault plane solution along the Karakoram fault show nearly right-lateral movement along with East-West extension (Kana et al., 2018). Along the central portion around 120 km, fault have displaced (Searle, 1996; Searle et al., 1998), however at the southern end the fault only moved around 65 km (Murphy et al. 2000, 2002). The initiation of Karakoram fault should have been started

around 9-10 Ma (Murphy et al., 2002; Robinson et al., 2004, 2007), which is notably younger than the initiation age of the Altyn Tagh fault at about 55–45 Ma (Yin et al. 2002, 2008). Murphy et al. 2000 used the collected Fault-slip data at each mapped area along the Karakoram fault system to characterize its regional slip direction.

The study area is situated in the eastern Karakoram region of northern Ladakh and extends from Siachen glacier system in NW to Shyok-Nubra confluence in South East. This region is tectonically disturbed (Rai, 1983). The dextral strike slip Karakoram fault with a length of around 800 Km is passing through this region and it separates rocks of the Karakoram and Ladakh terrains. The Karakoram fault runs almost parallel to the main body of Siachen glacier. The other major tectonic features of this region are Karakoram shear zone, Shyok Suture zone and Khalsar thrust (Figure 2.1). The intervention of strongly mylonitized granite gneiss, volcanic, slate, phyllite-limestone intercalations ,conglomerate, amphibolites and serpentinite in the frontal Asian Plate margin and Shyok Suture Zone along the Nubra – Shyok Valleys forms the Karakoram Shear Zone (KSZ) (Jain and Singh, 2009). This is very narrow in width (1-5Km) and extends for nearly 200 km in Nubra valley, SSZ is an association of dismembered ultramafics, basalt, gabbro, and sediments having chert, shale and Orbitolina-bearing limestone (Jain and Singh, 2009). Karakoram Batholith Complex (KBC) comprises of various lithology such as Biotite granite, Leucogranite, metamorphics. Monotonous vertical cliffs of biotite-muscovite granite in upper parts of Nubra

valley beyond Panamik constitute the main body of the Karakoram Batholith (Jain and Singh, 2009).

The data of local seismological network comprising of four broad band recording station installed in Nubra-Shyok region, Jammu & Kashmir (Figure 2.1) has been used in the present work. This seismological network is installed in highly mountainous region and altitudes of the recording stations lies between 3180 to 3455 m from mean sea level (Table 2.1, Figure 2.2). The four recording station used the same type of instrumentation i.e. the Trillium 120P broadband seismometer and Taurus 24 bit data acquisition system (Figure 2.3), these instrument are operational in continuous mode. The seismic data was recorded at 100 samples per second.

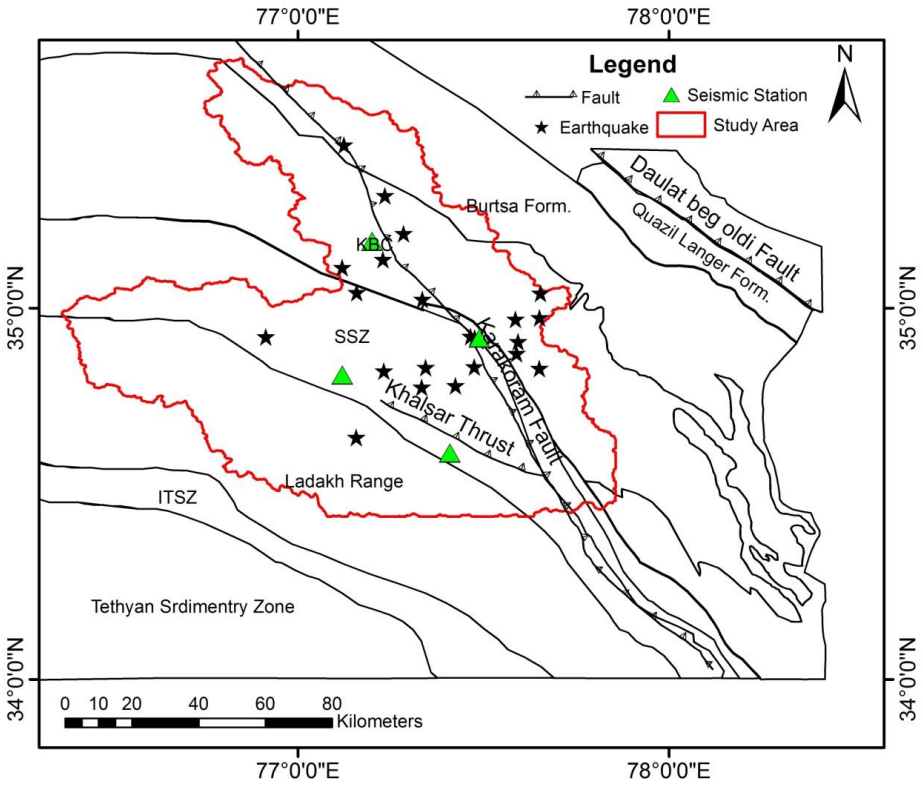

Figure 2.1: Earthquake events along with location of seismic stations shown on the tectonic map of the region (modified after Jain and Singh 2009; Rajinder et al., 2017a)

A total of thirty earthquakes recorded at this network have been used in the present study. The location of recording stations and earthquake events is shown in Figure 2.1. The hypocentral parameters of the earthquake events used in the this study are given in, Table 2.2. An example of the seismograms recorded at all the four stations is shown in, Figure 2.4.

Table 2.1: Geographical coordinates of stations used in the present work.

Sr. No.	Station Name	Station Code	Latitude (Degree)	Longitude (Degree)	Elevation (m) M.S.L.
1	Sasoma	SASO	77.49 E	34.92 N	3430
2	Parta	PTPR	77.41 E	34.61 N	3180
3	Base	BASE	77.20 E	35.18 N	3455
4	Chalunka	CHLK	77.12 E	34.82 N	3180

Figure 2.2: Field photograph of 'Sasoma' seismic observatory in Nubra-Shyok, region.

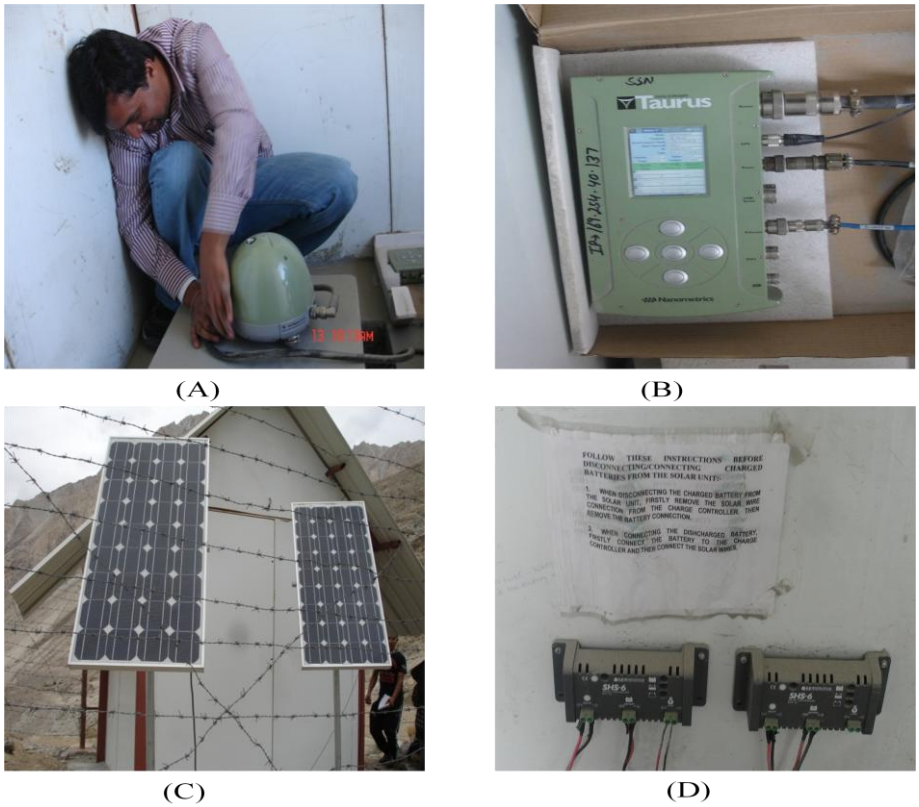

Figure 2.3: Major components of field seismic observatory of Nubra-Shyok, region, (A) Trillium-120 P, Sensor, (B)Taurus data recording system and (C) Battery, (D) Solar Panel.

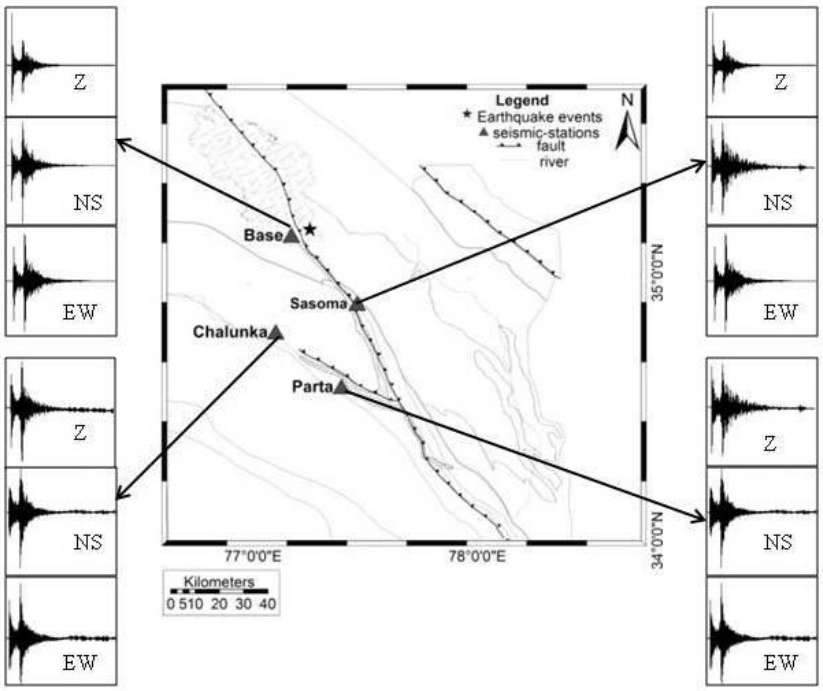

Figure 2.4: Three component waveform seismic data of the event occurred on 28.10.2010.

Table 2.2: The parameters of the earthquake used for estimation of Coda Q.

	Origin Time		Hypocentral Parameters			
Sr. No.	**Date-Month-Year**	**Hr.Min.Sec**	**Long.(E)**	**Lat.(N)**	**Depth (KM)**	**Mw**
1	01-01-2010	10.19.13	77.37	35.528	10	2.5
2	08-01-2010	13.24.10	77.23	35.131	10	3.7
3	14-01-2010	08.32.51	77.425	34.791	10	3.8
4	17-01-2010	07.09.52	77.232	34.831	10.3	2
5	22-01-2010	02.51.07	77.466	34.924	3.2	2.6
6	08-02-2010	04.14.22	77.477	34.92	10	4.2
7	10-02-2010	03.19.14	77.159	35.042	56.2	1.7
8	11-02-2010	01.42.44	77.507	35.323	10	1.8
9	11-02-2010	11.51.19	77.59	34.878	9	1
10	14-02-2010	06.09.34	77.651	34.838	80.6	1.7
11	23-04-2010	00.02.05	77.735	35.297	10	1.8
12	29-04-2010	12.28.33	77.654	35.04	12	2.6
13	14-05-2010	02.27.26	76.644	35.721	16.8	3.7
14	11-07-2010	13.40.10	77.125	35.439	120	2.1
15	16-07-2010	21.51.17.2	77.336	35.024	9.5	1.8
16	12-08-2010	03.06.03	77.594	34.91	14.2	2.5
17	16-08-2010	00.30.59	77.652	34.974	12.8	3.2
18	24-08-2010	11.21.14	77.282	35.49	10.9	3.2
19	02-09-2010	03.04.035	77.476	34.842	45.7	4.4
20	05-09-2010	04.15.02	77.587	34.97	8.7	2.7
21	06-09-2010	23.30.15	77.334	34.787	6.5	3.6
22	09-09-2010	16.13.12	77.345	34.84	12.3	4.5

23	11-09-2010	05.11.53	77.661	34.951	47.6	2.8
24	17-09-2010	14.11.16	77.661	35.926	13.2	4.1
25	19-09-2010	03.12.18	77.235	35.303	0.1	3.6
26	01-10-2010	02.00.27	77.158	34.652	10.7	3
27	15-10-2010	01.34.38	77.158	34.652	46	2.6
28	28-10-2010	10.43.14	77.285	35.201	10	4
29	02-12-2010	12.21.24	76.914	34.923	10	3
30	19-12-2010	11.18.21	77.12	35.109	10	3.4

2.3. Methodology

The single backscattering method (Aki and Chouet, 1975) have been used in the present work for estimation of Coda wave quality factor. According to this method coda amplitude, A(f, t) in a seismogram can be written as follows.

$$A(f,t) = S(f)\, t^{-a} \exp^{(-\pi ft/Qc)} \qquad (2.1)$$

where f denotes frequency and S(f) denotes the source function, and is considered a constant as it is independent of time and radiation pattern. 'a' denotes the geometrical spreading factor and considered 1 for body waves.

By taking logarithm of equation (2.1), it is linearized as given below:

$$\ln[A(f,t)] = \ln S(f) - \ln(t) - (\pi ft/Q_c) \qquad (2.2)$$

$$\ln[A(f,t)] + \ln(t) = \ln S(f) - (\pi ft/Q_c)$$

$$\ln[A(f,t)t] = C - b\,t \qquad (2.3)$$

where in equation (2.3), the term 'b' and 'C' represent $\pi f/Q_c$ and In S(f), respectively. Equation (2.3) is an equation of straight line. Hence, Q_c can be determined from the slope of the ln[A(f, t) t] versus 't' curve (Figure 2.5).

The coda waves of 30 seconds duration, observed on all the event-station pairs, have been analysed in the present work. At these window lengths all the seismograms are band pass filtered at different central frequencies (Table 2.3). The Q_c values corresponding to different central frequencies are used to calculate the frequency dependent coda-Q relation.

Table 2.3: Band pass filter applied to local earthquake data.

Low Cut-off (Hz)	High Cut-off (Hz)	Central frequency (Hz)
1	3	1.5
2	4	3
4	8	6
6	12	9
8	16	12
12	24	18
16	32	24

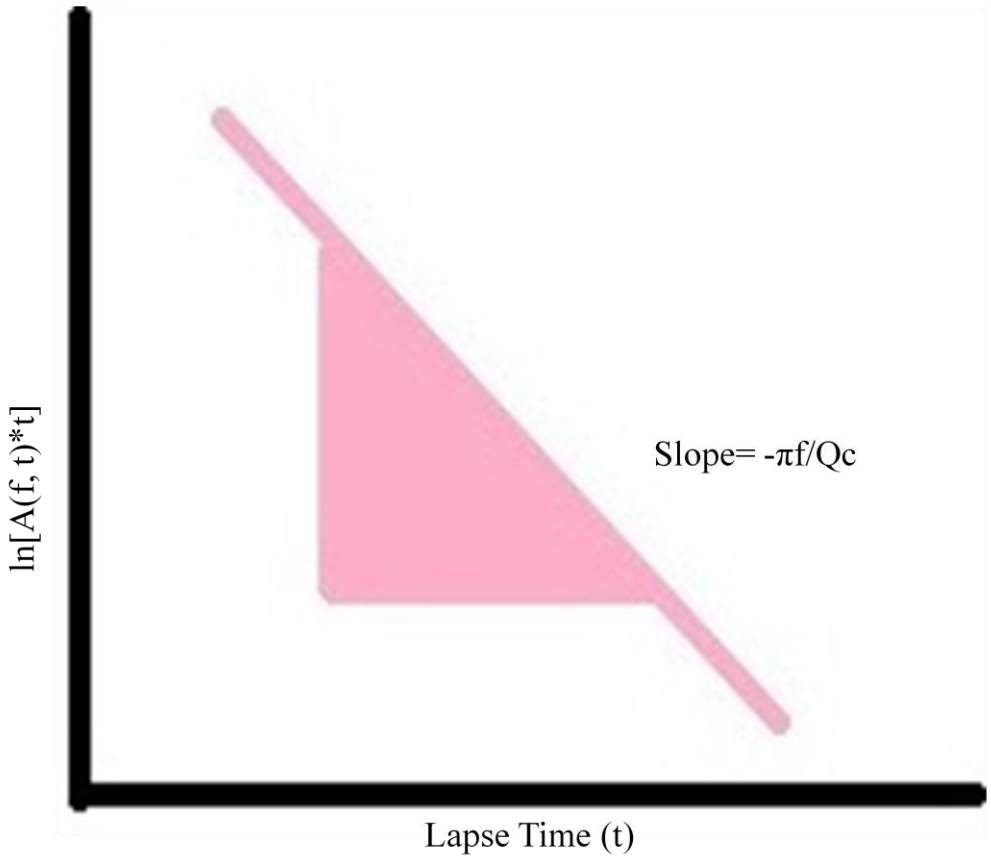

Figure 2.5: Plot of logarithmic 'coda amplitude' versus ‘Lapse time’.

2.4. Results and Discussions

Coda waves of 30 seconds window length, at different central frequency of 1.5, 3, 6, 9, 12, 18 and 24 Hz, have been analyzed to estimate Q_c relation for the Nubra-Shyok region. In the present work, Q_c relation of form $Q_o f^n$ has been determined at four seismic stations and the Q_c value obtained at each station is further used to determine regional Q_c relation for Nubra-Shyok region. The number of events at BASE, SASOMA, CHALUNKA and PARTA stations are 15, 11, 13 and 12, respectively. The slope of linear equation (2.3) between logarithmic coda amplitudes and lapse time gives the Q_c values at different central frequencies (Figure 2.5). The value of Q_c is obtained at different central frequencies for the earthquake happened on 16-07-2010 and

recorded at BASE station (Figure 2.6). Thus several values of Q_c are obtained at each central frequency corresponding to several number of events i.e. Q_c values vary from 69 to 339 at 1.5 Hz and 1385 to 4789 at 24 Hz at BASE station; 113 to 222 at 1.5 Hz and 2269 to 4442 at 24 Hz at CHALUNKA station; 21 to 327 at 1.5 Hz and 1274 to 4934 at 24 Hz at SASOMA station; 127 to 326 at 1.5 Hz and 2540 to 4984 at 24 Hz at PARTA station (Figure 2.7(A)). The mean value of Q_c is calculated at each frequency and it is further used to develop Q_c relation of form $Q_o f^{n}$ at each recording station (Figure 2.7(B)).

The final values of Q_c obtained at each station is further used to calculate regional Q_c relation for Nubra-Shyok region (Figure 2.8). The best fit line gives $(121\pm7.2)f^{(1.0\pm0.04)}$, which represent regional attenuation characteristics of the Nubra-Shyok, region of Himalaya. The $Q_o f^{n}$ relation is used for separating different regions into stable and active regions. The parameter 'Q_o' and 'n' in this relation characterize heterogeneities and level of tectonic activity of the region, respectively. This relation propose low values of Q_o (<200) for tectonically and seismically active regions and high Q_o (>600) for seismically stable region and intermediate values for moderate regions (Kumar et al., 2005). Regions with higher 'n' (>0.8) value manifest local heterogeneities. It is seen that the calculated value of Q_o varies in between 121±7.2 and 'n' varies in between 1.0±0.04 indicating tectonically active and highly heterogeneous region.

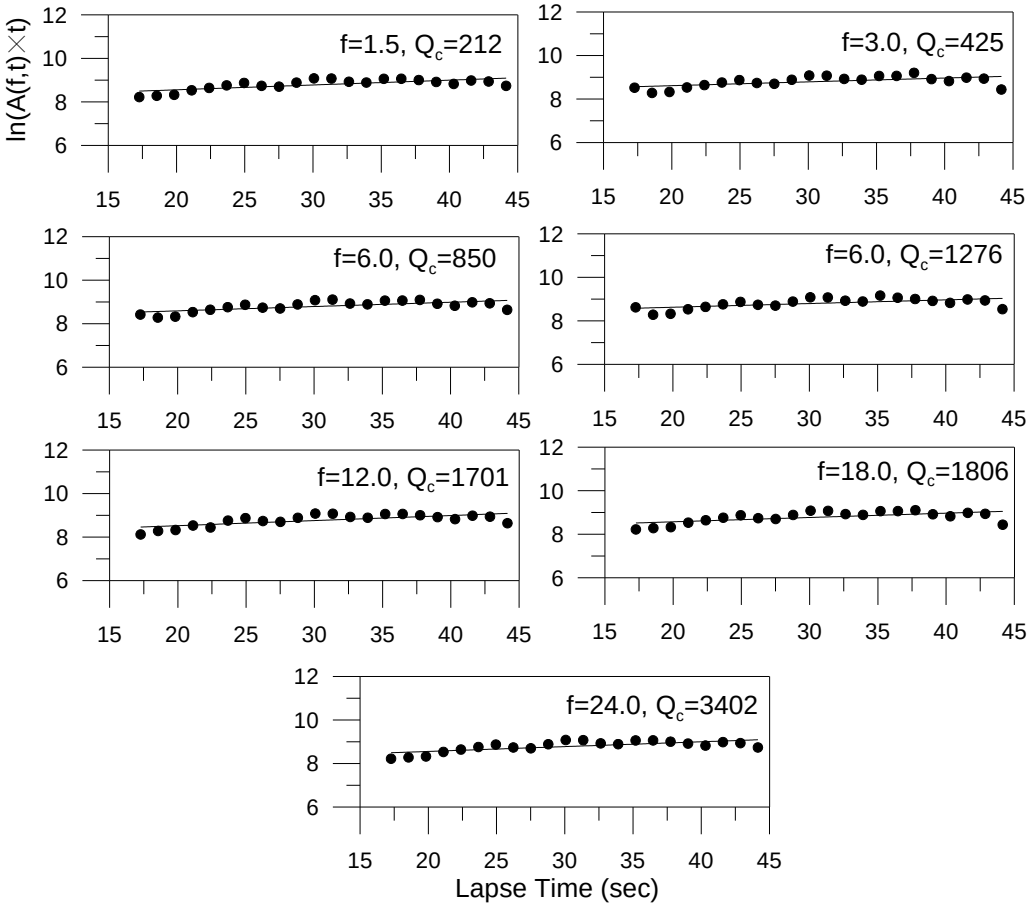

Figure 2.6: Plot between logarithmic coda amplitudes and lapse time for different central frequencies at Base station for the events occurred on 16-07-2010.

A comparison of Q_c obtained in the present work has been made with available Q relations in Himalaya region. It is seen from Table 2.4 that for Himalayan region, 'Q_o' and 'n' varies from 28 to 158 and 0.71 to 1.3, respectively. Comparison of present relation with available relations of Himalaya region is made (Figure 2.9) and it revealed that the relation obtained in present work lies well within the range of values that are justified for tectonically active Himalaya regions.

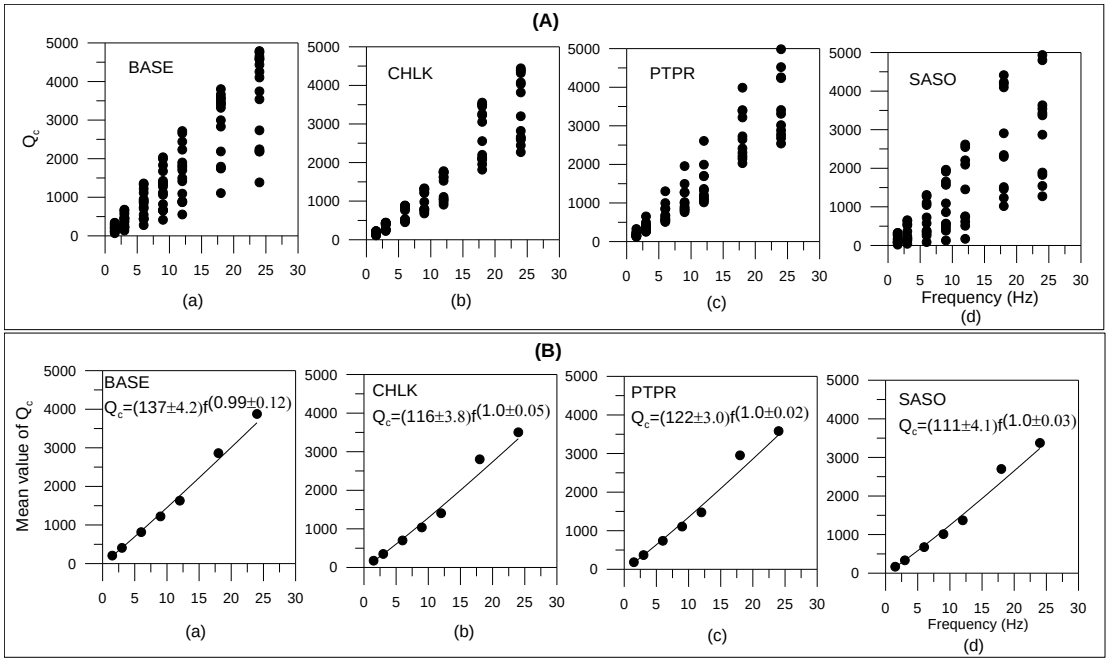

Figure 2.7: (A) Plot of obtained Q_c values as a function of frequency and (B) Mean values of Q_c as a function of frequency

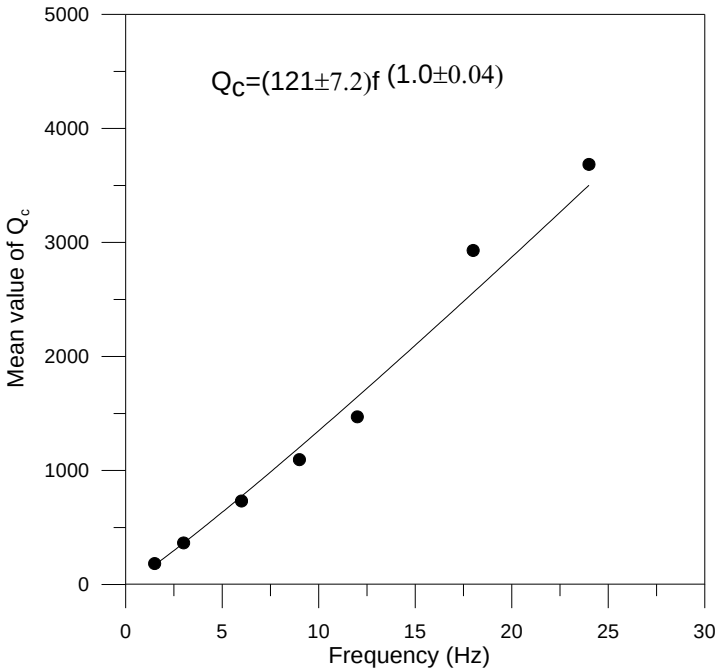

Figure 2.8: Regional $Q_c(f)$ relationship for Nubra-Siachen region based on the obtained value of Q_c at different stations.

Table 2.4 Q(f) Relationship for Himalayan region, India.

Himalaya region, India		
Attenuation relation	**Region**	**Reference**
Q(f) =126f $^{0.95}$	Garhwal Himalaya, India	Gupta et al. (1995)
Q(f) =30f $^{1.21}$	Garhwal, India	Mandal et al. (2001)
Q(f) =86f $^{1.02}$	NE Himalaya, India	Gupta and Kumar (2002)
Q(f) =92f $^{1.07}$	Kumaon Himalaya, India	Paul et al. (2003)
Q(f) =158f $^{1.05}$	NW Himalaya, India	Kumar et al. (2005)
Q(f) = 112f $^{0.97}$	Garhwal Himalaya, India	Joshi (2006)
Q(f) =87f $^{0.71}$	Garhwal region, India	Sharma et al.(2009)
Q(f) = 104f $^{1.3}$	Kumaon Himalaya, India	Singh et al. (2012a)
Q(f) =61.8f $^{0.992}$	Garhwal Himalaya	Singh et al. (2012b)
Q(f) =119f $^{0.99}$	Garhwal-Kumaon Himalaya	Mukhopadhyay and Sharma (2010)
Q(f) = 28f $^{1.2}$	Kumaon Himalaya, India	Parveen Kumar et al. (2015)

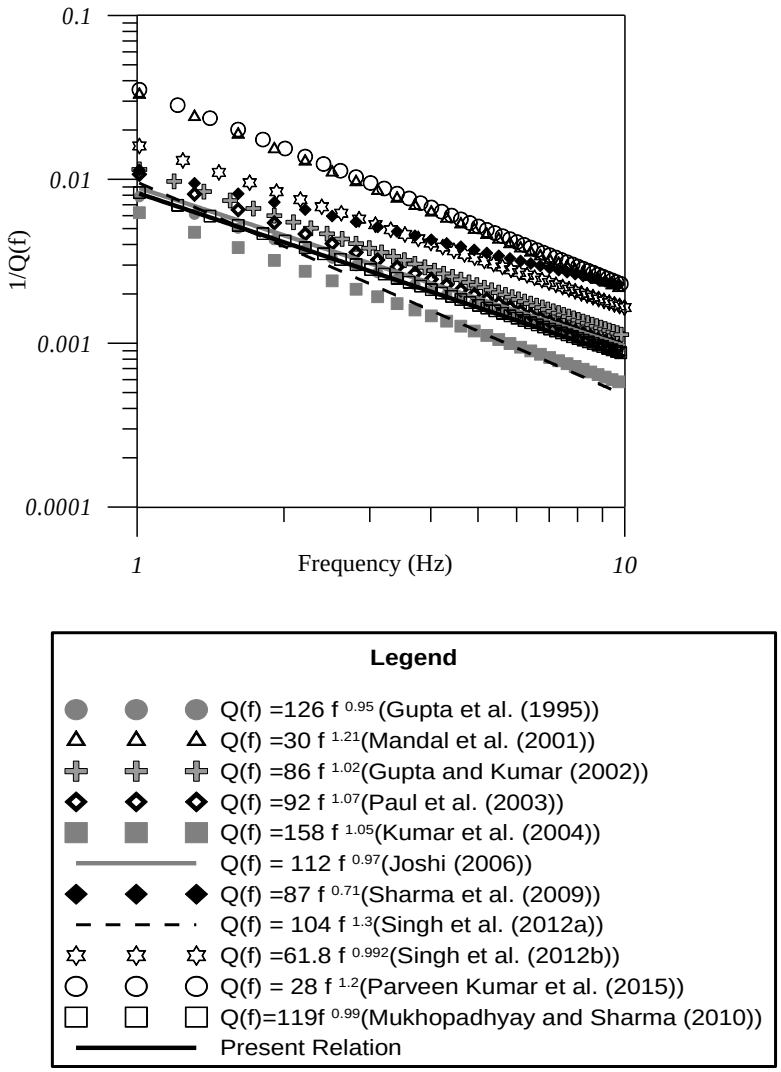

Figure 2.9: Comparison of $Q_c(f)$ relation obtained in present work with the available relation of Himalayan region.

2.5 Conclusions

In the present work, attenuation characteristics have been determined for Nubra-Shyok region, Himalaya, India as it is a virgin area regarding the attenuation studies. In this paper single back scattering method has been used to obtain regional Q_c relation for Nubra-Shyok region, Himalaya, India. Data of thirty events recorded at four stations in Nubra-Shyok region have been used in this study. In this work Q_c relation at each station is obtained individually. The values of Q_c obtained at four different stations further used

to obtain a regional regression relation of form $Q_c(f) = (121\pm7.2)f^{(1.0\pm0.04)}$,which represent the attenuating property of rocks in the Nubra-Shyok region. Low value of Q_o and high value of 'n' obtained in the present $Q_c(f)$ relation shows that the region is seismically active and characterized by local heterogeneities.

CHAPTER 3

EARTHQUAKE SOURCE PARAMETERS STUDY

3.1 Introduction

The studies of earthquake source parameters gives a prospect to study the faulting processes operating in the region and stress regime of the Nubra-Shyok region. The of study area is seismically active and located in Higher Himalaya. This region has a great potential for tourism and adventurous activities. Various construction activities are in progress in this region. The knowledge of earthquake source parameters will obviously help in the safe construction of various infrastructure.

The earthquake source parameter study in India, started in 1990s. The digital data of local earthquake recorded by telemetered array in Garhwal was used in the first earthquake source parameter study in India. Thereafter numerous earthquake source parameter studies have been carried out in the parts of Northeast India, Kumaon Himalaya, Garhwal Himalaya, Himachal Pradesh and shield part of India (Sharma and Wason, 1994, Kumar et al., 2008; Kumar, 2011, Kumar et al., 2013). However, the study of earthquake source parameters in Nubra-Shyok, region has not been reported by any worker.

Earthquake occurrences, release the certain amount of strain energy accumulated in the rocks. This release of strain energy causes sudden drop of stress stored by the rocks. Our understanding about the earthquake source parameters (seismic moment, stress drop, corner frequency and stress drop)

and spectral characteristics of body waves improved many folds, owing to advancement in the seismic source theory. Brune (1970), proposed a circular model to calculate source parameters. Far and near field displacement amplitude spectrum was used as a function of the physical parameters at the source. This model describes the nature of seismic spectrum radiated from the seismic source by considering the physical process of the energy release. The source model relates the corner frequency and low frequency asymptote to source dimension, seismic moment and stress drop. The model proposed by Brune (1970) have been used in various source parameters studies (Tucker and Brune, 1977; Fletcher, 1980; Hanks and Boore 1984; O'Neill, 1984; Andrews, 1986; Sharma and Wason, 1994; Bansal, 1998). Several other prominent workers contribute to the source parameters studies in different part of world such as Abercombie and Leary (1993); Zobin and Hasakov (1995), etc. The earthquake source parameters in Himalayan and nearby region have been studied by various workers (Singh et al., 1979; Sharma and Wason, 1994, 1995; Kumar et al., 2006; 2012; 2013a, b, c; 2014a, c; Paidi et al., 2013). However, no source parameters studies using local Broadband data have been carried out in this difficult terrain of NW Himalaya, because climatic conditions in this region is too harsh for operating and regular monitoring of seismic instruments. In context with above reference the source parameters are calculated for local earthquake events in Nubra-Shyok region, NW Himalaya. The earthquake events used in the present study comprises of the digitally recorded seismic waveform data by four broadband seismic stations installed in Nubra-Shyok region during January 2010 to February 2011 (Table3.1). These four BBS are operational in continuous mode. Each station is equipped

with a trillium 120-P, three-component broadband sensor, and a Taurus 24-bit digitizer with a synchronised GPS. All four stations are recording data at 100 samples per second. The source model relates the low frequency asymptote and corner frequency to seismic moment, stress drop, and source dimension.

3.2 Methodology

The flow chart of methodology adopted for estimation of earthquake source parameters from raw seismic data recorded at four seismic observatories of Nubra-Shyok, region, given in, Figure 3.1.

Circular model (Brune, 1970) is considered for the events as local earthquakes of low magnitude have been used for the present work. This model is quite good for estimation of earthquake source size and stress drop for such earthquakes (Madariaga and Ruiz, 2016). In this earthquake source model signal spectrum is computed from the raw unfiltered seismic data recorded by the seismograph, using the Fourier transform. The sensitivity factor of the recording instrument is applied to the spectrum for scaling. Thereafter signal attenuation effect removed from the signal spectrum using the attenuation relationship developed for the study area (Rajinder et al., 2017a). The flat spectral level and corner frequency are estimated. The other Brune parameters (seismic moment, source radius, moment magnitude and stress drop) are calculated using flat spectral level and corner frequency value.

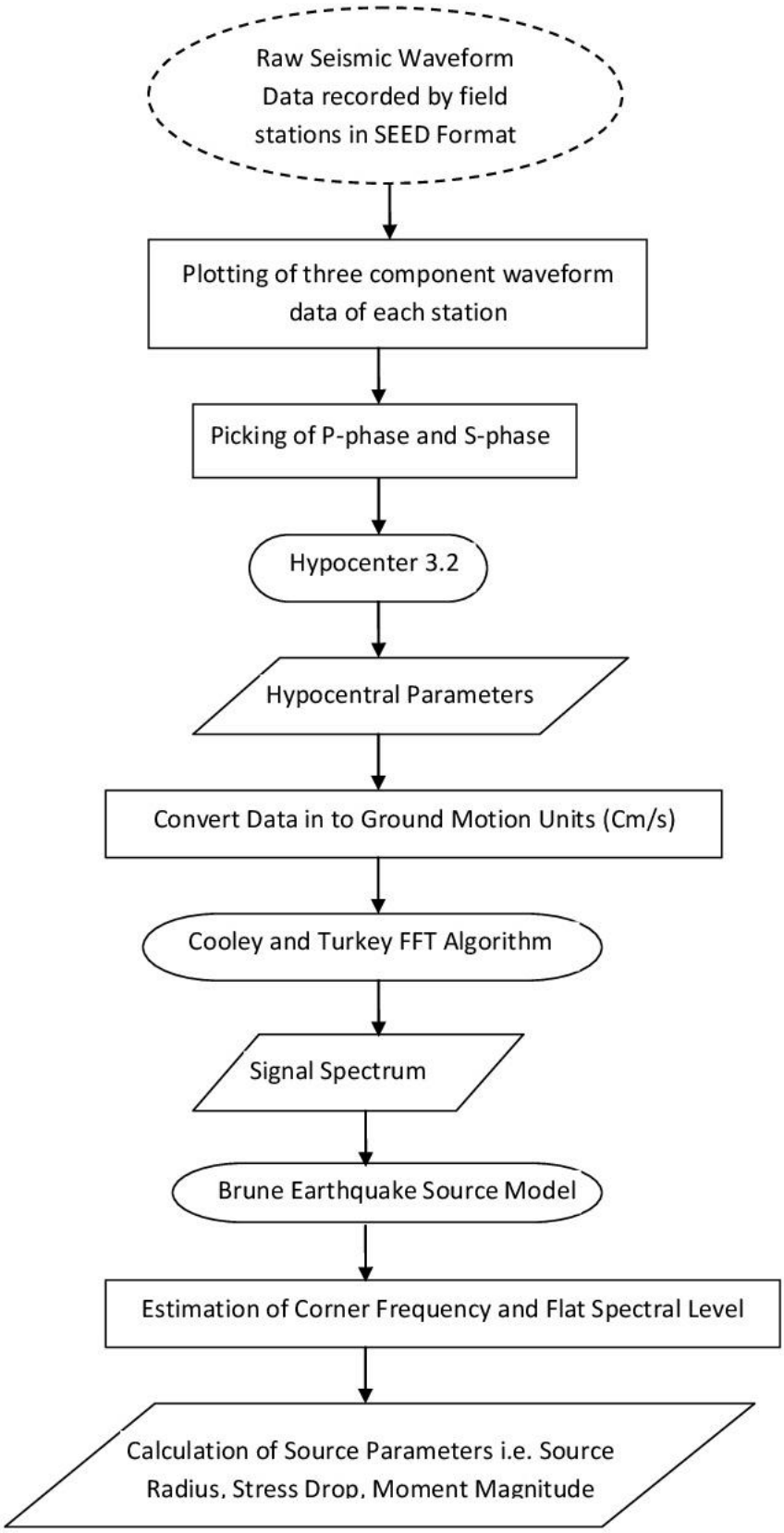

Figure 3.1: Methodology adopted to estimate earthquake source parameters

Earthquake source parameters such as seismic moment, source radius and stress drop of 17 local events recorded during the period Jan. 2010 to Feb. 2011 (Table 3.1) have been estimated by analyzing the P-wave spectra of the events. A total data window length of 800 seconds (Figure 3.2) with four seconds for P-phase is used for all events. This length is sufficient to resolve corner frequency above 0.92 Hz. The Fast Fourier Transform (FFT) algorithm of Cooley and Turkey (1965) is applied to compute the signal spectrum. The FFT algorithm gives Fourier transform 'X(k)' of a real time signal 'x(n)' by following equation.

$$X(k) = \sum_{n=0}^{N-1} e - \frac{2\pi ink}{N} x(n) \qquad (3.1)$$

where 'X(k)' denotes a difficult series in frequency domain.

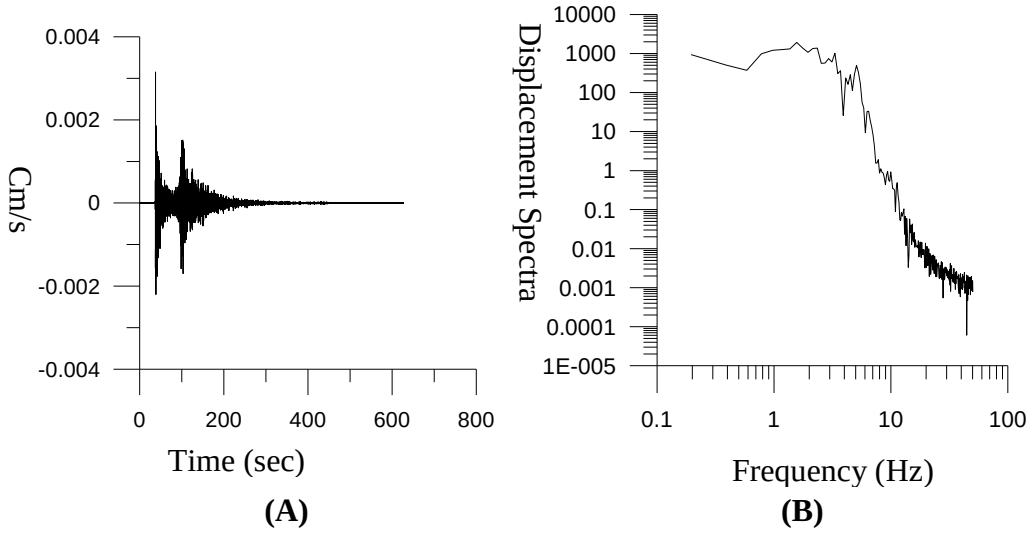

Figure 3.2: (A) An example of earthquake time series recorded at BASE station and (B) Displacement spectra of P-phase.

The flat spectral level (Ω_0) and corner frequency (fc) were estimated from spectral analysis of the recorded digital waveforms (Figure 3.2 (B)). The

Brune spectra, was fitted using a procedure given below, to the corrected observed P-wave displacement spectra at all four stations following the formula (Brune, 1970, 1971)

$$D(f,R) = \left(\Omega_0 \mathrm{GS(R)} e^{-\pi ft/Q}\right)\left[1+\left(\frac{f}{f_c}\right)^2\right] \qquad (3.2)$$

where D(f) is the displacement spectrum, Ω_0 is flat spectral level, f is frequency in Hertz, t is travel time, GS(R) is the geometrical spreading, and R is the source receiver distance. The term $e^{-\pi ft/Q}$ accounts for the attenuation of seismic waves at high frequencies and describes an elastic attenuation of waves. The coda Q frequency dependent relation of the form $Q_c=Q_0 f^n$ developed for all four seismic of Nubra-Shyok, region (Figure 2.7B, Chapter 2) are used in equation (3.2).

The value of flat spectral level (Ω_0) estimated from spectral analysis is used to estimate the seismic moment by following Keiles-Borok (1959) and Brune (1970, 1971) as given as in equation (3.3). These parameters are further used to calculate circular source radius (r), seismic moment (Mo), with the help of following equations:

$$M_o = \left(\frac{4\pi\rho V^3}{FR_{\theta\Phi}}\right)\Omega_0 \qquad (3.3)$$

Where V is the P-wave velocity in the source zone (= 6.0 km/s), ρ is average density (= 2.67 g/cm^3), $R_{\theta\Phi}$ is average radiation pattern (= 0.63), F is the free surface effect (= 2), Ω_0 is long period spectral level.

The value of seismic moment obtained from equation (3.3) for every earthquake event is used to estimate the earthquake moment magnitude following Aki (1971) and Hanks & Kanamori (1979), equation (3.4).

$$M_w = \frac{2}{3}\text{Log}M_0 - 10.7 \qquad (3.4)$$

The value of source radious (r) and stress drop ($\Delta\sigma$) are estimated following Brune (1970) and Brune (1971), by making use of corner frequency (f_c) estimated and seismic moment (M_0) from seimic spectral analysis of seismic signal for every earthquake event.

$$r = {}^{2.34V}/_{2\pi f_c} \qquad (3.5)$$

$$\Delta\sigma = 7M_0/16r^3 \qquad (3.6)$$

3.3 Results and Discussion

The source parameters such as stress drop source radius and seismic moment of local events have been computed using Brune's source model (1970) by estimating the corner frequency and low frequency spectral level using displacement spectra (Table 3.1). The coda wave quality factor estimated for all four seismic stations (Figure 2.7B) have been used in the estimation of earthquake source parameters of Nubra-Shyok, region. The seismic moment for earthquake events with magnitudes ranges between 2.7 to 5.0, ranges between 2.1 x 10^{20} to 3.34 x 10^{23} dyne-cm and the circular source radius (r) lies in the range 532.3 m to 1.296 km.

The variation of estimated source radii of earthquakes with seismic moment has random nature (Figure 3.3), which infers that source dimension is independent to earthquake size in terms of seismic moment for this magnitude range in the Nubra-Shyok, region.

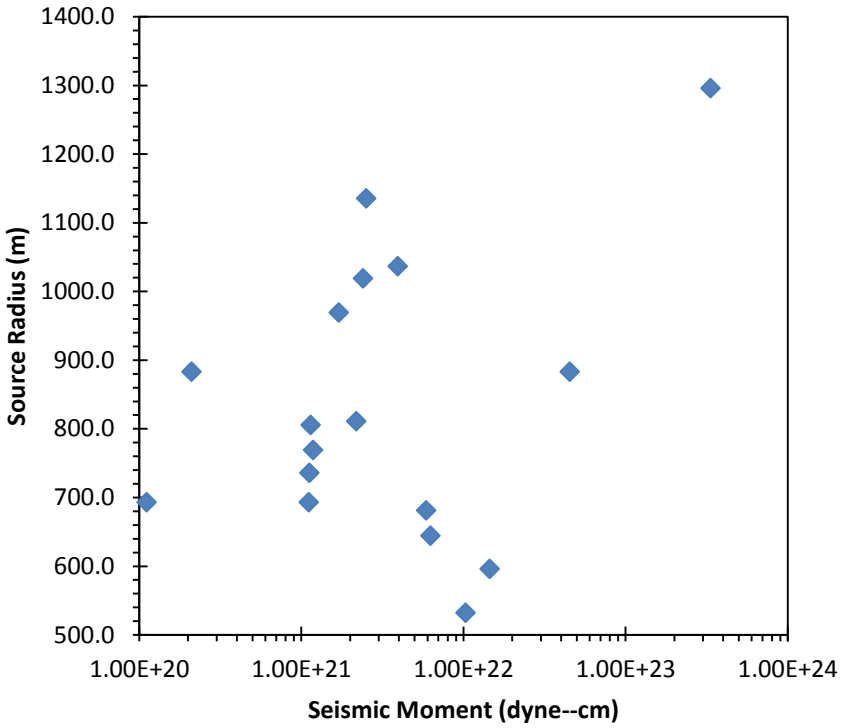

Figure 3.3: Plot of seismic moment versus source radius.

Table 3.1: The hypocenter and source parameters of the earthquakes studied.

S. No.	Date	Time	Lat. (° North)	Long. (° East)	Depth (Km)	f_C (Hz)	r (m)	Seismic Moment (M_0)	Stress Drop ($\Delta\sigma$)	M_W
1	30-05-2010	04:22	35.769	77.321	4.5	1.48	805.6	1.14E+21	1.0	2.8
2	07-12-2010	13:32	35.102	76.793	9.5	2.0	596.2	1.45E+22	29.9	2.7
3	15-07-2010	15:35	35.749	70.561	10.0	0.92	1296.0	3.34E+23	61.7	3.6
4	24-08-2010	08:34	36.49	71.282	6.3	1.75	681.3	5.88E+21	8.1	3.5
5	19-09-2010	04:12	36.931	71.478	0.1	1.35	883.2	4.52E+22	28.7	3.3
6	21-10-2010	08:05	32.841	72.978	10.0	1.35	883.2	2.10E+20	0.1	3.6
7	25-10-2010	04:33	37.645	73.746	10.0	1.05	1135.6	2.51E+21	0.7	3.3
8	28-10-2010	15:46	31.067	75.587	10.0	2.24	532.3	1.03E+22	29.9	3.3
9	11-09-2010	21:19	35.732	70.746	10.0	1.47	811.1	2.18E+21	1.8	3.3
10	14-11-2010	02:27	35.699	75.761	11.6	1.55	769.3	1.18E+21	1.1	3.7
11	22-11-2010	22:02	36.027	76.357	5.5	1.72	693.2	1.11E+20	0.1	3.5
12	25-11-2010	09:27	37.908	72.541	10.0	1.85	644.5	6.25E+21	10.2	3.8
13	12-02-2010	20:13	35.249	74.246	10.0	1.62	736.0	1.12E+21	1.2	3.8

14	12-03-2010	18:00	34.023	76.802	2.0	1.72	693.2	1.11E+21	1.5	4.4
15	12-07-2010	19:21	36.283	71.647	7.3	1.23	969.4	1.70E+21	0.8	4.0
16	19-12-2010	07:22	35.109	70.692	10.0	1.15	1036.8	3.93E+21	1.5	4.1
17	02-07-2011	16:22	36.671	71.236	10.0	1.17	1019.1	2.40E+21	1.0	5.0

The stress drops obtained in this study ranges between 0.1 to 61.7 bars. This observation is in-line with the other region of Himalaya studied so far. About 60 bars is the average stress drop observed for Himalayan earthquakes. Most of these events have seismic moment less than 10 bars. Similar low stress drop observations have been reported in earlier studies in the other parts of Himalaya (e.g., Sharma and Wason 1994; Kumar et al. 1994, 2012b; Wason and Sharma 2000; Paul et al. 2007; Paul and Kumar 2010). In the study area low stress drop events have been occurring along with high stress drop events. The occurrences of low stress drop events can be explained by two types of models: low effective stress models (Brune et al. 1986) and partial stress drop models (Brune 1970). Brune et al. (1986) explained low effective stress events happens either due to complex fault geometry or due to asperities on the fault causing the fault locks soon after the rupture passes, and the average slip over the fault cannot reach a value corresponding to average dynamic stress drop over the whole fault. The availability of low effective stress to accelerate the fault held responsible for low stress drop earthquakes (Brune, 1970). The increasing trend exhibits by stress drop with seismic moment for magnitudes less than 3.8 and becomes constant for higher magnitude events (Figure 3.4), this observation is in line with several studies reported for Himalayan region (e.g., Sharma and Wason, 1994, 1995; Kumar et.al., 2006; 2012; 2013a, c; 2014a, b, c; Paidi et al., 2013).

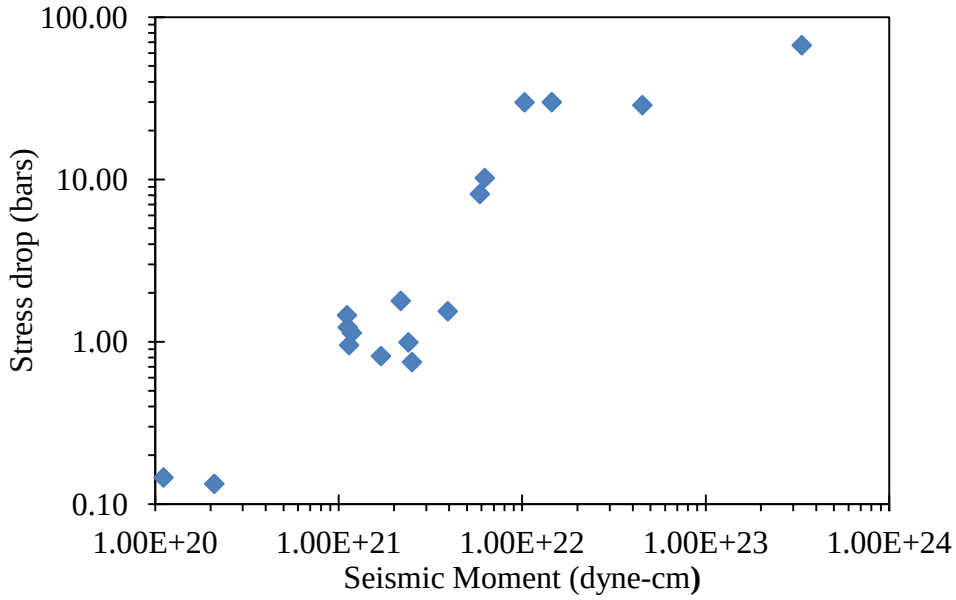

Figure 3.4: Plot of seismic moment versus stress drop.

3.4 Conclusions

The 17 local events studied have seismic moments between 2.1 x 10^{20} dyne-cm to 3.34 x 10^{23} dyne-cm and their moment magnitude ranges between 2.7 to 5.0. The source dimension in terms of the radius of circular fault varies from 532.3 m to 1.296 km. The stress drops of these earthquakes ranges between 0.1 to 61.7 bars and found in agreement with the other seismically active regions of Himalaya. The average stress drop observed in earlier studies for Himalayan earthquakes is about 58 bars. For better understanding of the source parameters of local earthquakes more data will be useful from this region. However, these initial results show promise for spectral characterization of local micro seismic events.

CHAPTER 4

PATTERN OF LOCAL SEISMICITY IN THE STUDY AREA

4.1 Introduction

The alpine mountains of Himalaya are result of ongoing orogeny, which started in Cenozoic era (Wang et al., 2001) and it is a product of northward movement of Indian plate and its collision with Eurasian plate and subsequent under thrusting of Indian plate (Dewey and Bird, 1970; McKenzie and Sclater, 1971, Yin and Harrison, 2000). Different models have been proposed by various research workers to explain the origin of the Himalaya (Gansser, 1964; Valdiya, 1980; Seeber and Armbruster, 1981). The collision has also resulted into large scale thrusting and the same is progressed southward forming the Main Central Thrust (MCT) and Main Boundary Thrust (MBT). The Indus-Tsangpo Suture Zone (ITSZ) located about 250 Km north of MCT and marks the pre-collision boundary along which the Indian plate subducted below the Eurasian plate and the subduction ended in Eocene times (Gansser, 1964).

The Himalayas, spanning length of around 2500 km is a consequence of continental collision (Valdiya, 1980, Seeber and Armbruster, 1981, Ni and Barazangi, 1984). The Himalayan region is known for its high seismicity for small to large magnitude earthquakes. The convergence between the Indian and the Eurasian plates, with continent–continent collision is considered prime factor responsible for the seismicity of the alpine Himalayan region. Several large and great earthquakes have occurred in Himalayan region (Table 4.1).

Beside these large magnitude earthquake numerous small magnitude earthquake has also been reported in the Himalaya.

The occurrences of significant earthquakes in Himalaya and its geodynamics have been presented by Seeber & Armbruster (1981); Khattri (1999) and Bilham & Gaur (2000). Several prominent features of tectonics and related seismicity arising from continental- continental collision of Indian-Eurassion plate and subsequent subduction of Indian plate under Eurasian plate in and around karakoram Himalaya have been reported by Fu et al. 2000; Zeng et al. 2000. The occurrence of earthquakes at intermediate depth under Karakoram range and western Tibet are common (Chen and Molnar, 1983). However, most continental earthquakes occur at shallow depths in the upper crust. The two depth-levels of earthquake occurrence under the continents are being reported, with the majority of the earthquakes happening in the upper crust, an aseismic crustal layer, and occasional deeper earthquakes that were assumed to be in the uppermost continental mantle (Chen and Molnar,1983).

Table 4.1: Large and great earthquakes occured in Himalayan region (Kana et al., 2018).

Sr No	Year	Magnitude	Region	Reference
1	1803	7.7	Kumaon	
2	1833	7.7	Nepal	
3	1897	8.1	Shilong	
4	1905	7.8	Kangra	
5	1934	8.3	Bihar/Nepal Border	
6	1950	8.6	Assam	

7	2005	7.6	Kashmir
8	2015	7.8	Nepal
9	2015	7.5	Hindu-Kush

4.2 Seismicity Studies around the Karakoram Region

The seismicity of Karakoram region of Himalaya has been studied by various researchers but the waveform seismic data of Nubra-Shyok, region situated in eastern Karakoram was not available. However, this work provides the scope to study the waveform seismic data recorded by Nubra region network comprising of four broadband seismographs. This region did not experience any major earthquake till date (as per the literature/record available). However micro, small & large earthquakes frequently experienced by local residing in this region (pers. communications, unpublished report of SASE). The Nubra-Shyok region is exhibit moderately seismically susceptible characteristics (Mridula et al., 2016).

The fault plane solutions for the Karakoram event obtained from moment-tensor inversion and forward modelling show predominantly thrust faulting with some strike-slip components (Guangwel & Ni 1989). The composite fault plane solutions determined from the study of first P-wave motion around Karakoram fault shows major thrust faults with small strike slip component (Paul et al., 2011). The shallow earthquake events are mainly happened in Pamir and Karakoram fault zone and their focal mechanism solutions are correlated with the tectonic features of the region (Fan et al. 1994). A 90-Km-deep event beneath the Karakoram is interpreted by Fan et al.

(1994) as occurring in the subducted Asian lithosphere; the fact that the P axis of this event is oriented parallel to the descending plate suggests down dip compression within the Asian lithosphere. The Mohorovicnic discontinuity was mapped using teleseismic receiver functions in Northwest Himalaya and Ladakh region (Rai et al., 2006). The three component earthquake data recorded by the linear array of 16 broadband seismographs started from Delhi (NDI) to Taksha (TKS), situated around the Karakoram Fault in Nubra region of Western Himalaya was used and crust thickness around 40 Km at Delhi (NDI) station was observed (Rai et al., 2006). The crust thickness is increasing towards Himalayan mountains and observed around 50 km thick crust under the foothills of Himalaya and around 65 km depth under Higher Himalaya. The crust thickness around 75 km around the Karakoram Fault in Nubra region of Himalaya was observed. Singh et al. (2005) proposed a model explaining the tectonic and seismicity characteristic of Hindukush Himalaya by making use of tectonic and seismic activity of the region. A lower-crustal low velocity layer under the Khardung (KDG) seismic station located in the North of the ITSZ, in Ladakh is observed by Oreshin et al. (2008). Caldwell et al. (2009) reported the extension of low-velocity layer towards Taksha situated in the North of Khardung. This low velocity layer is continuous in Nubra region and centred at ~30 km depth. This low velocity layer shows a good spatial correlation with the high resistivity layer reported by Arora et al. (2007) with the help of magneto telluric studies.

4.3 Methodology

The flow chart of methodology adopted for this study is given in Figure 4.1. The three component seismic waveform data recorded by four broadband seismic stations from 2010 to 2012 have been used for present analysis. The earthquake events used in the present study are tabulated in Table 4.2, and their geographical location are plotted in Figure 4.2. An example of three component seismic signal data of 19.08.2010 earthquake recorded at BASE seismic observatory is given in Figure 4.3. For computation of hypocentral parameters of local earthquakes three types of data is required such as phase data of local earthquake, accurate geographical co-ordinates along with elevation of recording stations and the local velocity model of the region covered by the recording stations. Computationally efficient and stable computer program is a major requirement to allow conversion of travel time data to estimate hypocentral parameters (Kumar 2011; Kumar et al. 2014a).

The 'HYPOCENTER 3.2' (Lienert, 1994) incorporated in SEISAN environment has been used for the estimation of hypocentral parameters of local earthquakes. This computer program makes use of Geiger Method (1912), in this method earthquake location is defined as an inverse problem. The phase data picked from earthquake seismogram is used to decipher the earthquake hypocentral parameters and origin time. The phase data in a seigram is a function of model parameters and it can be written as below.

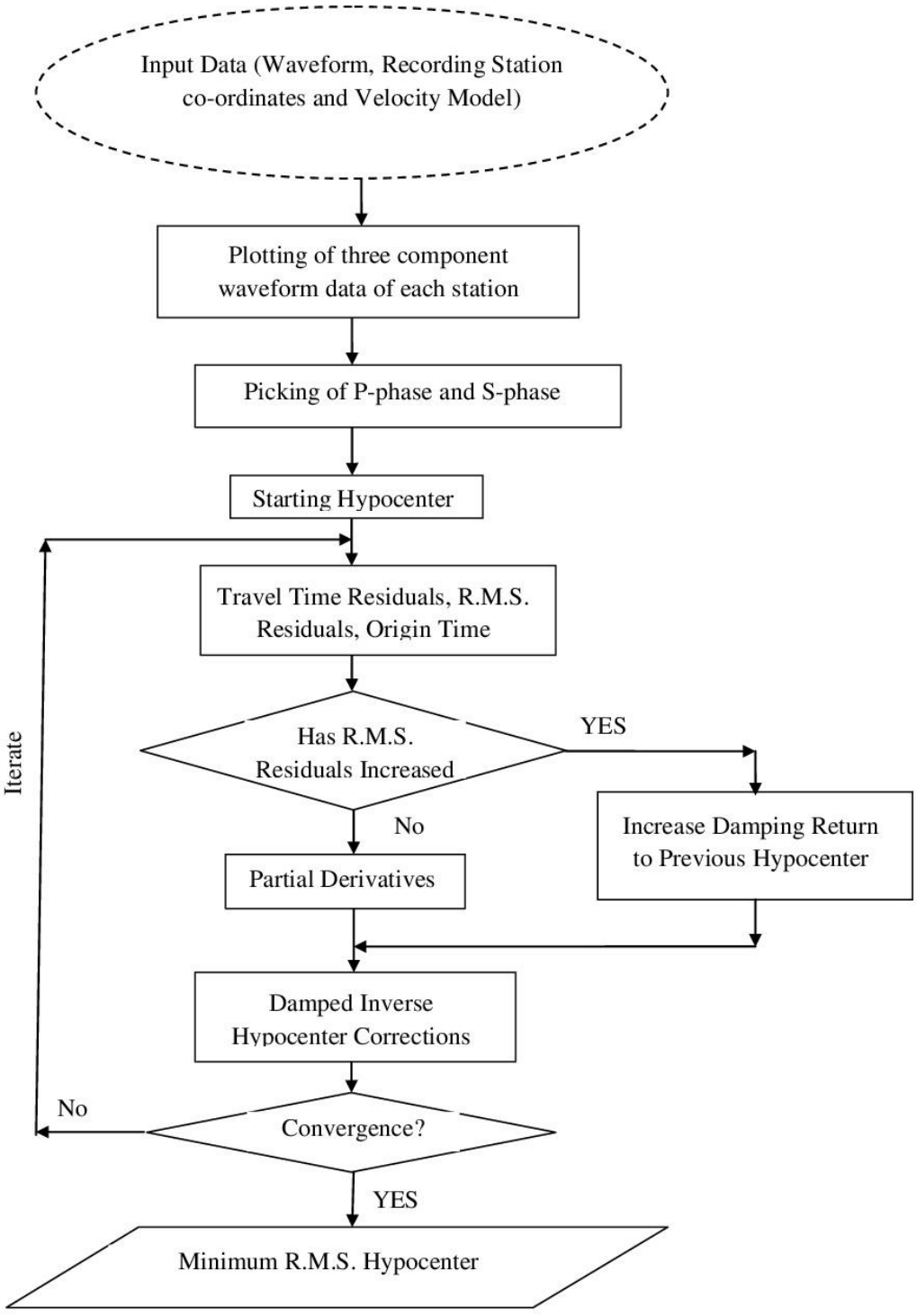

Figure 4.1: Flow chart of Methodology.

$$\Delta d_i = \sum_j G_{ij} \Delta m_j \qquad (4.1)$$

Where Δd_i represents the data matrix i.e. the arrival time observation of various phases of seismogram, G_{ij} represents the partial derivative matrix and Δm_j is a model parameter matrix. The equation (4.1) is solved for four model parameters (latitude, longitude, depth and origin time). There is one equation for each observed phase time data. In the present work four stations, recording three component gives 12 equations corresponding to every phase data. Hence twelve equations needs to be solved for four unknowns (Latitude, Longitude, Depth and Origin Time).

$$\begin{bmatrix} \Delta d_1 \\ \Delta d_2 \\ \Delta d_{\_} \\ \Delta d_{12} \end{bmatrix} = \begin{bmatrix} G_{11} & G_{12} & G_{13} & G_{14} \\ G_{21} & G_{22} & G_{23} & G_{24} \\ G_{\_\_} & G_{\_\_} & G_{\_\_} & G_{\_\_} \\ G_{121} & G_{122} & G_{123} & G_{124} \end{bmatrix} \begin{bmatrix} \Delta m_1 \\ \Delta m_2 \\ \Delta m_3 \\ \Delta m_4 \end{bmatrix}$$

Now the above matrix is an over determined problem and it can be solved as follows:

$$G^T \Delta d = G^T G \Delta m$$

$$\Delta m = (G^T G)^{-1} G^T \Delta d = G^{-g} \Delta d \qquad (4.2)$$

or $$\Delta m_j = \sum_i G_{ji}^{-g} \Delta d_i$$

The operator $(G^T G)^{-1} G^T$, which acts on the data to yield the model is called the generalized inverse of G and it is written as G^{-g}. It provides the best least square solution, because it give the smallest squared misfit.

The equation (4.2) provides the hypocentral location of earthquake and origin time of earthquake. The seismic velocity model determined by Caldwell et al. (2009) at Taksha (TKS) seismic station and geographical co-ordinates of four recording stations (Table 2.1) have been used for estimation of hypocentral parameters of local earthquakes. The P-and S-phase arrival times are picked manually making use of earthquake analysis software seisan (Haversuskov and Moller, 2003). The P-and S-phase were identified on the unfiltered data, to avoid any time shift due to filtering.

The starting earthquake location parameters are provided in the beginning of this model and the expected value for data is predicted. The changes are made in the starting location to remove the error in the earthquake location. The iterative changes are made in the earthquake location until it converges and misfit is removed. The moment magnitude (M_W) has been estimated using Hanks & Kanamori (1979) given as below.

$$M_w = \frac{2}{3}\log M_0 - 10.7 \qquad (4.3)$$

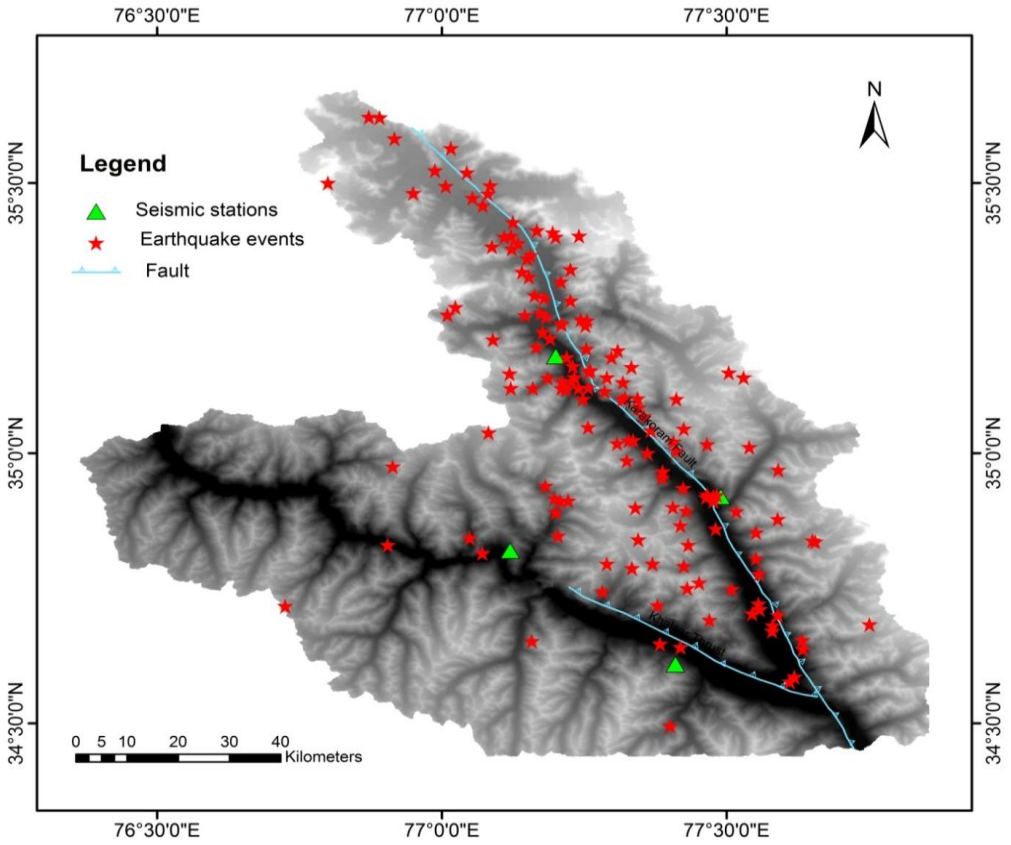

Figure 4.2: Earthquake events and major tectonic units (adopted from Phillips, 2008) in the study area.

Table 4.2: Hypocentral parameters of earthquake events

	Origin Time		Hypocentral Parameters						
Sr No.	**DD-MM-YYYY**	**HR:MIN:SEC**	**Long.**	**Lat.**	**Depth (km)**	**M_W**	**RMS**	**ERH (Km)**	**ERZ (Km)**
1	01-01-2010	10:19:57	77.37	35.828	10	2.5	0.4	4.7	3.7
2	03-01-2010	04:06:09	77.466	34.923	53.2	3.2	0.21	5	1.9
3	08-01-2010	05:45:42	77.16	35.12	10	3.7	0.36	3.2	2.7
4	14-01-2010	08:32:09	77.419	34.866	0.1	2.5	0.47	4.3	1.2
5	14-01-2010	17:24:54	77.425	34.791	10	3.1	0.58	2.4	3.9
6	22-01-2010	02:51:40	77.466	34.923	3.2	3	0.39	4.6	3.8
7	25-01-2010	22:12:18	77.582	35.237	15.8	2.8	0.89	1.7	3.4
8	08-02-2010	03:21:12	77.477	34.92	10	4.2	0.76	3.4	2.6
9	09-02-2010	11:26:00	76.951	35.136	10	3	0.63	5	1.7
10	10-02-2010	03:19:00	77.109	35.062	7.3	2.9	0.42	1.2	3.6
11	11-02-2010	01:42:00	77.507	35.323	10	2.4	0.53	4.3	4.9

12	11-02-2010	11:51:03	77.59	34.878	10.4	2.6	0.56	5	3.7
13	14-02-2010	06:09:44	77.651	34.838	0	2.8	0.39	4.8	1.7
14	18-02-2010	01:20:07	77.37	34.795	16.2	2.6	0.57	5.2	3.5
15	25-02-2010	12:19:50	77.751	34.683	98.7	3.6	0.17	3.7	2.9
16	26-02-2010	03:07:23	77.656	34.836	10	2.9	0.34	4.9	2.6
17	06-03-2010	20:01:56	77.182	34.939	8.6	1.9	0.12	4.3	3.8
18	12-03-2010	07:05:18	77.379	34.718	10	2.1	0.26	2.9	3.1
19	21-03-2010	01:42:18	76.725	34.717	96	2.4	0.69	1.3	4.9
20	28-03-2010	12:55:00	76.905	34.83	52.8	2.2	0.34	3.7	1.9
21	16-04-2010	12:19:50	77.044	35.519	51.2	2.9	0.43	2.6	2.1
22	23-04-2010	00:28:45	78.735	33.297	10	1.8	0.56	1.8	2.6
23	25-04-2010	20:01:56	77.153	35.326	54	3.2	0.71	2.8	1.9
24	29-04-2010	06:43:12	77.654	33.04	2.7	2.6	0.63	4.3	3.2
25	02-05-2010	13:32:13	77.464	34.918	56.7	4.1	0.59	3.1	2.7
26	06-05-2010	21:51:17	77.383	34.647	68	2.7	0.89	1.7	3.9
27	07-05-2010	13:26:00	77.248	35.1	14	4.4	0.63	2.6	3.2
28	14-05-2010	02.27.26	76.644	35.721	56.2	3.7	0.72	1.7	2.8
29	17-05-2010	03.06.03	77.328	35.023	92	3.2	0.45	3.2	1.7
30	19-05-2010	07:41:00	77.21	35.238	63.7	2.7	0.26	1.6	2.8
31	20-05-2010	04:06:09	77.387	34.954	2.7	2.6	0.12	1.9	2.9
32	28-05-2010	05:45:42	77.248	35.1	11.1	3.1	0.47	1.1	3.6
33	29-05-2010	08:32:09	77.308	35.018	6.5	2.8	0.38	2.5	5
34	30-05-2010	17:24:54	77.425	35.045	5.7	3.9	0.78	3.8	1.3
35	03-06-2010	02:51:40	77.2	34.89	4.3	2.7	0.24	4.7	1.9
36	04-06-2010	22:12:18	77.258	35.15	2.1	4.2	0.26	1.6	1.9
37	06-06-2010	03:21:12	77.024	35.27	8.1	3.9	0.53	3.4	2.7
38	08-06-2010	05:45:42	77.226	35.34	9	3.8	0.45	4.3	3.6
39	09-06-2010	08:32:09	77.119	35.147	45	4.2	0.47	2.8	3.4
40	10-06-2010	17:24:54	77.333	35.159	43	3.6	0.59	0.9	4.1
41	23-06-2010	02:51:40	76.8	35.5	1.4	3.7	0.32	1	3.7
42	24-06-2010	22:12:18	77.795	35.4	12.3	2.5	0.26	2.7	1.8
43	11-07-2010	03:21:12	77.2	35.4	12.8	3.7	0.89	0.5	4.9
44	12-07-2010	13:32:13	76.793	35.102	9.5	3.1	0.67	1.1	0.9
45	16-07-2010	21:51:17	77.336	35.024	9.8	1.8	0.58	1.2	1.8
46	21-07-2010	13:26:00	77.466	35.016	0.1	3	0.12	3.4	4.6
47	26-07-2010	01:42:00	76.872	35.622	72	3.2	0.45	1.2	4.3
48	28-07-2010	11:51:03	76.917	35.582	9.7	4.3	0.38	4.7	2.6
49	01-08-2010	06:09:44	76.988	35.523	7.4	3	0.36	1.7	1.6
50	03-08-2010	01:20:07	77.141	35.335	10	2.8	0.16	1.5	2.7

51	06-08-2010	12:19:50	77.18	35.287	1.7	4	0.23	0.8	1.9
52	12-08-2010	03.06.03	78.594	34.19	6.7	2.5	0.39	3.7	4.3
53	16-08-2010	00.30.59	78.331	33.974	10	3.2	0.48	2.6	4.3
54	18-08-2010	17:24:54	77.298	35.177	12	3	0.59	1.2	4.9
55	19-08-2010	14:11:29	77.219	35.177	16.8	2.3	0.66	3.6	1.2
56	24-08-2010	16:25:32	71.282	36.49	10	3.15	0.38	1.8	3.2
57	31-08-2010	20:17:10	77.355	35.068	13.7	3.6	0.12	1.6	3.4
58	02-09-2010	00:21:12	77.044	35.519	14.5	2.6	0.49	4.3	4.9
59	05-09-2010	04:15:47	77.591	34.969	71.2	2.2	0.27	1.7	3.7
60	06-09-2010	23.30.15	77.334	34.787	87.2	3.6	0.72	1.7	2.8
61	07-09-2010	14:36:54	77.431	34.75	15.4	2.4	0.45	3.2	1.7
62	09-09-2010	16.13.12	77.345	34.84	63.6	4.5	0.26	1.6	2.8
63	10-09-2010	13.18.15	77.412	35.004	11.1	2.7	0.12	1.9	2.9
64	15-09-2010	21:21:32	77.452	34.76	26	2.8	0.47	1.1	3.6
65	17-09-2010	14.11.16	77.661	35.926	13.2	4.1	0.38	2.5	5
66	01-10-2010	02.00.27	77.158	34.652	10	3	0.78	3.8	1.3
67	03-10-2010	10:19:57	77.081	35.48	12	2.6	0.24	4.7	1.9
68	09-10-2010	04:06:09	77.401	34.495	10	3.3	0.26	1.6	1.9
69	11-10-2010	05:45:42	77.59	34.7	9	4	0.53	3.4	2.7
70	13-10-2010	08:32:09	77.085	35.495	6	2.8	0.45	4.3	3.6
71	14-10-2010	17:24:54	77.156	35.366	10	2.1	0.47	2.8	3.4
72	15-10-2010	01:34:12	77.887	34.69	10	3	0.59	0.9	4.1
73	18-10-2010	11:47:21	77.309	35.19	10	2.8	0.32	1	3.7
74	22-10-2010	12:39:42	76.725	35.44	10.3	3.3	0.26	2.7	1.8
75	26-10-2010	15:33:18	76.786	35.334	37.7	2.8	0.89	0.5	4.9
76	28-10-2010	01:16:29	77.21	35.24	3.2	2.8	0.67	1.1	0.9
77	01-11-2010	04:03:11	77.125	35.427	5.9	3.2	0.58	1.2	1.8
78	02-11-2010	10:01:16	77.58	34.671	4.9	2.3	0.12	3.4	4.6
79	07-11-2010	07:15:18	77.552	34.805	6.2	3.9	0.45	1.2	4.3
80	09-11-2010	01:42:18	70.746	35.732	10	3.6	0.38	4.7	2.6
81	10-11-2010	12:55:42	77.556	34.721	83	2.6	0.36	1.7	1.6
82	13-11-2010	19:49:00	77.537	35.362	4.6	3.4	0.16	1.5	2.7
83	14-11-2010	20:01:56	77.367	35.042	8.2	3.7	0.23	0.8	1.9
84	15-11-2010	07:05:18	77.619	34.586	10	3.9	0.39	3.7	4.3
85	02-12-2010	01:42:18	74.246	35.249	10	3	0.48	2.6	4.3
86	03-12-2010	12:55:00	76.802	34.023	2	2.54	0.59	1.2	4.9
87	06-12-2010	02:55:03	77.54	35.011	0.1	3.5	0.66	3.6	1.2
88	09-12-2010	07:29:27	77.412	35.1	9.8	3.8	0.38	1.8	3.2
89	18-12-2010	20:01:20	77.153	35.326	10	2.6	0.12	1.6	3.4

90	19-12-2010	04:18:17	76.692	35.109	10	3.3	0.49	4.3	4.9
91	01-01-2011	10:15:47	77.29	34.795	9.4	2.2	0.27	1.7	3.7
92	20-01-2011	22:43:56	77.552	34.853	10	4.2	0.4	4.7	3.7
93	08-02-2011	16:52:59	77.43	35.398	132.4	3.2	0.21	5	1.9
94	13-02-2011	11:52:19	77.195	35.408	10	2	0.36	3.2	2.7
95	18-05-2011	10:19:57	77.177	35.224	5.7	71.2	0.47	4.3	1.2
96	05-07-2011	04:06:09	77.29	35.14	9.8	2.2	0.58	2.4	3.9
97	05-07-2011	05:45:42	77.517	34.892	10	3.7	0.39	4.6	3.8
98	10-07-2011	08:32:09	77.11	35.4	12	3	0.89	1.7	3.4
99	24-07-2011	17:24:54	77.09	35.21	11	4.2	0.76	3.4	2.6
100	04-09-2011	14:11:29	77.049	34.843	10	2.2	0.63	5	1.7
101	05-09-2011	16:25:32	77.208	34.911	15	1.7	0.42	1.2	3.6
102	06-09-2011	20:17:10	77.071	34.815	10	2.2	0.53	4.3	4.9
103	25-09-2011	06:47:49	76.679	35.39	10	3.1	0.56	5	3.7
104	16-10-2011	00:31:18	77.937	34.702	14	2.3	0.39	4.8	1.7
105	24-10-2011	10:17:10	77.24	35.12	57	2.6	0.57	5.2	3.5
106	29-10-2011	20:53:29	76.598	35.298	45	1.7	0.17	3.7	2.9
107	01-11-2011	18:37:00	77.863	34.563	10	3.5	0.34	4.9	2.6
108	02-11-2011	15:18:44	76.761	35.135	16.8	1.7	0.12	4.3	3.8
109	02-11-2011	03:21:12	77.211	35.132	4.3	2.8	0.26	2.9	3.1
110	06-11-2011	11:26:54	77.244	35.247	55.9	3	0.69	1.3	4.9
111	11-11-2011	03:19:39	77.228	35.133	1.2	4.2	0.34	3.7	1.9
112	12-11-2011	01:42:51	76.779	35.405	47	2	0.43	2.6	2.1
113	12-11-2011	11:51:03	77.412	35.332	42	3.6	0.56	1.8	2.6
114	17-11-2011	20:17:10	77.082	35.038	2.9	2.6	0.71	2.8	1.9
115	21-11-2011	00:03:00	76.621	35.303	45	1.8	0.63	4.3	3.2
116	27-11-2011	05:27:00	77.433	34.83	110	2.1	0.59	3.1	2.7
117	30-11-2011	00:34:00	77.997	34.862	10	1.9	0.89	1.7	3.9
118	02-12-2011	10:19:37	77.007	35.12	9.5	3.8	0.63	2.6	3.2
119	08-12-2011	14:06:09	77.82	35.18	4.3	2.7	0.39	3.7	4.3
120	09-12-2011	11:45:42	77.955	35.58	97.8	3.2	0.48	2.6	4.3
121	12-12-2011	08:32:09	77.173	35.259	10	3.2	0.59	1.2	4.9
122	14-12-2011	17:24:54	77.167	35.412	49.5	3	0.66	3.6	1.2
123	29-12-2011	02:51:40	77.15	35.36	63.7	2.4	0.38	1.8	3.2
124	30-12-2011	22:12:18	77.183	35.252	1.9	4.3	0.12	1.6	3.4
125	18-02-2012	03:21:12	77.233	35.14	10	2.6	0.49	4.3	4.9
126	23-02-2012	11:26:00	77.345	35.084	10	3.9	0.27	1.7	3.7
127	02-03-2012	03:19:00	77.424	34.935	100.7	3	0.4	4.7	3.7
128	29-03-2012	01:42:00	77.558	34.711	125	2.1	0.21	5	1.9

129	09-04-2012	11:51:03	77.581	34.681	10	2.8	0.36	3.2	2.7
130	18-04-2012	06:09:44	76.95	35.481	2.7	3.9	0.47	4.3	1.2
131	19-04-2012	01:20:07	77.088	35.382	10	2.7	0.58	2.4	3.9
132	20-04-2012	12:19:50	77.166	35.196	12	2	0.39	4.6	3.8
133	21-04-2012	03:07:23	77.257	35.048	13.7	3.8	0.89	1.7	3.4
134	27-04-2012	20:01:56	77.34	34.899	3.2	4	0.76	3.4	2.6
135	28-04-2012	07:05:18	77.261	35.153	10	3.8	0.63	5	1.7
136	01-05-2012	01:42:18	77.286	35.114	7.8	2.6	0.42	1.2	3.6
137	07-05-2012	12:55:00	77.23	35.161	3.8	4.4	0.53	4.3	4.9
138	11-05-2012	10:38:12	77.257	35.121	10	2.5	0.56	5	3.7
139	13-05-2012	22:36:41	77.317	35.099	8.7	3.4	0.39	4.8	1.7
140	15-05-2012	12:21:44	76.891	35.621	9.4	3.8	0.57	5.2	3.5
141	16-05-2012	09:43:07	77.016	35.564	49.8	3.7	0.17	3.7	2.9
142	16-05-2012	00:57:09	77.054	35.472	43.7	4.1	0.34	4.9	2.6
143	17-05-2012	18:22:54	77.122	35.402	90.2	2.9	0.12	4.3	3.8
144	18-05-2012	03:40:40	77.163	35.292	48.4	3	0.26	2.9	3.1
145	20-05-2012	11:18:39	77.19	35.212	10	4.2	0.69	1.3	4.9
146	21-05-2012	17:26:41	77.209	35.317	53.8	2	0.34	3.7	1.9
147	27-05-2012	01:08:29	77.252	35.236	9.4	2.3	0.43	2.6	2.1
148	27-05-2012	17:46:41	77.344	35.101	8.4	3	0.56	1.8	2.6
149	28-05-2012	00:38:12	77.123	35.378	59.2	3	0.71	2.8	1.9
150	29-05-2012	12:36:41	77.218	35.118	4	3.6	0.63	4.3	3.2
151	30-05-2012	10:19:57	76.927	35.653	12.1	4.3	0.59	3.1	2.7
152	04-06-2012	04:06:09	77.318	35.131	10	3.4	0.12	1.9	2.9
153	05-06-2012	05:45:42	76.887	35.635	61.7	3.7	0.47	1.1	3.6
154	08-06-2012	08:32:09	77.407	35.021	67.9	3.2	0.38	2.5	5
155	11-06-2012	17:24:54	77.186	35.139	10	3.9	0.78	3.8	1.3
156	12-06-2012	02:51:40	77.322	35.102	71.3	2.9	0.24	4.7	1.9
157	14-06-2012	22:12:18	77.325	34.986	7.4	2.4	0.26	1.6	1.9
158	15-06-2012	03:21:12	77.226	35.282	5.2	3.6	0.53	3.4	2.7
159	20-06-2012	11:26:00	77.282	34.744	12.8	3.8	0.45	4.3	3.6
160	22-06-2012	03:19:00	77.611	34.577	45.8	3.2	0.47	2.8	3.4
161	24-06-2012	01:42:00	77.419	34.641	94.3	3.5	0.59	0.9	4.1
162	29-06-2012	11:51:03	77.557	34.776	68.5	2.3	0.32	1	3.7
163	11-07-2012	06:09:44	77.481	34.86	10	2.8	0.26	2.7	1.8
164	14-07-2012	01:20:07	77.545	34.703	74.9	4.2	0.89	0.5	4.9
165	17-07-2012	12:19:50	77.007	35.494	6.8	3.7	0.67	1.1	0.9
166	18-07-2012	03:07:23	77.134	35.388	0.9	2.1	0.58	1.2	1.8
167	23-07-2012	20:01:56	77.361	35	10	2.3	0.12	3.4	4.6

168	31-07-2012	07:05:18	77.634	34.637	47.9	3.8	0.45	1.2	4.3
169	01-08-2012	01:42:18	77.509	34.748	110.1	3.5	0.38	4.7	2.6
170	06-08-2012	12:55:00	77.47	34.691	320.1	2.9	0.36	1.7	1.6
171	12-08-2012	07:31:12	77.204	34.847	10	3.7	0.16	1.5	2.7
172	17-08-2012	10:38:12	77.504	35.149	10.7	3.6	0.23	0.8	1.9
173	26-08-2012	22:36:41	76.954	35.243	8.4	2.3	0.39	3.7	4.3
174	28-08-2012	12:21:44	77.072	35.458	10.2	3.4	0.48	2.6	4.3
175	01-09-2012	09:43:07	77.388	34.966	12	3.6	0.59	1.2	4.9
176	02-09-2012	00:57:09	77.01	35.256	74	3.2	0.66	3.6	1.2
177	05-09-2012	18:22:54	77.146	35.255	86	2.8	0.38	1.8	3.2
178	05-09-2012	03:40:40	77.254	35.193	73.7	3.9	0.12	1.6	3.4
179	09-09-2012	11:18:39	77.255	35.245	98.7	4.1	0.69	1.3	4.9
180	10-09-2012	17:26:41	77.633	34.654	12	4	0.34	3.7	1.9
181	07-10-2012	01:08:29	77.477	34.911	10	2.6	0.43	2.6	2.1
182	08-10-2012	17:46:41	76.629	35.46	10	1.9	0.56	1.8	2.6
183	09-10-2012	00:38:12	77.241	35.402	10	1.3	0.71	2.8	1.9
184	15-10-2012	12:36:41	77.121	35.12	14.6	12	0.63	4.3	3.2
185	15-10-2012	02:49:39	77.464	34.918	10	6.9	0.59	3.1	2.7
186	20-10-2012	07:31:12	77.429	34.893	10	2.6	0.89	1.7	3.9
187	25-10-2012	10:38:12	77.53	35.14	47.9	3.5	0.63	2.6	3.2
188	26-10-2012	22:36:41	77.21	35.12	12.9	3.2	0.39	3.7	4.3
189	06-11-2012	12:21:44	77.198	34.916	432.8	2.9	0.48	2.6	4.3
190	09-11-2012	09:43:07	77.483	34.922	134	2.8	0.59	1.2	4.9
191	16-11-2012	00:57:09	76.914	34.975	10	2.7	0.66	3.6	1.2
192	23-11-2012	18:22:54	77.406	34.9	10	2.1	0.38	1.8	3.2
193	28-11-2012	03:40:40	77.222	34.912	172	2.2	0.12	1.6	3.4
194	05-12-2012	19:43:07	76.917	35.12	218.9	3.9	0.49	4.3	4.9
195	24-12-2012	22:49:18	77.945	34.93	115.6	3	0.27	1.7	3.7
196	25-12-2012	10:49:38	77.684	35.238	126.7	2.8	0.4	4.7	3.7
197	17-01-2010	07.09.52	78.832	34.831	10.3	2	0.21	5	1.9
198	19-09-2010	12:43:17	71.478	36.931	0.1	3.5	0.36	3.2	2.7

4.4 Results and Discussions

The hypocentral parameters of local earthquake are estimated with the help of 'HYPOCENTER 3.2' (Lienert, 1994) from the phase data recorded at four seismic stations installed in Nubra-Shyok region. The standard error in

the estimation of hypocentral parameters for these events are < 0.5 seconds in origin time, < 5.0 Km in epicentre (ERH) and < 6.0 in focal depth (ERZ).

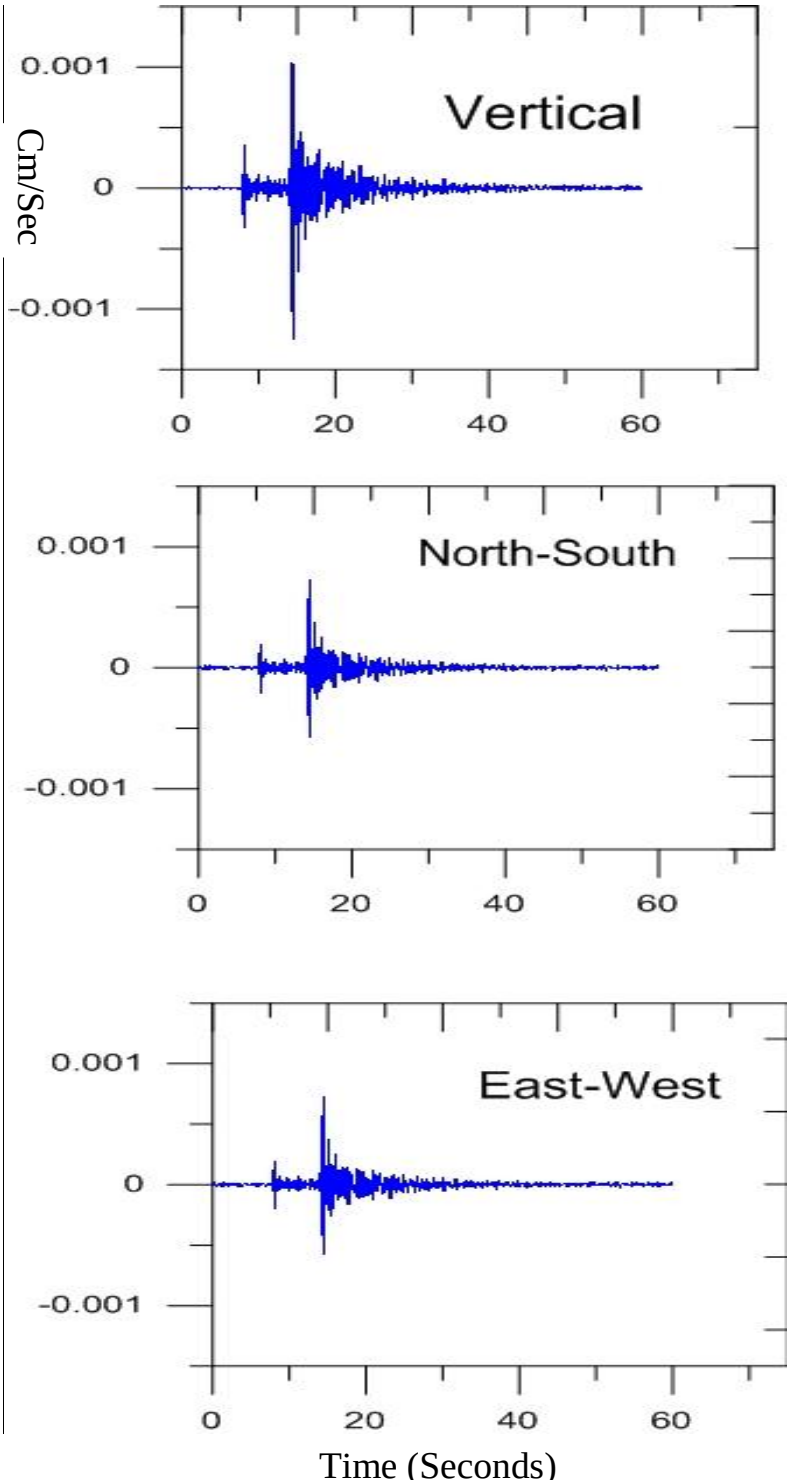

Figure 4.3: Three component seismogram of 19.08.2010 eartquake recorded at BASE seismic station.

The observed local seismicity is mainly occurred along the Karakoram Fault and few events are occurred at a depth of 40km or more, but no local event is reported in a depth range from 17-40 km below the surface of the Earth. This seismically inert layer (17-40 Km) shows that no stress gets accumulated in this layer. The plot of Number of earthquakes versus Focal Depth layer (Figure 4.4) shows good spatial correlation with the low resistivity layer in the mid crust of NW Himalaya determined from the magnetotelluric studies of NW Himalaya (Arora et al., 2007) and partially melted upper middle crust revealed by Rayleigh wave dispersion (Caldwell et. al., 2009). Due to the partially melted nature of mid-crust (depth range 17-40km) no stress is accumulated in the middle-crust, so no earthquake is reported in mid-crustal depth range in Nubra-Shyok region. This infers the presence of an aseismic mid-crustal layer sandwiched between tectonically active layers in Nubra-Shyok region. This aseismic layer is consistent with the geological section of the area (Figure 4.5).

The pattern of earthquake events (Figure 4.4) shows that the seismicity in the Nubra-Shyok region is mainly occurring at upper crustal depth. The upper crustal seismicity for the Karakoram region have also been reported by Kana et al. (2018), Hazarika et al., (2017) and Dassgupta et al. (2000). The most of the earthquakes happened in this region falls in the magnitude range of 4-5 and an earthquake with magnitude 6 occurred in 1917 is the largest reported earthquake in the region (Dassgupta et al. 2000). The local seismicity observed in this work and reported by other workers around this region infers that the Nubra-shyok region is seismically active. The value of Q_0 less than

200 obtained from the Coda Q relation $Q_c(f) = (121\pm7.2)f^{(1.0\pm0.04)}$ developed for the Nubra-Shyok region, shows that this region is tectonically and seismically active region. The earthquake source parameters estimated for this region is also in the range of other seismically active parts of Himalaya. Hence the study of local seismicity, attenuation characteristics and earthquake source parameters of Nubra-Shyok, region confirms that this region is seismically active.

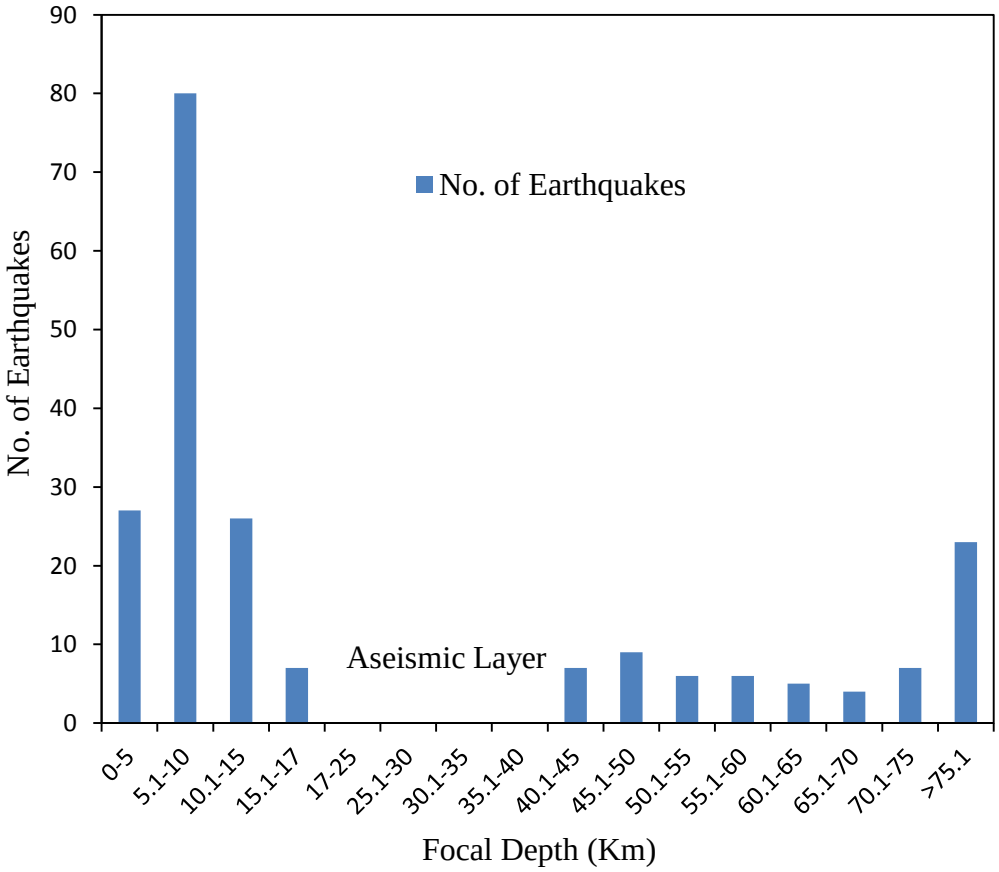

Figure 4.4: Plot of earthquake frequency versus depth range.

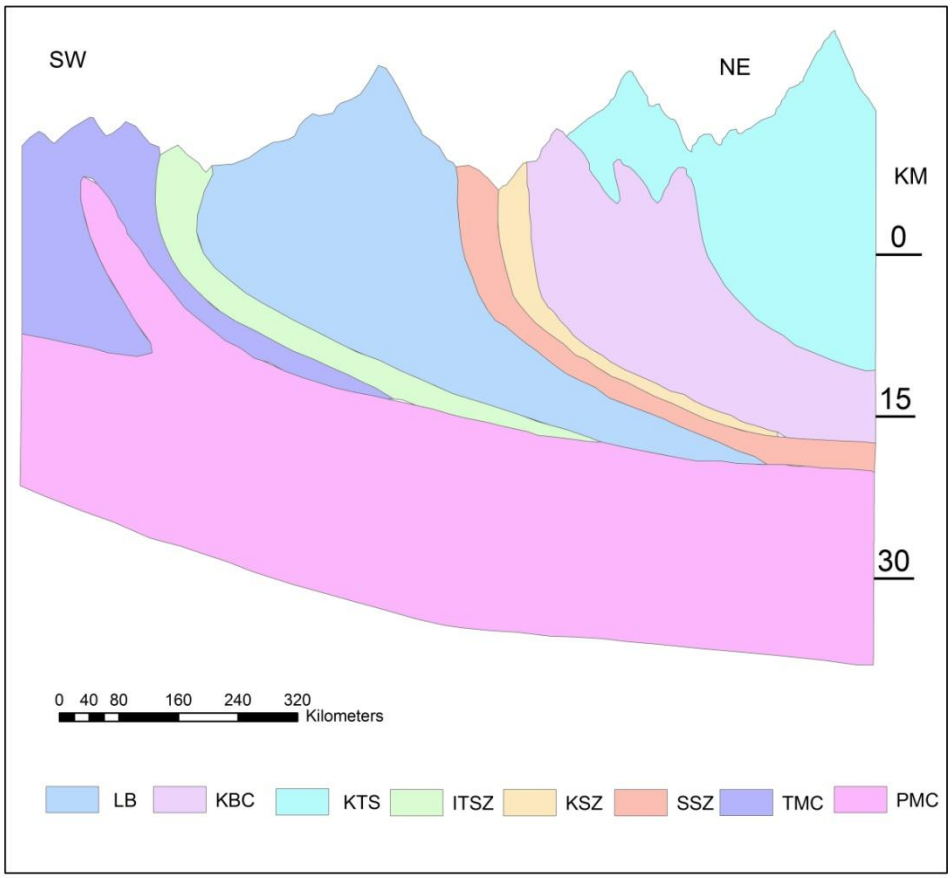

Figure 4.5: Geological cross-section through the Northern parts of NW Himalaya and Karakoram (modified after Jain and Singh, 2009): LB-Ladakh Batholith, KBC-Karakoram Batholith Complex, KTS-Karakoram Tethyan Sequence, ITSZ-Indus Tsangpo Suture Zone, KSZ-Karakoram Shear Zone, SSZ-Shyok Suture Zone, TMC- Tso Morari Crystallines and PMC-Partially Melted Crust.

4.5 Conclusions

The observed local seismicity for the period 2010-2012 in Nubra-Shyok region decipher that this region is seismically active. The pattern of local seismicity shows that the earthquake events happens mainly along the Karakoram Fault. The moment magnitudes of these events lies between 1.3 and 4.3. The depth distribution of earthquake events shows that most of the local earthquakes in this region have been occurred at upper part of the crust**.** Aseismic layer (17-40Km) sandwiched between two seismically active layers

is detected in Nubra-Shyok region. This aseismic layer shows the good spatial correlation with the low resistivity layer reported in the earlier studies. Results of this study support the proposed ‘partially melted crust for this region reported in earlier studies.

CHAPTER 5

AVALANCHE SUSCEPTIBILITY MAPPING

5.1 Introduction

The study region is highly mountainous and heavily glacerized region of NW Himalaya. Several prominent glaciers are present in the region (Figure 5.1). The Siachen glacier, largest glacier of Karakoram Himalaya and second largest outside the polar region, is the prominent glacier in the study area, with a strech of around 74 Km. Siachen glacier system covers about 700 Km^2 area and 1.3-3.2 wide (SAC, 2016). Westlries are the prominent source of precipitation in the Siachen region. The glacier mass budget of -0.03 ± 0.21 'melt water equivalent per annum' of Siachen Glacier was estimated using multi-sensor satellite imageries for the period 1999–2007 (Agarwal et al., 2017). A shift of 1.5 km in the position of snout from 1978 to 2013 was found using Landsat satellite imageries (Snehmani et al., 2016). The climatic condition of the Nubra-Shyok region is near to continental snow conditions (Sharma and Ganju, 2000). The temperature as low as -50 ^{0} C during winter season and around 27^0 C during summer season has been reported in the region (Bhutiyani et al., 2010; Dimri et al., 2010). The Nubra--Shyok region is characterized by scarce rainfall in lower reaches and moderate to heavy snow fall in the upper reaches. This region have experienced multitude of slope failure due to the presence of high relief and steep slopes (Bhutiyani et al., 2013; Dortch et al., 2009). Changing climatic conditions in Western Himalaya has led to the enhancement of natural hazard events such as floods,

landslides, cloud bursts and avalanches in the last three decades (Bhutiyani et al., 2013).

Snow avalanches is a major natural hazard in the snow covered mountain region, and posed a major threat to man and materials in higher Himalaya. Snow avalanches have engulfed thousands of human life in western Himalaya region and these deaths are termed as 'white death' (Singh and Ganju, 2002). Harsh climatic condition and snow avalanches are responsible for around 75% of the deaths in the Nubra-Shyok region (Rajinder et al., 2017b, Pandit and Mishra, 2014). The snow avalanches cannot be predicted accurately in space and time window, as the avalanche prediction is a very complex process and includes dynamic meteorological factors i.e. temperature, snowfall, wind speed, precipitation and its intensity and static terrain factors (McClung and Schaerer, 1993). An avalanche susceptibility map proves very useful for the evaluation of danger and planning for safe travel activities in snow covered regions. Geographical Information System (GIS) has proved its usage in the assessment of natural hazards. The major advantage of GIS in natural hazard evaluation is its capability of integration of large heterogeneous datasets, their management and analysis.

A significant reason while applying the Analytical Hierarchy Process (AHP) model is that this model provides a powerful potential for difficult decision problems (Malczewski, 2006). The AHP model has been effectively used for assessment of natural mass-movement problems (Nefeslioglu et al., 2013), including delineation of avalanche prone areas (Kumar et al., 2016, Snehmani et al., 2014, Seluck, 2013).

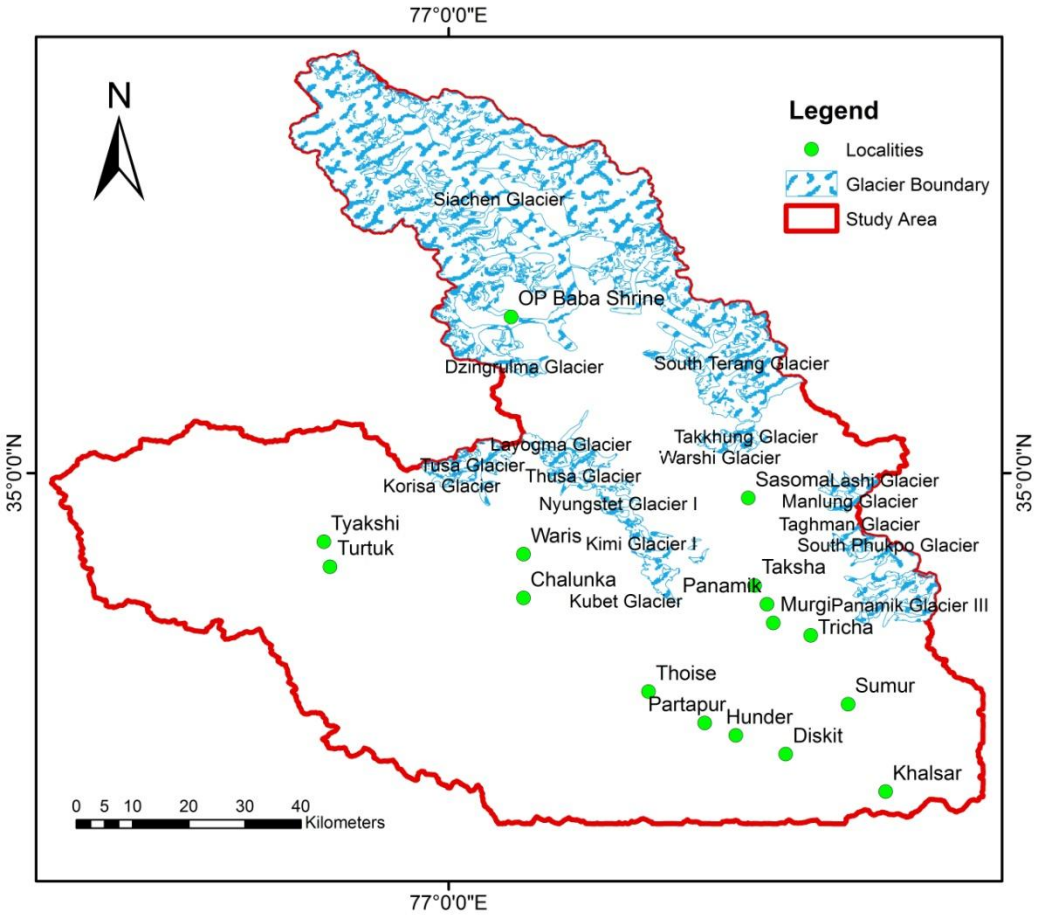

Figure 5.1: Study area along with boundary of major glaciers and major localities in the region.

An avalanche susceptibility map using static terrain factors (curvature, slope, land cover aspect and elevation) accountable for avalanche occurrence in Nubra-Shyok region, Himalaya was generated using expert judgements and Analytical hierarchy process model. The weight values for each avalanche contributory factor was assigned by comparing possible pairs in a matrix**.** Receiver operator characteristics-Area Under the Curve technique was applied for result verification in the present work. The calculated weight values of the slope factor is 0.47, which is found most significant, while the weight value of elevation factor is 0.25, were also found to be significant factor. The weight value of land cover was 0.05 and it create a least importance. The curvature

and aspect weight values were 0.12 and 0.11 respectively, and produce intermediate degree of importance. The avalanche susceptibility map of the Nubra-Shyok region was divided into five zones: (I) Very High (II) Moderate-to-High (III) Moderate (IV) Low (V) Very Low, and covers 27.5% , 28.0% 19.0%, 20.0%, and 4.8%, of the total area respectively. ROC-AUC method was applied to verify the study results. The value of Area under the curve (0.9112) shows that results of the present study are acceptable and 91.12% avalanche pixels are properly categorized.

5.2 Data Set and Methodology

Multiple source remote sensing data of spatial resolution 30×30 m was used to generate the five static terrain factors (Table 5.1). The Landsat 8 'operational land imager' imagery was used to produce the land cover map for the study region. ASTER GDEM was used to generate elevation, aspect, slope and curvature maps. This DEM resolution is sufficient enough to resolve the avalanches (Sleuck et al., 2013). The ASTER GDEM (spatial resolution of 30×30 m) is better in comparison to Carto DEM V1 and Carto DEMV1.1R1 made available by National Remote Sensing Centre (NRSC), Hyderabad and DEM generated in-house using the Cartosat-1 stereo orthokit, to use in the inaccessible areas of Western Himalaya, where available ground control points are limited (Singh et al. 2016a, 2016b, 2016c). Several data gaps were noticed in the freely available Carto DEM V1 and Carto DEMV1.1R1 in the higher reaches of study area. The remotely acquired image of Nubra-Shyok, region by Landsat 8 satellite on 10^{th} day of February, 2015 was used for producing the land cover GIS layer.

Table 5.1: Layers prepared for avalanche contributory factors for this study.

The flowchart of methodology applied to prepare the avalanche susceptibility map for Nubra-Shyok region is given in, Figure 5.2. The Survey

Sr. No.	Layer	Resolution
1	Land Cover	30 meters × 30 meters
2	Curvature	30 meters × 30 meters
3	Aspect	30 meters × 30 meters
4	Elevation	30 meters × 30 meters
5	Slope	30 meters × 30 meters

of India topographic map sheets (1:50,000 scale), satellite imagery and data of field investigation, have been used to produce an avalanche inventory map for Nubra-Shyok, region. The avalanche inventory map is a useful tool to know the active and potentially hazardous avalanche sites. The ASTER GDEM is used to derive the GIS layers of aspect, slope, curvature and elevation, while the land cover layer is derived from the Landsat imagery dated 10- February-2015. The five GIS layers (Table 5.1), were considered as the criteria for final avalanche susceptibility map. In the next step weight values of each GIS layer is calculated using the AHP model.

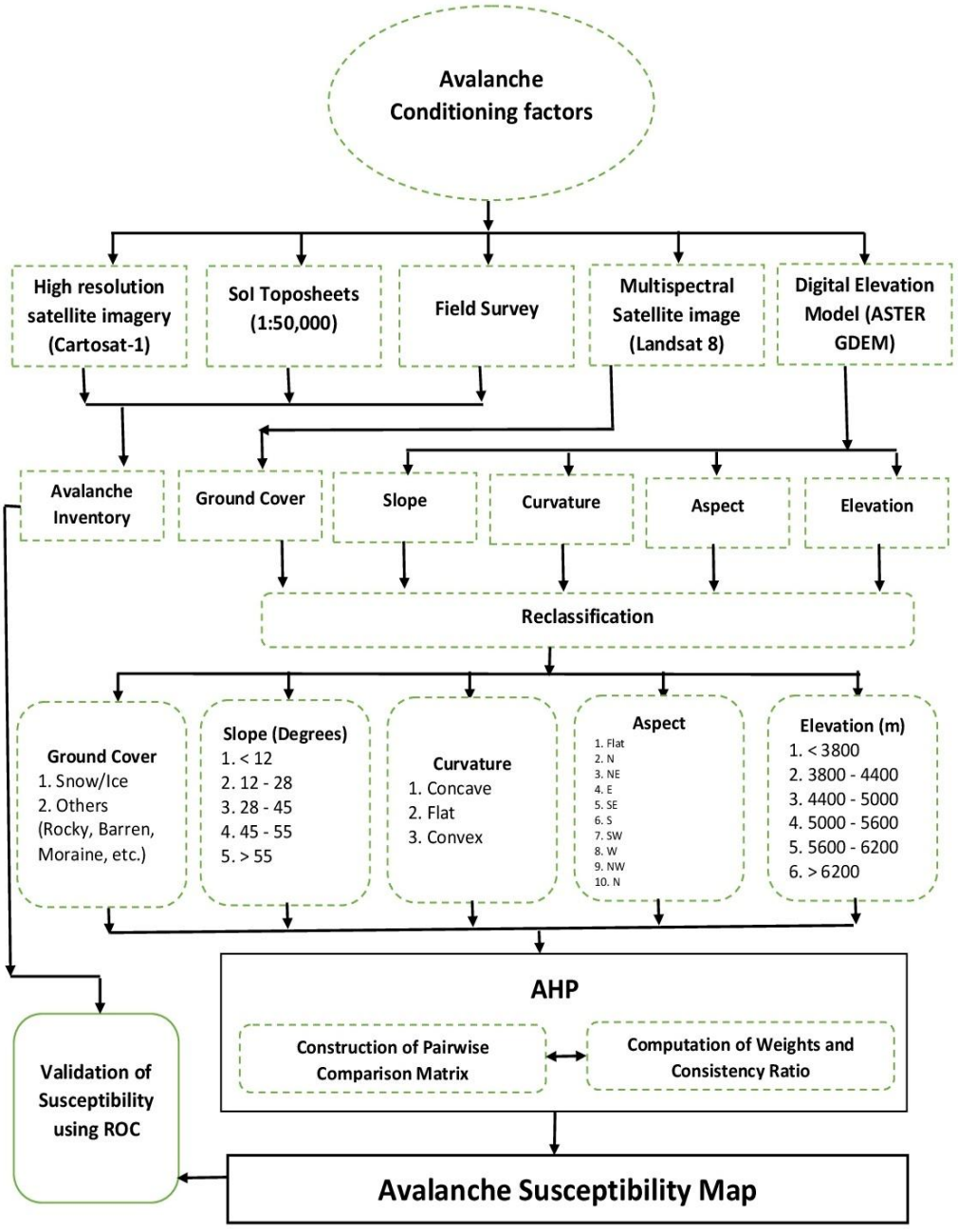

Figure 5.2: Flow chart of AHP based avalanche susceptibility mapping method.

AHP model was preferred in the present study because it does not require the dataset for training of model and it incorporates the expert knowledge and judgements in analysis. The AHP is a mathematical tool of analysing complex decisions problems with multiple criteria. AHP calculates

the required importance weighing factors associated with the GIS layers by making use of pairwise comparison matrix where all identified relevant criteria of GIS layer are compared against each other (Chen et al., 2009). The expert judgment in AHP was expressed using the a fundamental continuous scale from 1 (least important) to 9 (most important) (Satty and Vargas 1991).

The degree of consistency for judgments can also be assessed in AHP by calculating the consistency ratio (CR). The CR was calculated following Satty (1980), equation (5.1) .

$$\mathrm{CR} = \frac{\mathrm{CI}}{\mathrm{RI}} \qquad (5.1)$$

RI represents the average value of the CI produced using a random matrix that depends on the matrix order. The principal Eigenvalue, y_{max} was used to check the consistency of a matrix. The upper bound of the Eigenvalue is the same size as the element (n) in the matrix. A consistency index (CI) was used to define the degree of consistency. Higher the value of CI lowers the degree of consistency of matrix.

$$\mathrm{CI} = \frac{\mathrm{y_{max-n}}}{\mathrm{n}-1} \qquad (5.2)$$

A CR value greater than 0.1 needs reassessment of the judgments in the original matrix of pairwise comparisons, because the decision marker is less consistent. In this work, value of consistency ratio obtained for every estimated weight value of each class and every layer is within acceptable limits. The rating assigned to each class of criteria and the weight value calculated for each criteria were used to generate final avalanche susceptibility

map. Receiver Operator Characteristics-Area Under Curve (ROC-AUC) technique was applied to verify the outcome of this study.

5.3 Generation of Thematic Layers and Analysis of Avalanche Occurrence Factors

The avalanche hazard assessment is very complex because it involves several factors that affects avalanche occurrences. The terrain parameters, snowpack characteristics, weather parameters, natural and anthropogenic triggers contributes mainly to the avalanche hazard assessment. The different metrological condition leads to different type of bonding in snowpack as the snowpack develops from successive addition of layer on a slope under varying meteorological conditions (Schweizer et. al., 2003). The main reason behind occurrence of snow avalanches is additional stresses produced in the snowpack by natural phenomena such as addition of fresh snow and external triggering factors such as shaking produced by earthquake and/or anthropogenic activity. The avalanche occurs as and when the additional stresses produced by natural phenomena or manmade activity surpass the snowpack strength. The frequency of avalanches triggered naturally is more sturdily related to terrain parameters than weather factors (Smith and McClung,1997). Snowpack stability also depends upon the dynamic metrological parameters and these metrological parameters are governed by changing weather conditions. However, land cover, aspect, altitude, slope and curvature are static in nature. As sufficient knowledge about metrological parameters of Nubra-Shyok, region is not available and these are valid for short-term, hence this study is carried out using terrain parameters only.

5.3.1 Slope

The ASTER GDEM data was used to derive the slope map for Nubra-Shyok, region (Figure 5.3) and slope map is further categorized into five classes. Slope is considered essential static terrain factor for assessment of avalanche danger in the snow covered mountainous region. Rare snow avalanches occurs on mountain slopes below 25^0 (Ancey, 2009), however most of the hazardous snow avalanches is reported on snow covered mountains with slope greater than 30^0 but less than 45^0. Small avalanches is observed on a mountain slope less than 25^0 , as shear stress on such gentle slopes is so small to start the avalanche process. The steeper slopes (45^0 -55^0) does not support the snow accumulation, which results in frequent small avalanching, hence less amount of snow is available for avalanching, on such steep slopes. The slope values were divided into five classes (Table 5.2). The slope class (28^0-45^0) is most vulnerable for avalanche occurrence, hence assigned maximum weightage, while slope class $<12^0$ is least vulnerable to avalanche occurrence and hence assigned minimum weightage (Table 5.3).

Table 5.2: Slope classification used for avalanche susceptibility mapping

Class	Explanation
$<12^0$	Avalanching not reported practically.
12^0-28^0	Substantial hazardous avalanches reported in this slope class.
28^0-45^0	Most favourable slope class for avalanche occurrence, most of dangerous avalanches reported in this class

45^0-55^0	Mainly small avalanche reported in this class due to steepness of slope.
$>55^0$	This is the steepest slope class and earth's gravitational force keeps sliding the snow downslope, causing the low intensity avalanching frequently, therefore the snow accumulation is rare and hence danger of large avalanche is also rare.

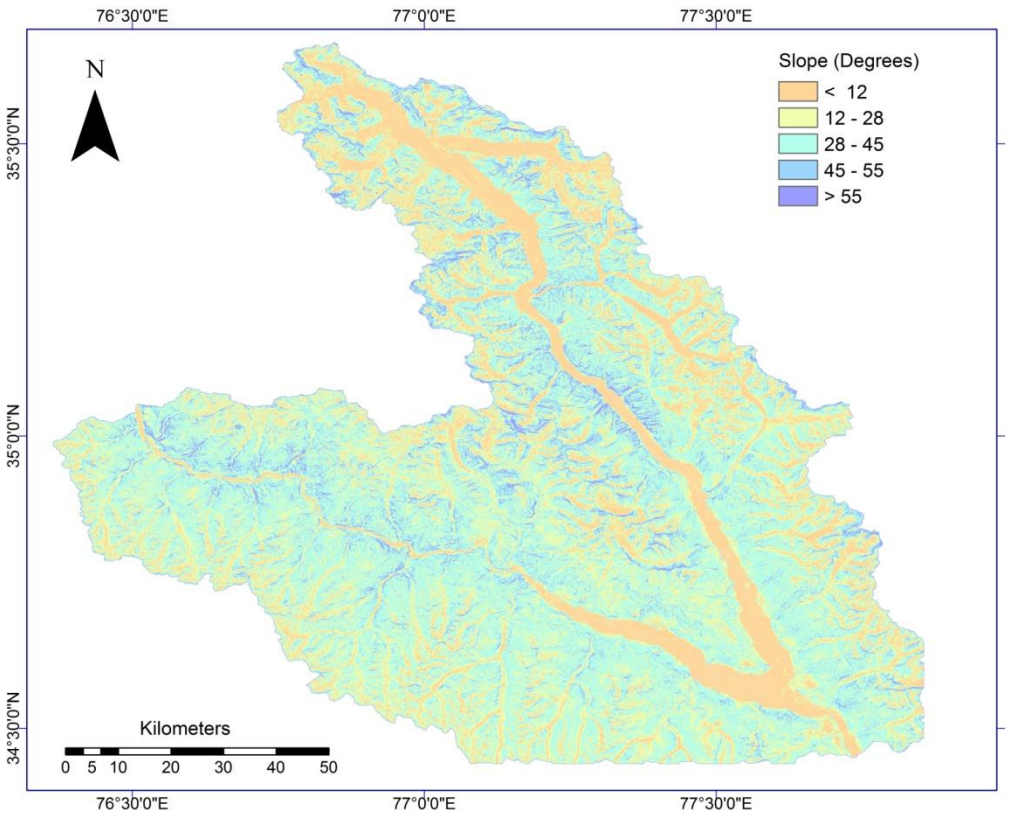

Figure 5.3: Slope layer prepared for avalanche susceptibility mapping

5.3.2 Elevation

The snow avalanche occurrence is not directly related to the elevation factor, however metrological parameters governing snowpack stability such as intensity and type of precipitation, temperature and wind speed, changes with elevation, so elevation is also considered important terrain factor in avalanche

susceptibility mapping. Generally, with the increase of elevation the wind speed also increases, which in turn increase the amount of wind-transported snow. The air temperature decrease with increase in elevation, hence at higher reaches snow remains available for avalanching for longer duration, however at lower elevation snow starts melting with increase in temperature. The snow avalanches are reported mainly between 2700 m to 6000m in Western part of Indian Himalaya (Ganju et al., 2002) and the dangerous avalanches are reported mainly between 5000 m to 5600m altitude range in the upper Himalaya zone (Sharma and Ganju, 2000).

The elevation varies from 2468m to 7709 m in Nubra-Shyok, region. The zone of origin for all dangerous avalanches in the Nubra-Shyok region lies above 5000m (Sharma and Ganju, 2000). The elevation class values were divided into various subclasses (Figure 5.4). The elevation group 5000 m to 5600m is most vulnerable for avalanche occurrence, hence assigned maximum importance while elevation class > 6200m is least vulnerable for avalanche occurrence and hence given minimum importance and other classes were assigned intermediary importance.

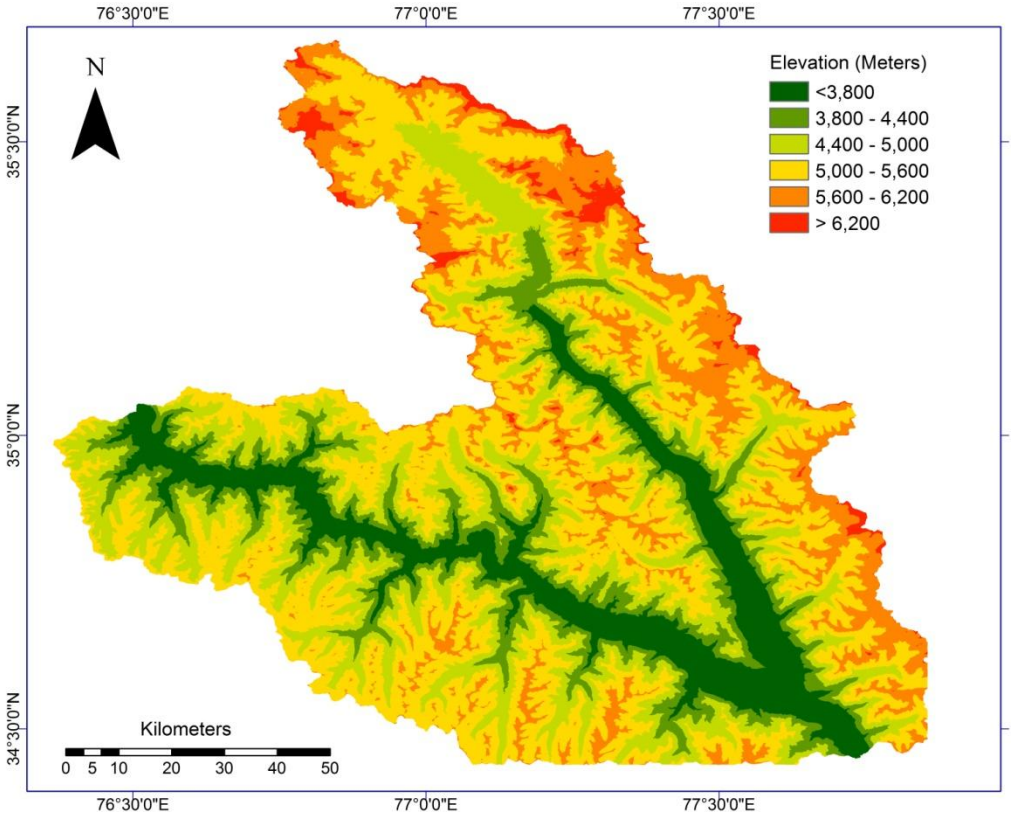

Figure 5.4: Elevation layer prepared for avalanche susceptibility mapping

Table 5.3: Ratings assigned to each class of layer

Layer	**Class**	**Ratings**
Slope	$<12^0$	1
	12^0-28^0	4
	28^0-45^0	9
	45^0-55^0	5
	$> 55^0$	3
Elevation	< 3800	1
	3800-4400	3
	4400-5000	4
	5000-5600	9
	5600-6200	5
	> 6200	2
Aspect	Flat	1

	North	9
	N-E	9
	E	3
	S-E	5
	S	3
	S-W	1
	W	1
	N-W	7
Curvature	Convex	9
	Flat	4
	Concave	1
Land Cover	Snow/Ice	9
	Others (Glacial moraines, Barren, Rocky,)	4

5.3.3 Aspect

The orientation of snow covered slope with respect to the sun has a direct bearing on the snowpack stability. The shaded slopes stay unstable for longer time while the sun facing slope stabilize more quickly in comparison to the shady slopes. The wind keeps on drifting the snow from the wind facing slopes and accumulating the drifted snow on leeward slopes, hence leeward slope are more treacherous in comparison to wind facing slopes. ASTER GDEM was used to produce aspect map for Nubra-Shyok, region, and aspect map was further divided into nine classes (Figure 5.5). Most of the avalanche slopes in Nubra-Shyok region are in northern aspect and these poses danger of snow avalanche during the whole year (Sharma and Ganju, 2000). Hence North-East and North aspect class are more vulnerable to avalanche occurrence, hence these were considered the important aspect classes.

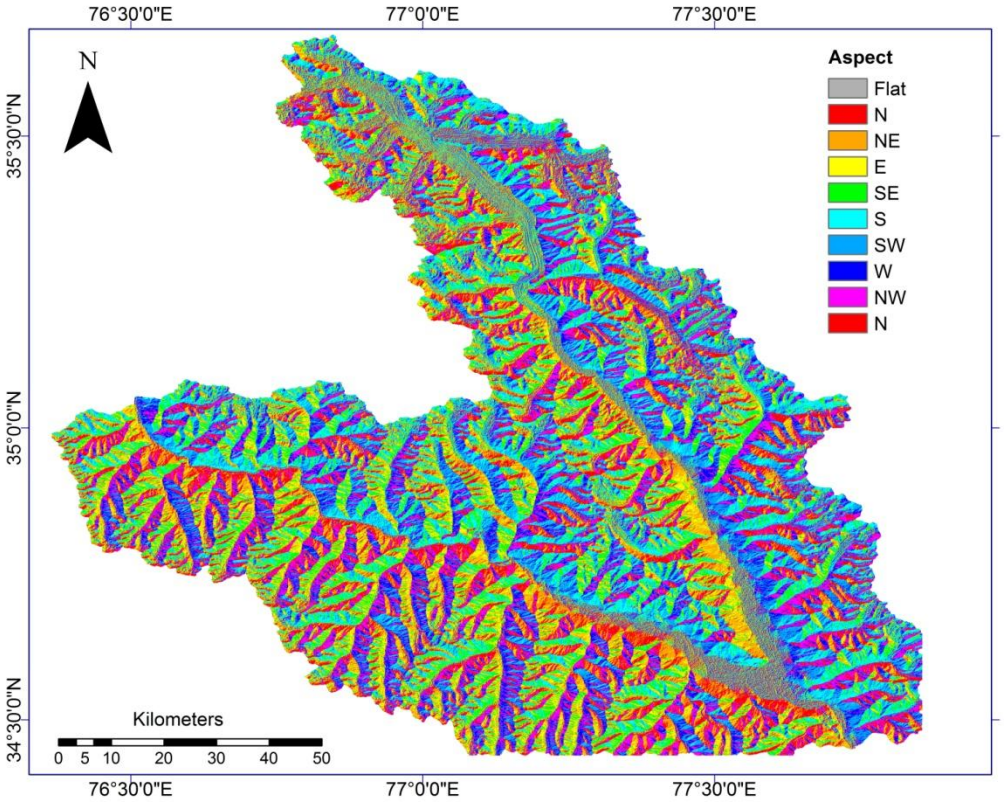

Figure 5.5: Aspect layer prepared for avalanche susceptibility mapping

5.3.4 Curvature

Curvature is also considered as the significant factor in the evaluation of avalanche susceptibility mapping (Maggioni and Gruber, 2003). As concave surface can hold large snow amount, hence snowpack on concave surfaces are more stable than on convex surfaces. Concave surface upkeep the stabilization of snowpack while the snow cover on convex surfaces is more unstable (Nagarajan et. al., 2014). The ASTER GDEM was used to produce the curvature map and curvature map was divided into three different classes: Concave, flat and Convex (Figure 5.6). The convex curvature is more vulnerable to avalanche initiation in comparison to concave surfaces, hence convex curvature class given more weightage than the concave, while the flat curvature class was assigned intermediate importance.

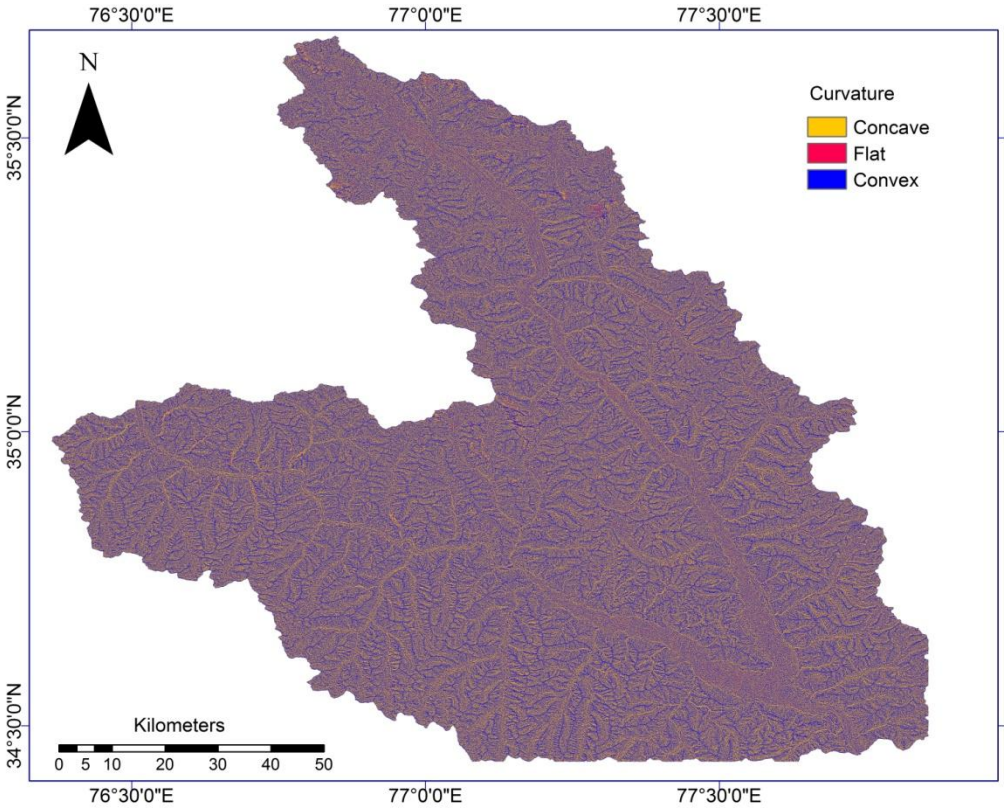

Figure 5.6: Layer of curvature prepared for avalanche susceptibility

5.3.5 Land Cover

Land cover was recognized as one of the important factor among the static terrain factors (Ganju et al., 2002). Good vegetation coverage may anchor the snow on slopes, hence in such areas less amount of snow would be available for avalanching. Avalanches can be anchored by dense forest area (Cioli et. al., 1998). As the upper Himalaya zone are devoid of vegetation and hence land conditions are not supporting to snow avalanches anchorage (Sharma and Ganju, 2000). During field visits, it is observed that there is no such vegetation in the Nubra-Shyok region that can anchor the avalanches, most of the land cover is either snow/ice covered or barren, hence the values of land cover is divided into two classes Snow/Ice and Non-snow including barren, rocky, glacial moraines, etc.) (Figure 5.7). The Snow/Ice class is

assigned the maximum weightage, while the other class was assigned minimum weightage.

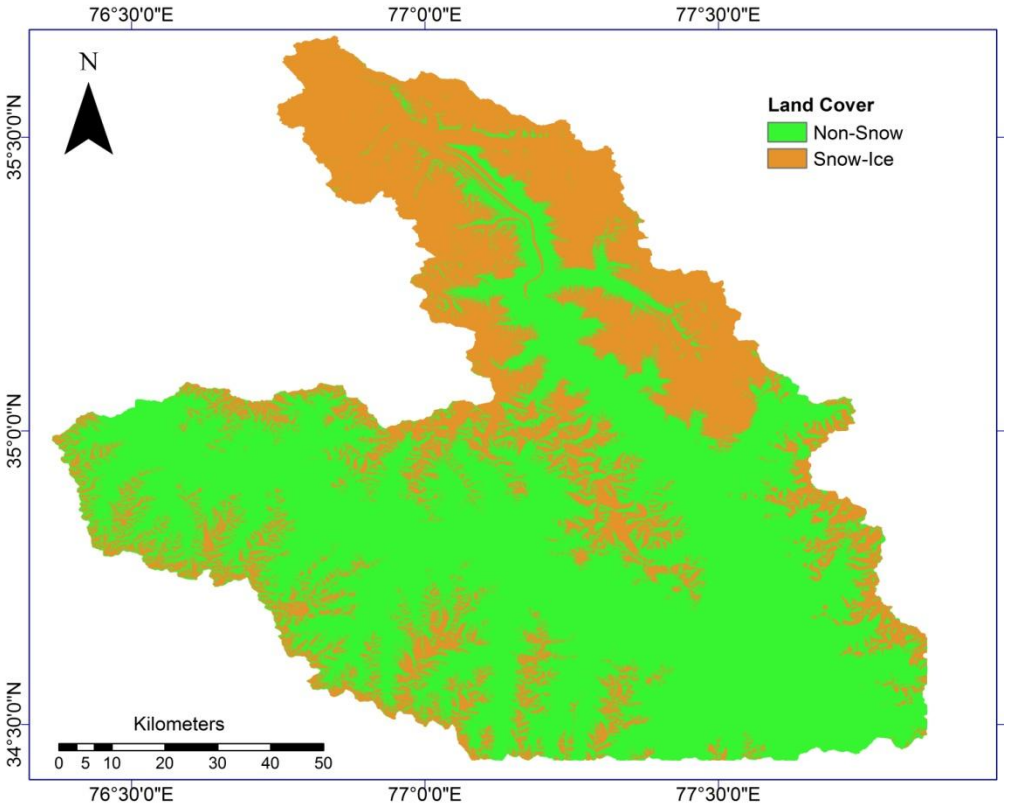

Figure 5.7: Land Cover layer prepared for avalanche susceptibility mapping.

5.4 AHP Model for Avalanche Susceptibility Mapping

AHP model has been used successfully for avalanche hazard studies (Kumar et al., 2016, Nefeslioglu et al., 2013, Seluck 2013, Snehmani et. al., 2014) landslide susceptibility studies (Komac, 2006; Kayastha et al., 2013; Shahabi et al., 2014; Shahabi et al., 2015; Basharat et. al., 2016; Hashim et. al., 2017) debris risk evaluation (Yang et al., 2011) and debris flow susceptibility assessment of (Chen et al. 2015). The prime goal of the present study was delineation of avalanche susceptibility zones of the Nubra-Shyok region, this was achieved by making use of fundamental evaluation factors

such as curvature, aspect, land cover elevation and slope (described in section 5.3). The characteristics of every class of each layer and its judgement of expert was used to assess and give the internal rating.

The weight value of each class in the GIS layer is calculated using the pairwise comparison matrix. The internal rating assigned to each class of every layer (Table 5.3) based on the engineering knowledge of the class in consonance with the Satty's (1980) scale, was used to prepare the comparison matrix to calculate the weight value of each class of all five layers used in present study (Table 5.4). The weight value of all five GIS layers were calculated by pair wise comparison matrix following AHP model (Table 5.5). In this work, value of consistency ratio obtained for every estimated weight value of each class and every layer is less than 0.10, which is well within in the limit as proposed by Saaty (1908).

Table 5.4: Pairwise comparision matrix for each class of every layer

Layer/Class							**Weight**
Slope							
	12	12-28	28-45	45-55	55		
12	1	1/4	1/9	1/5	1/3		0.0343
12-28	4	1	1/9	1/5	4		0.1073
28-45	9	9	1	9	9		0.5767
45-55	5	5	1/9	1	5		0.1834
55	3	4	1/9	1/5	1		0.0983
CR	0.055						
Elevation							
	<3800	3800-4400	4400-5000	5000-5600	5600-6200	>6200	
<3800	1	1/3	1/4	1/9	1/5	1/2	0.0311
3800-4400	3	1	1/4	1/9	1/5	3	0.0692
4400-5000	4	4	1	1/9	1/5	4	0.1169
5000-5600	9	9	9	1	9	9	0.5467

5600-6200	5	5	5	1/9	1	5				0.1944
>6200	2	1/3	1/4	1/9	1/5	1				0.0418
CR	0.043									
Aspect										
	Flat	N	N-E	E	S-E	S	S-W	W	N-W	
Flat	1	1/9	1/9	1/3	1/5	1/3	1	1	1/7	0.0213
N	9	1	1	9	9	9	9	9	9	0.3042
N-E	9	1	1	9	9	9	9	9	9	0.3042
E	3	1/9	1/9	1	1/5	1	3	3	1/7	0.0430
S-E	5	1/9	1/9	5	1	5	5	5	1/7	0.0904
S	3	1/9	1/9	1	1	1	3	3	1/7	0.0462
S-W	1	1/9	1/9	1/3	1/3	1/5	1	1	1/7	0.0214
W	1	1/9	1/9	1/3	1/3	1/5	1/3	1	1/7	0.0195
N-W	7	1/9	1/9	7	7	7	7	7	1	0.1497
CR	0.017									
Curvature										
	Concave	Flat	Convex							
Concave	1	1/4	1/9							0.06224
Flat	4	1	1/9							0.15806
Convex	9	9	1							0.7797
CR	0.035									
Land Cover										
	Snow/Ice	Others								
Snow/Ice	1	9								0.9
Others	1/9	1								0.1
CR	0.025									

Table 5.5: Pair wise comparison matrix for weight values of all five layers.

Layer	Land Cover	Curvature	Slope	Aspect	Elevation	Weight value
Land cover	1	2	7	2	5	0.05
Curvature	1/2	1	4	1	2	0.12

Slope	1/7	1/4	1	1/5	1/2	0.47
Aspect	1/2	1	5	1	2	0.11
Elevation	1/5	1/2	2	1/2	1	0.25
CR	0.0012					

The avalanche susceptibility map for Nubra-Shyok region was produced using weight value of each layer and every class of layer in equation (5.3).

$$\mathrm{ASI} = \sum_{i=1}^{n} (R_i \times W_i) \qquad (5.3)$$

Where, ASI stands for avalanche susceptibility index map, R_i represents the ratings of each class of the factors, and W_i is used for representing the weight values for each avalanche occurrence factors. The avalanche susceptibility index map was divided into five susceptible zones (Table 5.6 and Figure 5.8).

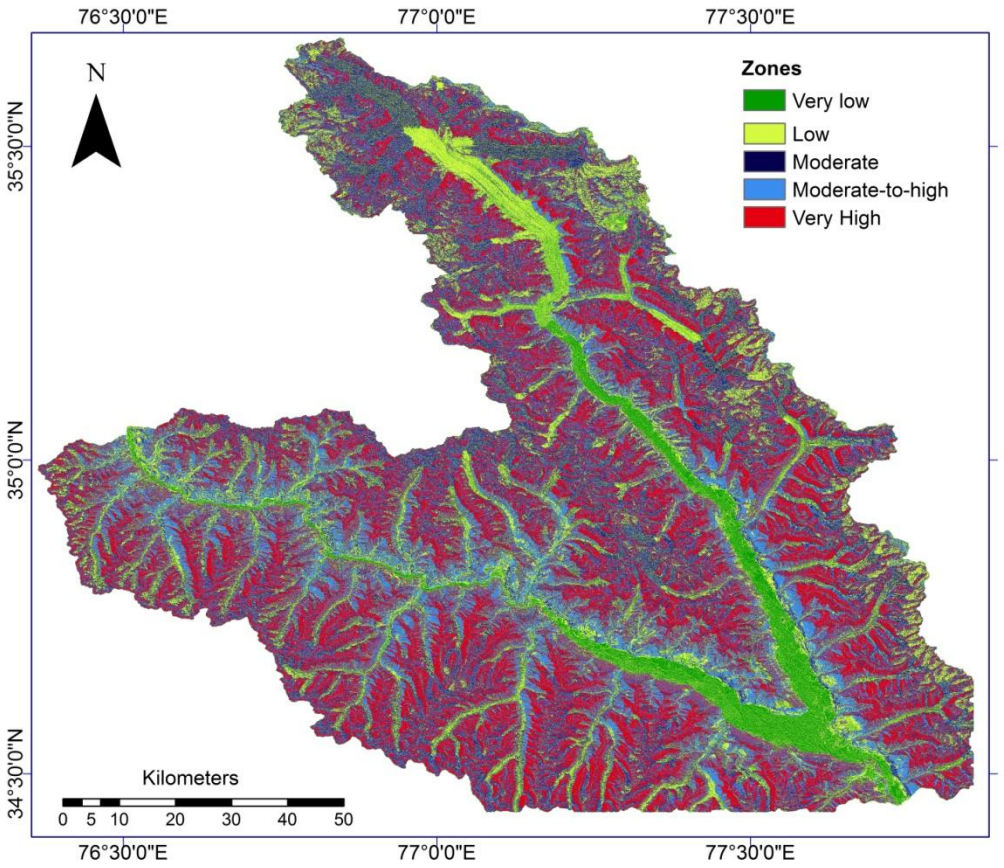

Figure 5.8: Avalanche susceptibility map of Nubra-Shyok region.

5.5 Results and discussion

The calculated weight value of the slope factor was 0.47, which is found most significant factor for avalanche occurrence. The other major significant avalanche occurrence factors were found elevation with weight value 0.25. The weight value of land cover factor was found 0.05, which receives the least importance. The weight values of aspect and curvature were 0.11 and 0.12, respectively and both these factors received approximately equal and intermediary degree of importance. The weight values of each class of GIS layers are given in, Table 5.4, while the weight value of each GIS layer is given in Table 5.5.

The land cover is the least significant factor while slope is the most significant terrain factor for avalanche occurrence, in Nubra-Shyok region. Hence, least weightage was assigned to the land cover factor and highest weightage was assigned to slope factor. The slope class 28^0-45^0 is most vulnerable to avalanche initiation (Table 5.3) in the study region and highest rating was assigned to this slope class. The snow/ice land cover class assigned the highest value of rating while other class which includes moraines, rocky, barren, etc. assigned the least rating. The second dominate terrain factor for avalanche occurrence in Nubra-Shyok region considered Elevation. The maximum occurrence of avalanches was observed in the elevation range of 5000 m to 5600 m (Sharma and Ganju, 2000), hence highest rating was given to this elevation class. Curvature and aspect contributing more or less equally to the avalanche phenomena in the Nubra-Shyok region. The concave surfaces retard the avalanche initiations while convex surfaces help in avalanche formation. Hence, concave curvature class were given least rating while the convex curvature class given highest rating. Northeast and North slopes are more vulnerable to avalanches in the Nubra-Shyok basin, hence highest rating was assigned.

Nubra-Shyok region avalanche susceptibility map was divided into five zones: - (i) Very High (ii) Moderate-to-High (iii) Moderate (iv) Low (v) Very Low. The spatial coverage of these five avalanche susceptible zones are 27.5%, 28.0%, 19.0%, 20.0%, and 4.8%, respectively (Table 5.6).

Table 5.6: Area of various avalanche susceptibility zones of Nubra-Shyok region.

Avalanche Susceptibility	**Area (Km^2)**	**%**
Very low	461.70	4.8
Low	1923.76	20
Moderate	1827.57	19
Moderate-to-high	2693.26	28
Very high	2645.17	27.5

5.6 Validation of Avalanche Susceptibility Map

Result validation is an essential step in the generation of an avalanche susceptibility map and to determine its prediction ability. The prediction ability of an avalanche susceptibility is generally estimated by using the information that is not used in the building process of map. An alternative to the above is the threshold calculations, is the ROC value and the AUC (Zweig and Campbell1993). It is very popular statistical assessment methods, especially for natural mass movements such as landslides. The results of this study was verified using the ROC-AUC method. The ROC curve is a graphical representation of the trade-off between false negative (sensitivity) and false positive rates (specificity) for every possible cut-off. An ideal Area under the curve value is 1, and the value less than 0.5 is considered as worse, while the values in the range 0.5-1 is considered good for acceptance (Hanley et. al., 1983). In the this work AUC value 0.9112 was obtained (Figure 5.9). The results validation process shows

that 91.12% avalanche pixels were properly categorized in the avalanche susceptibility map and these results are acceptable.

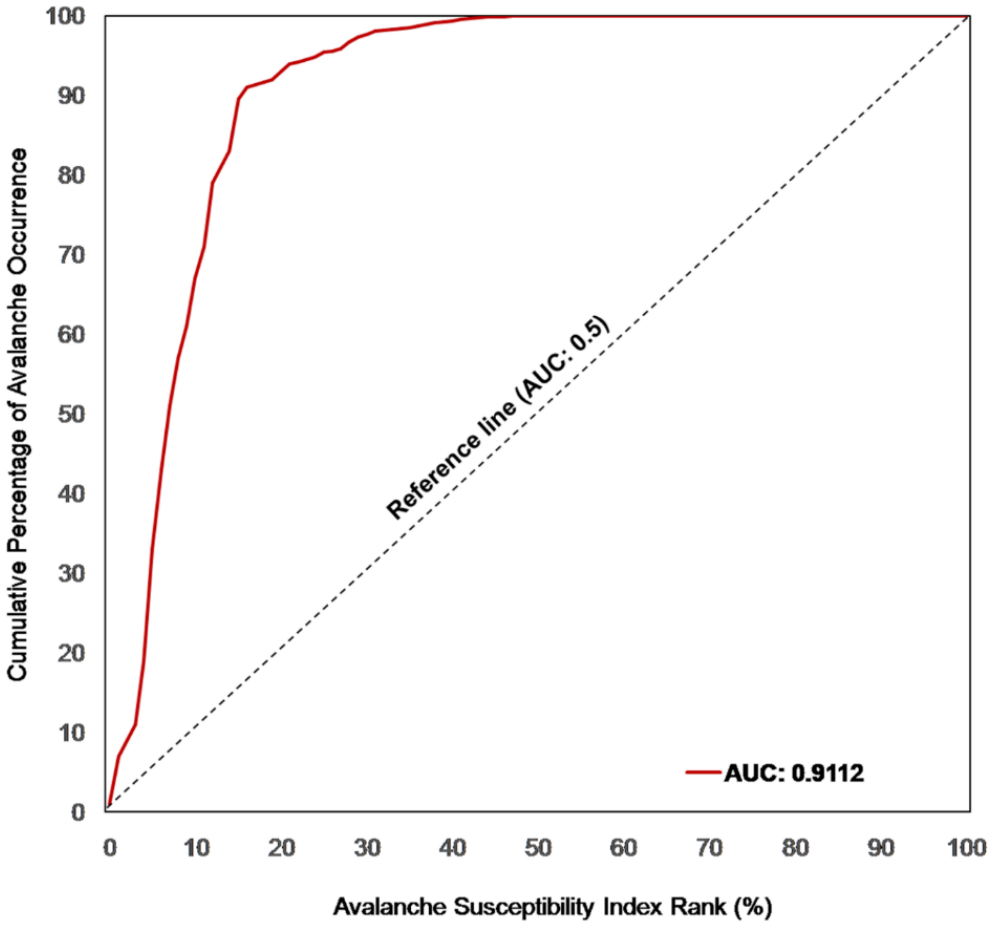

Figure 5.9: Result validation of avalanche susceptibility map using ROC-AUC technique.

5.7 Conclusions

In this work avalanche inventory map was prepared, creation of avalanche occurrence static terrain factors and their analysis and contribution to avalanche susceptibility is also evaluated. The confirmation of results is also carried out. Five numbers of static terrain factors responsible for avalanche occurrences, such as curvature, elevation aspect, land cover and slope, were used as an input data generation of avalanche susceptibility map

for Nubra-Shyok region. Depending upon the significance and availability, these terrain factors were analyzed very judiciously. The avalanche susceptibility map of Nubra-Shyok region demonstrate that 27.5% of the area is in very high susceptibility zone and only 4.8% of the the area is in very low susceptibility zone. In the validation process ROC-AUC value was found 0.9112 and hence, this means avalanche susceptibility map of Nubra-Shyok region produced in this study is 91.12 % accurate. The results of this study confirms that GIS-based AHP method is appropriate to identify and locate the avalanche prone areas. This avalanche susceptibility map may be used by the policy makers for better planning of infrastructure growth in the region and safe movement across the region.

CHAPTER 6

IMPLICATIONS OF EARTHQUAKE ACTIVITY ON SNOW AVALANCHE OCCURENCES

6.1 Introduction

Earthquakes have caused destruction to infrastructure and human lives across the globe. The impact of earthquakes is more pronounced in the hilly regions with a possibility of slope failure. The landslide, rock fall, liquefaction etc. are the prominent natural hazard related to earthquakes in hilly terrains. One of such natural hazards related to earthquake is snow avalanches in the snow bound mountainous regions. The occurrence of avalanches mainly depends upon the terrain characteristics, metrological and snowpack conditions. The snow cover over a slope can be destabilized by several external triggering factors; out of which earthquake is one of the most common external triggering factors for highly mountainous snow covered areas with high seismicity (Podolskiy et al., 2010 (a), 2010(b)). Strong ground motion generated as a result of earthquakes can persuade different disastrous geological processes including slope failure phenomena such as Landslide, rock fall, rockslide, debris flow, etc (Hewitt et al., 2008) and avalanche is a process among these in snow cover mountainous terrain (Chernous et al., 2004, Podoloskiy et al. 2010 a, b, Schaer, 2012). Huge Life and property loss may occur, when an unstable snowpack is disturbed by an earthquake, resulting catastrophic avalanches (LaChapelle, 1968). The Huascaran avalanche in 1970, is the most devastating example of an earthquake-induced

avalanche that killed thousands of people (Chernous et al. 2002). Several avalanches were triggered by Gorkha earthquake in Nepal in 2015 and these earthquake induced avalanches engulfed the lives of hundreds of peoples.

In the present work, earthquake induced snow avalanches are studied in Nubra-Shyok region. Thousands of people most of them were army personals have been killed in this region by snow avalanches. Around the Nubra-Shyok region, casualties due to avalanches were not only happened in India but also in the adjacent countries like Pakistan (Pandit and Mishra, 2014). More than one hundred peoples were engulfed by the 2012 Gayari avalanche in Siachen Glacier. Snow avalanches and severe climatic conditions are responsible for around three-fourth of total deaths happened in Nubra-Shyok region (Rajinder et al., 2017b). Owing to high seismic activity and avalanche susceptibility in Nubra-Shyok region, the concern about earthquake triggered avalanches has increased in last few decades. Moreover, only single study has been carried out by Singh and Ganju (2002) in NW Himalaya, India about earthquake triggered snow avalanches and the results of this study were discussed by Podolisky et al. (2010a) and it feels that this region need more studies on earthquake triggered avalanches.

In the present work an effort has been made to investigate induced avalanches triggered by passive seismic activity within the distance of ~638 km from induced avalanches for Nubra-Shyok region. The spatial distribution of seismogenic avalanches, correlation of earthquake magnitude with avalanches and lower bound limit of earthquake magnitude responsible for triggering an avalanche is examined in the present work.

6.2. Study Area and Data Used

The study area has thousands of glaciers with varying lengths, Siachen glacier with length around 74 Km is the largest among them. Most of Himalayan glacier are fed by snow fall from the moisture laden South West Indian Monsoon (SWIM), while the Nubra-Shyok, region receives the snowfall from mid-latitude westslries during winter season. Most of the snow fall received by the study region at high altitudes during winter season and this snow mass persist for longer duration due to extended winter season and weak thaw freeze cycle. High relief along with steep slopes exists in the study region, which cause huge number of slope failures of large magnitude (Dortch et al. 2009). In the last thirty years, climate change in the North West Himalaya responsible for accelerating the natural calamities like cloud bursts, snow avalanches, landslides and flood (Bhutiyani et al., 2013).

Nubra-Shyok region is tectonically active and its major tectonic unit is dextral strike slip Karakoram fault (KF) that divide rocks of Karakoram and Ladakh terrains and it passes through the main trunk of Siachen glacier. The Karakoram Fault is seismically active and mainly responsible for shallow earthquakes in the present study region (Kana et al., 2018, Imsong et al., 2017, Hazarika et al., 2017, Rajinder et al., 2016). The tectonic activity can also be verified from attenuation relation of form $Qc(f) = Qo\ f^{n}$; $(121\pm7.2)f^{(1.0\pm0.04)}$ i.e. frequency dependent coda wave quality factor relationship established for Nubra-Shyok region. Low Qo (<200) and high n (>0.8) values reveal that present study region is tectonically active and comprises local heterogeneities (Rajinder et al., 2017a). The source parameters of local earthquakes calculated for the study region also in the range of earthquake source parameters of

seismically active parts of Himalaya (Rajinder et al., 2015). The local seismicity in the present study region is shallow focus and mainly occurred along the Karakoram Fault (Rajinder et al., 2016). Due to tectonic activity along with heavily glacierized, this region is very much vulnerable to the snow avalanches. The susceptibility map of snow avalanche prepared for Nubra-Shyok region by using static terrain parameters such as: land cover, slope, curvature, aspect and elevation also shows that this region is highly susceptible to avalanches (Rajinder et al., 2017b).

The earthquakes occurred within the radius of ~600 km from Nubra-Shyok region is utilized for the present work. Earthquakes hypocentral parameters reported by India Meteorological Department (IMD), other published work and computed by using data of local broad band seismic network established in Nubra region, India is employed for this work. The earthquake data of magnitude $1.7 \leq M_w \leq 6.0$ occurred during the period of 2002-2012 in Nurbra-Shyok region; reported by IMD, SASE and published work is implemented to study seismogenic snow avalanches in this region. The parameters of avalanche occurrence reported by Snow and Avalanche Study Establishment (SASE), Chandigarh, India for a decade (i.e. year 2002-2012) is incorporated for this work and parameter are given in, Table 6.1.

Table 6.1: Earthquake and avalanche parameters used for magnitude distance relation.

	Earthquake Parameters						Avalanche Parameters		
Sr. No.	**Date dd-mm-yyyy**	**Time hh:mm:ss**	**Lat (Deg.)**	**Long (Deg.)**	**Depth (km)**	**Mag. (M_w)**	**Lat. (Deg)**	**Long. (Deg.)**	**Distance (km)**
1	01-04-2002	10:53:25	34.75	76.38	10	2.1	35.11	77.14	80
2	07-04-2002	20:41:17.1	35.09	76.04	33	3.3	35.06	77.21	107
3	16-04-2002	16:00:5.6	31.10	77.46	35	2.9	34.49	76.86	381
4	16-04-2002	16:08:14	37.58	72.86	33	3.6	34.49	76.86	497
5	04-06-2002	18:32:6.3	35.10	75.74	33	3.6	35.10	76.92	107
6	04-06-2002	18:32:6.3	35.10	75.74	33	3.6	35.10	76.92	107
7	23-12-2002	15:20:17.2	36.28	76.61	33	3.8	35.12	77.16	138
8	23-12-2002	1:58:17.6	35.98	74.68	96	3.9	35.12	77.15	243
9	06-01-2003	23:21:13	32.83	76.07	33	2.9	35.18	77.04	276
10	10-01-2003	2:36:1.5	33.00	76.25	26	3.2	35.12	77.15	250
11	30-01-2003	10:41:15.8	36.21	76.43	9	4.2	34.78	76.73	161
12	30-01-2003	10:41:15.8	36.21	76.43	9	4.2	34.75	76.72	164
13	03-02-2003	23:2:23.7	31.87	76.86	12	2.8	35.17	77.11	367
14	18-02-2003	16:17:35.3	37.81	74.09	15	3.6	34.82	76.75	409
15	21-02-2003	10:46:33	35.21	76.06	33	3.8	34.83	76.75	76
16	02-03-2003	15:23:32.4	33.56	75.64	33	4.3	35.14	77.19	226
17	03-03-2003	16:01:10.9	33.76	77.52	38	2.0	34.96	76.96	143
18	03-03-2003	20:37:52.9	33.64	72.66	33	3.9	34.93	76.86	412
19	03-03-2003	20:37:52.9	33.64	72.66	33	3.9	34.93	76.86	412
20	05-03-2003	18:20:55.6	33.19	76.27	10	2.6	35.05	77.14	222
21	09-03-2003	23:38:24.8	33.44	77.6	10	3.6	35.18	77.11	54
22	09-03-2003	22:18:21.6	35.59	77.42	10	1.9	35.18	77.11	54
23	15-03-2003	11:53:38.1	35.31	75.54	33	3.6	34.81	76.80	128
24	22-03-2003	1:46:22.5	35.87	74.99	33	4.0	35.19	77.06	202
25	06-04-2003	3:43:31.8	37.78	72.93	200	3.6	34.76	76.73	479
26	16-04-2003	13:54:52.9	34.08	76.48	33	3.6	34.80	76.71	83
27	21-04-2003	23:50:31.8	31.42	77.70	4	3.0	35.04	77.14	406
28	27-04-2003	19:17:22.3	32.72	76.78	5	2.9	34.80	76.71	231
29	29-04-2003	9:35:54.7	32.9	76.73	33	2.6	34.82	76.76	214
30	11-05-2003	16:34:52.3	33.12	75.71	0	4.6	35.04	77.18	252
31	11-05-2003	16:34:52.3	33.12	75.71	33	4.6	35.04	77.18	252
32	12-05-2003	3:48:29.8	31.64	77.02	10	2.9	35.13	77.18	388
33	12-05-2003	3:48:29.8	31.64	77.02	10	2.9	35.13	77.18	388

34	13-05-2003	19:30:44.6	37.22	79.09	90	4.8	35.11	77.11	295
35	13-05-2003	19:30:44.6	37.22	79.09	90	4.8	35.11	77.11	295
36	07-09-2004	4:1:1.6	36.16	78.12	15	3.9	34.82	76.74	195
37	14-11-2004	9:10:26.4	36.60	72.05	86	4.8	35.18	77.08	480
38	14-12-2004	16:41:57.9	32.72	74.53	10	2.7	34.50	76.83	290
39	09-02-2005	15:55:55.8	34.79	73.19	96	4.2	34.76	76.74	324
40	11-02-2005	16:55:33.8	35.86	73.18	378	3.6	34.94	76.93	355
41	14-02-2005	21:00:42.6	37.46	73.38	15	4.2	34.94	76.94	425
42	15-02-2005	21:48:36.5	31.54	74.85	05	3.8	35.05	77.05	440
43	20-02-2005	8:18:54.6	34.25	74.45	15	3.7	35.01	76.96	244
44	26-02-2005	18:41:9.2	33.18	76.83	15	2.8	34.95	76.92	196
45	08-04-2005	17:7:40.2	31.62	76.88	10	3.2	34.96	76.94	371
46	14-04-2005	8:25:46.7	32.80	76.36	15	2.5	35.18	77.17	275
47	14-04-2005	7:11:27	32.41	76.31	10	4.7	35.18	77.12	316
48	18-04-2005	20:10:33.2	32.65	76.29	06	4.0	35.02	76.99	271
49	19-04-2005	16:20:3.2	34.70	73.63	37	3.2	35.18	77.14	324
50	20-04-2005	7:5:21.9	31.07	74.32	20	3.3	35.00	76.97	502
51	01-05-2005	13:4:11.4	32.63	75.91	10	3.0	35.19	77.05	303
52	07-05-2005	6:27:58.5	33.54	73.20	10	3.9	35.01	76.99	384
53	23-05-2005	5:43:30.8	37.41	72.96	33	3.3	35.15	77.09	447
54	23-05-2005	00:25:21.6	31.15	78.59	10	3.6	35.14	77.08	465
55	03-06-2005	20:36:51	32.20	78.04	20	2.5	34.49	76.87	276
56	06-06-2005	21:55:18.4	32.28	75.72	33	2.8	34.98	77.06	324
57	20-06-2005	22:52:28.5	36.13	77.78	10	3.6	35.02	77.06	140
58	25-06-2005	12:21:10.6	32.90	75.87	10	2.2	35.05	77.05	262
59	14-07-2005	2:38:22.5	36.51	77.10	182	4.1	35.02	76.98	166
60	24-07-2005	00:49:2.4	37.16	78.32	10	3.6	35.18	77.07	247
61	04-08-2005	16:17:21.7	32.41	76.42	10	2.6	35.17	77.08	313
62	15-11-2005	21:55:51.1	34.62	73.54	10	3.8	35.04	77.05	324
63	27-11-2005	12:59:30.8	34.98	72.77	10	4.6	34.79	76.72	361
64	28-11-2005	7:39:52.8	34.46	73.22	10	3.6	34.97	76.92	343
65	30-11-2005	4:27:13.1	34.53	73.34	10	3.3	35.01	76.98	337
66	01-12-2005	15:38:27.2	34.91	73.01	10	5.0	35.02	76.98	362
67	03-12-2005	5:18:38	34.86	73.17	10	3.8	35.02	76.98	348
68	28-12-2005	8:33:48	36.00	75.16	37	3.7	34.97	76.93	197
69	28-12-2005	22:04:28.5	34.88	73.23	10	4.9	34.96	76.93	337
70	28-12-2005	20:22:0.2	34.87	72.76	10	4.2	34.96	76.92	379
71	04-01-2006	12:4:38.2	34.51	72.84	10	4.2	34.94	76.91	375
72	04-01-2006	12:31:11.9	34.66	72.75	--	4.1	35.04	77.05	394

73	07-01-2006	12:32:30.8	34.21	73.33	10	3.8	34.95	76.93	339
74	07-01-2006	7:24:43.5	34.49	72.38	65	3.9	34.97	76.92	418
75	08-01-2006	3:23:11.1	34.68	72.37	10	3.5	35.01	76.96	420
76	03-02-2006	9:59:54.2	34.16	74.58	33	2.9	34.84	76.80	217
77	04-02-2006	2:53:37.2	32.08	77.11	15	2.5	34.81	76.79	305
78	07-02-2006	13:54:57.9	34.74	72.52	10	3.4	34.80	76.76	387
79	09-02-2006	19:59:18	35.25	73.33	10	3.4	34.81	76.81	320
80	13-02-2006	2:00:22.4	34.81	72.89	10	3.6	34.80	76.80	356
81	13-02-2006	6:59:20.6	35.22	72.06	10	3.3	34.80	76.80	434
82	15-02-2006	3:7:33.5	34.23	78.51	10	2.6	34.95	76.95	164
83	19-02-2006	23:4:30.6	36.40	74.78	33	3.0	35.11	77.22	263
84	19-02-2006	18:8:18.8	35.00	73.10	275	3.0	35.14	77.22	375
85	20-02-2006	10:9:41.3	34.15	73.61	33	2.8	35.19	77.05	335
86	21-02-2006	9:23:51.6	31.91	76.99	8	2.6	34.97	76.95	340
87	21-02-2006	14:3:4.6	34.84	72.83	20	2.9	34.97	76.95	375
88	22-02-2006	10:25:47.6	35.00	73.44	10	3.3	35.17	77.04	328
89	22-02-2006	22:59:35.2	34.80	73.00	10	4.0	35.24	77.04	371
90	22-02-2006	7:2:38.1	34.49	72.29	10	3.2	35.17	77.04	440
91	23-02-2006	18:13:50.9	32.90	75.85	20	2.6	34.81	76.76	228
92	23-02-2006	19:23:4.2	35.97	73.59	38	3.9	34.94	76.94	324
93	25-02-2006	14:11:16.7	33.99	75.14	30	3.1	34.80	76.80	177
94	25-02-2006	0:1:7.7	33.50	75.54	10	2.3	34.80	76.80	185
95	26-02-2006	13:4:14.5	31.42	73.52	26	3.2	34.80	76.76	482
96	27-02-2006	11:58:46.2	34.58	73.19	10	3.7	35.19	77.05	358
97	02-03-2006	12:46:25.9	34.48	73.38	10	4.4	34.47	76.87	320
98	06-03-2006	17:4:58.6	36.21	75.13	38	3.4	34.49	76.80	244
99	09-03-2006	9:51:0.1	32.87	76.55	33	2.9	34.96	76.92	235
100	13-03-2006	18:12:20	34.74	73.56	20	3.2	35.04	77.05	320
101	24-03-2006	3:37:1.2	34.26	73.48	10	3.7	35.01	76.96	329
102	26-03-2006	6:59:8.2	34.67	73.04	10	3.8	35.07	77.19	381
103	27-03-2006	1:47:4.2	32.97	76.44	10	2.9	34.98	77.06	230
104	03-04-2006	20:43:3.3	34.13	73.41	10	3.6	34.48	76.86	319
105	04-04-2006	11:40:8.3	33.69	75.78	33	3.7	34.48	76.86	132
106	04-04-2006	9:12:24.2	34.56	72.76	10	4.6	34.48	76.86	376
107	10-04-2006	2:23:1.8	34.72	72.97	10	3.9	34.79	76.79	349
108	14-04-2006	15:19:5.6	34.83	72.74	10	3.4	35.05	77.05	393
109	15-04-2006	11:51:19.3	34.44	73.74	10	3.3	34.97	76.93	298
110	17-04-2006	16:12:38.3	37.58	72.14	33	5.0	35.01	76.98	519
111	21-04-2006	23:20:55.4	32.60	76.60	33	3.8	34.47	76.87	209

112	21-04-2006	23:20:55.4	32.60	76.60	33	3.8	35.12	77.16	285
113	23-04-2006	20:36:44.2	34.69	73.04	33	3.1	34.96	76.92	355
114	05-05-2006	8:14:26.5	34.58	73.44	10	3.4	34.81	76.80	308
115	09-05-2006	13:30:22	32.64	76.56	10	4.3	35.05	77.05	271
116	10-05-2006	14:42:51.9	33.01	76.31	25	3.0	34.47	76.87	171
117	10-05-2006	14:42:51.9	33.01	76.31	25	3.0	35.01	76.99	231
118	10-05-2006	4:51:4.6	35.05	73.66	33	3.4	34.48	76.78	292
119	24-05-2006	19:19:14.9	37.63	72.55	326	3.8	35.04	77.04	494
120	01-06-2006	13:41:43.6	34.04	72.58	10	3.5	34.98	76.93	412
121	19-06-2006	8:32:47.3	34.46	72.89	33	3.4	34.49	76.87	364
122	30-06-2006	1:35:45.7	36.35	72.3	33	4.3	34.82	76.75	437
123	01-07-2006	15:35:31.3	34.62	72.85	10	3.4	34.47	76.88	369
124	03-07-2006	23:0:7.2	36.00	73.01	10	3.4	34.49	76.87	388
125	06-07-2006	19:27:27.9	34.54	72.03	38	3.3	35.06	77.09	465
126	08-07-2006	13:31:22.8	35.21	73.50	33	4.6	34.48	76.86	317
127	09-07-2006	3:40:54.6	32.67	76.18	4	2.7	34.97	76.92	264
128	17-07-2006	2:9:8.8	31.68	78.31	15	2.8	34.48	76.86	339
129	01-08-2006	17:54:46.4	35.17	74.07	10	3.6	34.48	76.89	269
130	06-12-2006	14:36:9.8	34.21	73.39	10	3.0	34.96	76.92	334
131	02-03-2007	17:24:16.9	35.13	72.94	10	3.0	34.83	76.78	352
132	04-03-2007	17:44:15.5	35.14	72.57	30	3.9	34.97	76.93	397
133	10-03-2007	18:18:10.6	32.38	76.56	10	2.6	35.05	77.05	300
134	23-03-2007	4:51:16.8	33.40	75.26	10	2.5	35.01	76.99	239
135	08-06-2007	15:29:25.5	34.48	73.29	15	4.5	34.50	76.85	326
136	09-07-2007	20:49:1.5	36.91	73.05	10	3.9	34.50	76.84	434
137	12-01-2008	1:5:13.1	35.97	75.23	37	3.5	35.18	77.15	195
138	20-01-2008	7:54:22.2	32.38	76.45	10	2.6	35.20	77.06	318
139	07-02-2008	18:01:50.6	34.39	74.10	59	3.1	34.81	76.77	249
140	16-02-2008	18:19:52.1	38.00	74.21	33	3.8	34.88	76.77	415
141	19-02-2008	22:18:36	33.11	76.18	34	2.3	34.80	76.76	196
142	20-02-2008	2:36:4.5	33.88	74.31	37	3.6	34.76	76.71	241
143	23-02-2008	4:15:17.6	34.02	76.91	33	2.9	35.03	77.21	115
144	24-02-2008	19:7:23.9	31.36	73.77	10	3.3	34.92	76.75	483
145	28-02-2008	21:49:42.3	37.51	72.35	137	4.4	34.75	76.73	498
146	11-03-2008	6:13:38.3	34.35	74.20	47	4.1	34.50	76.84	242
147	02-04-2008	20:43:28.2	36.94	74.00	33	3.4	35.14	77.09	342
148	13-04-2008	10:45:2.6	32.60	76.38	10	3.5	34.83	76.77	250
149	21-04-2008	10:38:20.6	34.34	72.54	10	3.2	35.14	77.18	433
150	23-04-2008	6:27:1	33.31	76.19	10	3.2	35.05	77.05	208

151	25-04-2008	6:40:59.7	31.89	77.29	33	3.5	35.08	77.21	355
152	26-04-2008	17:31:40.2	33.65	72.04	10	3.3	34.80	76.72	449
153	31-05-2008	5:15:36	32.96	75.69	10	3.6	35.19	77.83	317
154	10-12-2008	16:25:33.1	33.32	77.28	10	3	34.47	76.86	134
155	21-12-2008	5:25:10	35.71	73.07	96	4.6	35.01	77.09	372
156	31-12-2008	15:46:23.6	31.93	79.76	33	3.7	35.03	77.01	428
157	14-01-2009	12:47:3.2	32.93	76.19	10	2.8	35.11	77.12	256
158	26-01-2009	17:50:42.1	33.95	76.20	10	2.3	35.01	76.97	138
159	26-01-2009	16:00:30.9	32.99	75.97	10	3.2	35.02	76.98	244
160	27-01-2009	6:6:10.6	36.09	76.68	33	4.0	35.09	77.12	118
161	08-02-2009	14:33:11.9	34.50	73.10	10	4.4	35.11	77.22	382
162	12-02-2009	2:12:20.5	31.57	77.43	18	3.2	35.09	77.21	391
163	15-02-2009	23:27:50.3	37.58	76.65	33	3.5	34.83	76.77	306
164	25-02-2009	4:4:21.5	30.73	79.71	10	3.5	34.81	76.77	530
165	27-02-2009	3:13:57.4	37.93	73.01	33	3.5	34.97	76.93	481
166	03-03-2009	1:10:11.8	33.98	78.60	10	3.2	35.09	77.22	177
167	04-03-2009	16:48:22	36.60	77.49	96	3.7	34.94	76.95	191
168	12-03-2009	16:21:36.1	32.49	76.36	10	3.6	34.79	76.76	258
169	13-03-2009	00:34:18.5	36.85	76.63	10	3.4	34.96	76.92	212
170	15-03-2009	9:14:17.3	32.38	76.63	10	3.8	34.76	76.73	264
171	18-03-2009	12:44:32.3	32.03	75.67	10	3.1	35.10	77.10	366
172	19-03-2009	5:24:39.4	34.43	73.50	10	4.0	35.02	77.05	331
173	20-03-2009	4:35:22.9	35.24	72.05	10	4.1	35.12	77.16	464
174	24-03-2009	10:40:44	37.80	72.31	33	4.0	34.81	76.77	520
175	29-03-2009	12:30:51.9	32.96	76.18	10	2.9	34.70	76.91	205
176	04-04-2009	1:23:30.1	32.66	76.46	10	2.8	34.96	76.92	259
177	06-04-2009	7:1:24	34.95	72.73	10	4.4	35.06	77.09	397
178	10-04-2009	21:01:12.6	34.59	72.41	10	3.6	34.80	76.77	399
179	30-04-2009	11:58:23.8	33.33	74.6	33	3.0	35.05	77.05	296
180	11-05-2009	7:7:47.1	37.22	72.71	14	4.5	34.97	76.93	454
181	03-01-2010	04:06:09	34.92	77.46	53.2	3.2	35.04	77.06	39
182	08-02-2010	03:21:12	34.92	77.48	10	4.2	34.82	76.75	68
183	09-02-2010	11:26:00	35.13	76.95	10	3.0	34.60	76.76	62
184	10-02-2010	03:19:00	35.06	77.10	7.3	2.9	35.04	77.05	6
185	18-02-2010	01:20:07	34.79	77.37	16.2	2.6	34.97	76.92	45
186	07-03-2010	21:11:00	36.06	74.56	10	2.6	34.94	76.91	246
187	11-03-2010	23:07:00	34.98	76.39	10	2.3	34.98	76.45	4
188	13-03-2010	20:28:00	32.93	79.83	10	2.4	35.12	77.14	347
189	22-03-2010	11:14:00	33.09	75.89	10	2.5	35.04	77.05	242

190	06-04-2010	10:13:00	34.23	73.12	10	3.3	35.11	77.11	377
191	08-04-2010	22:41:00	32.72	78.12	14.8	3.9	35.01	76.95	276
192	16-04-2010	12:19:50	35.51	77.04	51.2	2.9	34.83	76.78	80
193	02-05-2010	13:32:13	34.91	77.46	56.7	4.1	35.05	77.05	40
194	07-05-2010	13:26:00	35.10	77.24	14	4.4	35.08	77.39	13
195	19-05-2010	07:41:00	35.23	77.21	63.7	2.7	34.85	76.78	59
196	20-05-2010	04:06:09	34.95	77.38	2.7	2.6	35.05	77.05	33
197	24-06-2010	22:12:18	35.40	77.79	12.3	2.5	35.23	77.09	66
198	16-07-2010	21:51:17	35.02	77.33	9.8	1.8	34.85	76.79	54
199	26-07-2010	01:42:00	35.62	76.87	72	3.2	35.17	77.08	53
200	03-08-2010	01:20:07	35.33	77.14	10	2.8	35.40	77.04	11
201	19-08-2010	14:11:29	35.17	77.21	16.8	2.3	35.17	77.08	12
202	11-09-2010	05.11.53	34.95	77.66	47.6	2.8	35.17	77.09	58
203	15-09-2010	21:21:32	34.76	77.45	26	2.8	35.17	77.09	56
204	03-10-2010	10:19:57	35.48	77.08	12	2.6	34.50	76.83	111
205	09-10-2010	04:06:09	34.49	77.40	10	3.3	34.51	76.76	59
206	11-10-2010	05:45:42	34.70	77.59	9	4.0	34.51	76.76	79
207	14-10-2010	17:24:54	35.36	77.15	10	2.1	35.19	77.05	22
208	19-10-2010	05:42:00	34.53	71.65	10	3.4	34.51	76.76	467
209	10-11-2010	12:55:42	34.72	77.55	83	2.6	34.49	76.80	74
210	23-01-2011	14:13:00	32.45	76.21	46.2	2.8	35.04	77.03	297
211	23-01-2011	14:13:00	32.45	76.21	46.2	2.8	35.04	77.06	298
212	07-02-2011	16:22:00	36.64	71.22	10	3.5	35.14	77.16	560
213	08-02-2011	16:52:59	35.39	77.43	132.4	3.2	35.13	77.17	38
214	09-02-2011	04:36:38	36.10	73.60	15	5.0	35.06	76.95	324
215	13-02-2011	11:52:19	35.40	77.19	10	2.0	35.08	77.21	36
216	21-03-2011	09:48:59	36.50	70.90	166	5.7	35.05	77.05	577
217	04-09-2011	14:11:29	34.843	77.049	10	2.2	35.13	77.10	32
218	05-09-2011	16:25:32	34.91	77.20	15	1.7	35.13	77.10	26
219	27-09-2011	11:02:59	36.70	76.70	84	4.9	34.50	76.80	244
220	24-10-2011	10:17:10	35.12	77.24	57	2.6	35.19	77.06	19
221	26-10-2011	16:17:32	31.50	76.80	5	3.5	34.47	76.87	330
222	02-11-2011	15:18:44	35.13	76.76	16.8	1.7	34.50	76.84	71
223	07-11-2011	11:59:30	36.60	71.10	205	6.0	34.47	76.87	573
224	12-11-2011	11:51:03	35.33	77.41	42	3.6	35.06	77.14	39
225	09-12-2011	11:45:42	35.58	77.95	97.8	3.2	35.28	77.05	88
226	29-12-2011	2:51:40	35.36	77.15	63.7	2.4	35.03	76.89	44
227	18-02-2012	3:21:12	35.14	77.23	10	2.6	34.98	76.94	32
228	20-02-2012	13:59:24	35.80	79.70	10	4.9	35.12	77.15	243

229	29-03-2012	01:42:00	34.71	77.55	125	2.1	34.78	76.79	70
230	18-04-2012	06:09:44	35.48	76.95	2.7	3.9	35.24	77.15	33
231	21-04-2012	03:07:23	35.04	77.25	13.7	3.8	35.18	77.09	21
232	27-04-2012	20:0156	34.89	77.34	3.2	4.0	35.09	77.29	22
233	28-04-2012	7:5:18	35.15	77.26	10	3.8	35.15	77.11	14
234	10-05-2012	22:00:40	30.20	79.40	5	3.9	35.18	77.09	594
235	11-05-2012	10:38:12	35.12	77.25	10	2.5	35.18	77.09	16
236	16-05-2012	9:43:07	35.56	77.01	49.8	3.7	35.21	77.09	40
237	17-05-2012	18:22:54	35.40	77.12	90.2	2.9	35.21	77.09	22
238	27-05-2012	1:08:29	35.23	77.25	9.4	2.3	34.50	76.80	92
239	28-05-2012	00:38:12	35.37	77.12	59.2	3.0	35.40	76.89	22
240	29-05-2012	12:36:41	35.11	77.21	4	3.6	34.51	76.80	78
241	03-06-2012	23:19:04	35.30	80.40	10	3.1	34.51	76.80	340
242	08-06-2012	8:32:09	35.02	77.40	67.9	3.2	35.40	76.89	63
243	22-06-2012	3:19:00	34.57	77.61	45.8	3.2	34.51	76.80	75
244	11-07-2012	6:9:44	34.86	77.48	10	2.8	35.40	76.89	81
245	12-08-2012	7:31:12	34.84	77.20	10	3.7	35.40	76.89	68
246	10-09-2012	17:26:41	34.65	77.63	12	4.0	35.03	77.16	61
247	25-10-2012	10:38:12	35.14	77.53	47.9	3.5	34.93	76.89	63
248	26-10-2012	22:36:41	35.12	77.21	12.9	3.2	34.98	76.94	29
249	19-12-2012	08:08:00	34.77	83.31	10	4.2	34.96	76.92	583

6.3. Methodology

In this work, earthquake events of period 2002-2012 with epicenter lie within ~600 km radius from Nubra-Shyok region is prepared to study earthquake induced snow avalanches in this region. The final database is prepared by using the hypocenteral parameters provided by (1) IMD, Delhi, earthquakes listed from (serial number 1 to 180 in Table 6.1), (2) computed by using the waveform data of local network installed in the Nubra region by SASE, (serial number 181 to 249 in Table 6.1). The wave form data of local BBS network are used to estimate hypocenter parameters of earthquake using the SEISAN software (Haversuskov and Ottemueller, 1999), which based on

'HYPOCENTER 3.2' program (Lienert, 1994) for earthquake locations. The major inputs for the software to compute hypocentral parameters are wave form data, velocity model of the study region and geographical co-ordinates together with elevation of recording sites. The velocity model provided by Caldwell et al. (2009) for the Nubra region is implemented for the present work and geographic location of recording station (Table 2.1).

Avalanche occurrence data of Nubra-Shyok region was compiled in association of earthquake data for the period 2002-2012 occurred in this region. The lower limit of earthquake ground motion parameters (i.e. Magnitude) associated with avalanche triggering is determined for this work. Relation between earthquake magnitude and distance of induced snow avalanche from epicenter is obtained using the least-squares linear regression mean. The obtained distance of induced snow avalanche from epicenter of earthquake is compared with the earthquake induced landslide studies (Keefer 1984) and earthquake induced avalanche studies (Podolskiy et al., 2010a), which reveal resemblance with present study.

6.4. Results and Discussion

The avalanches in the mountainous snow bound region can be released by the strong ground motion (Podolskiy et al., 2010a, b), which are generally produced artificially by explosions and naturally by earthquakes. The strong ground motion produced by explosion affects up to few kilometers, however the strong ground motion produced by earthquake affects up to hundreds of kilometers (LaChapelle, 1968; Higashiura et. al., 1979; Singh and Ganju, 2002; Podolskiy et al., 2010a). Hence snow avalanches triggered due to the earthquakes happened within the radius of ~600 km is studied in the present

work. Singh and Ganju (2002) observed avalanche occurrence in the absence of snow-metrological parameters for the period 1995-2000, in NW Himalaya India, further they observed that earthquakes have direct bearings on avalanche occurrences in snow bound region of North Western Himalaya. As the NW Himalaya, India region has high seismic and avalanche activity so in the present work the effect of seismicity on the avalanche occurrence is studied in Nubra-Shyok region of Western Himalaya, India.

The seismicity around the Nubra-Shyok region is examined to analyze earthquake induced snow avalanches in this region. The earthquake occurred during the year 2002-2012, within the radius of ~600 km from the Nubra-Shyok region is shown in Figure 6.2, a total of 1467 earthquakes are happened in this region during 2002-2012. The hypocentral parameters of earthquakes are estimated from waveform seismic data of local seismic installed in the present study region available for the year 2010-2012. For the period 2002-2009, hypocentral parameters reported by IMD, Delhi for this region (Figure 6.1) is used to study seismogenic snow avalanches. During this decade, a total of 1448 snow avalanches are taken place in this region out of these 347 avalanches are triggered due to the earthquakes during the period of 2002-2012 (Figure 6.2A). The year 2005 and 2006 consist highest number of induced avalanches corresponding to large number of earthquake happened in these year (Figure 6.2A). The date of occurrence of earthquake and snow avalanche (Table 6.1), confirms that large numbers of avalanches are triggered by earthquakes in Nubra-Shyok region, India. A total of 249 earthquakes with magnitude range 1.7 - 6.0 are responsible for triggering 347 snow avalanches

in this region and number of induced snow avalanches corresponding to the magnitude of earthquake is represented in, Figure 6.3B.

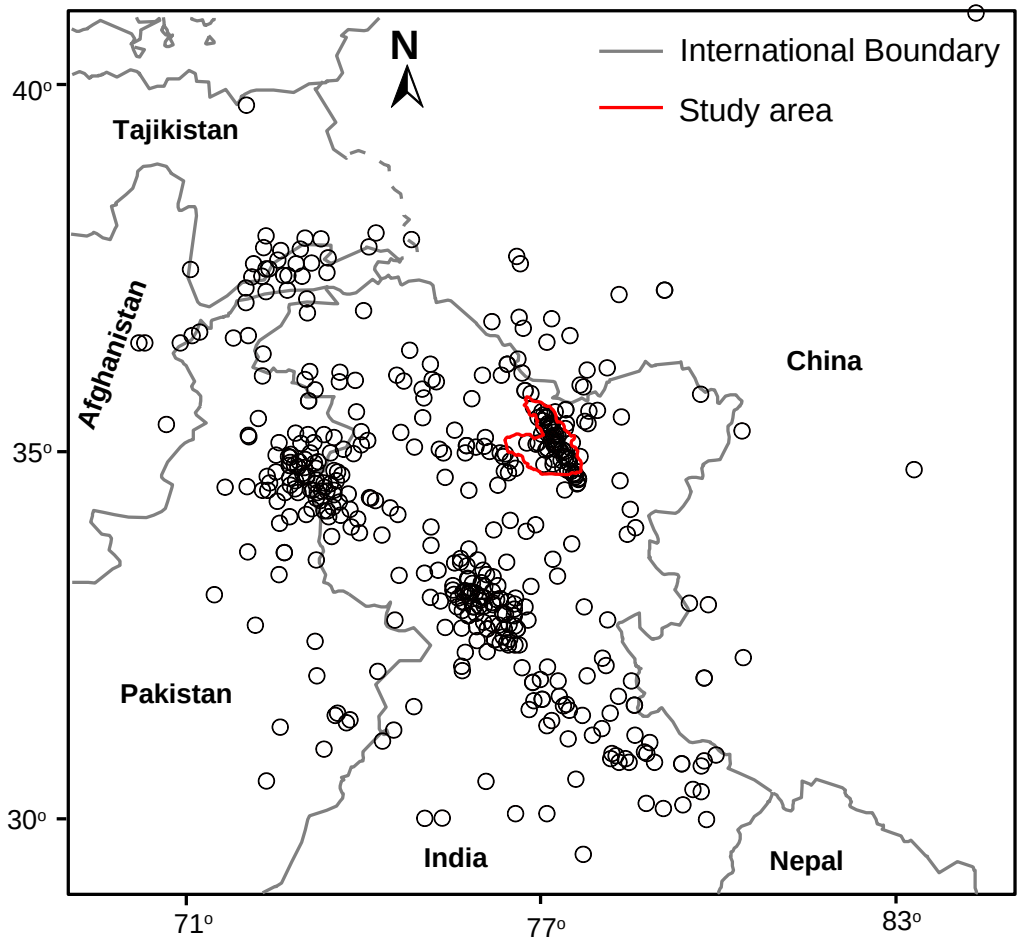

Figure 6.1: Seismicity map around the Nubra-Shyok region during the 2002-2012.

The maximum number of snow avalanches is triggered by the earthquakes having magnitude range of $2.0 \leq M_w \leq 4.9$, similar observation has been observed by the Singh and Ganju (2002) for the Western Himalaya, India. A total of 347 avalanches are triggered due to earthquakes out of which, the location of 249 avalanches are available and provided by the SASE. The

locations of these induced avalanches are plotted on avalanche susceptibility map (Figure 6.3). The geospatial analysis of various avalanche potential zones of study area are made with the location of reported avalanche sites and found that 1.66%, 16.95%, 21.38 %, 27.23% and 38.72% of avalanches are reported in Very Low Susceptible zone, Low Susceptible zone, Moderate Susceptible zone, Moderate-to-High Susceptible zone and Very High Susceptible zone, respectively. Minimum value of magnitude of an earthquake responsible for triggering a snow avalanche in present study region is made by using the plot between earthquake magnitude and distance of induced snow avalanche from epicenter (Figure 6.4). In the present work, lowest magnitude associated with triggering of an avalanche is 1.7 (M_w), at a distance of 4.4 km from the epicenter of earthquake.

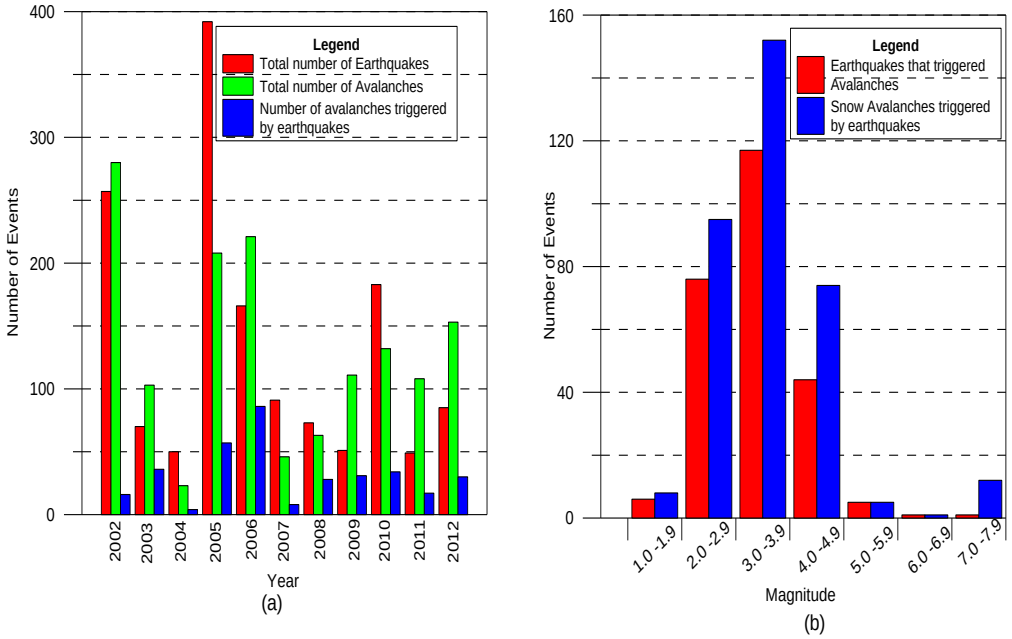

Figure 6.2: (A) Total number of earthquakes, snow avalanches and seismogenic snow avalanches corresponding to various years and (B) Number

of seismogenic avalanches and earthquakes corresponding to their magnitude in Nubra-Shyok region, India.

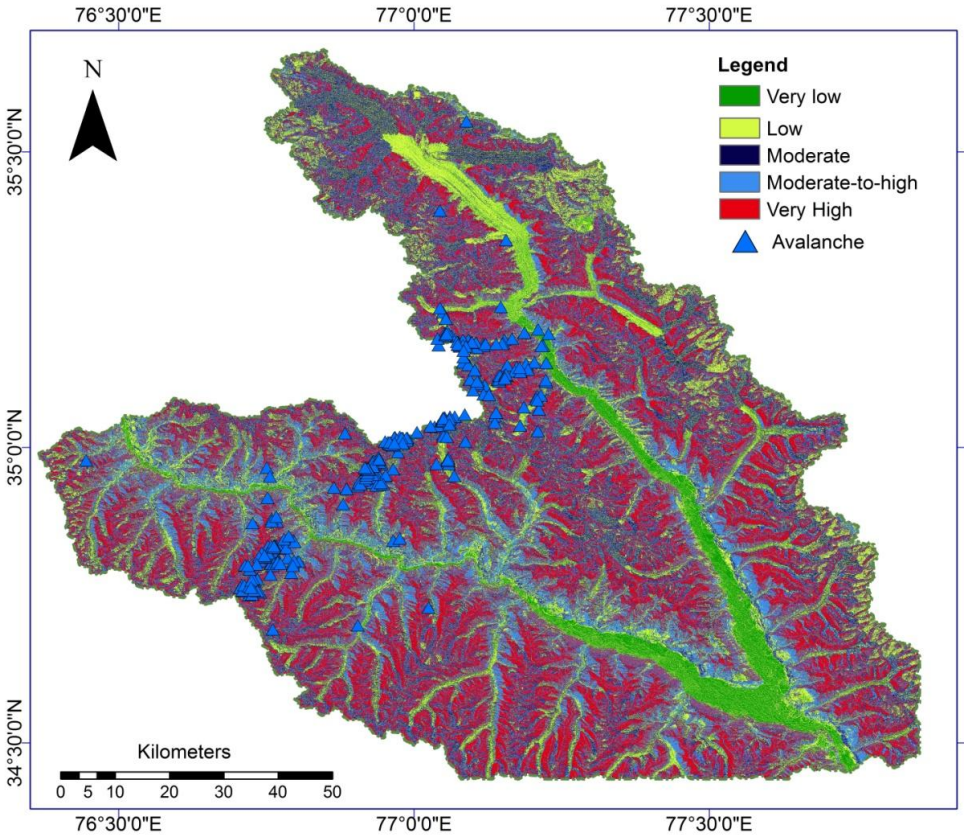

Figure 6.3: Seismogenic avalanche on the avalanche susceptibilty map of the region. Different colors represent different avalanche susceptibility zone (Modified after Rajinder et al, 2017b).

None of the avalanche is observed triggered by earthquake with magnitude less than 1.7 in this region. The lower limit of magnitude of earthquakes for triggering an avalanche upto the maximum distance of 594 km from the epicenter of earthquake is approximated by using the relationship between magnitude and source-to-site distance for earthquake triggered

avalanches from Least squares linear regression mean (Figure 6.4) and given in equation (6.1).

$$M_w = 0.002016 * X + 1.4 \qquad (6.1)$$

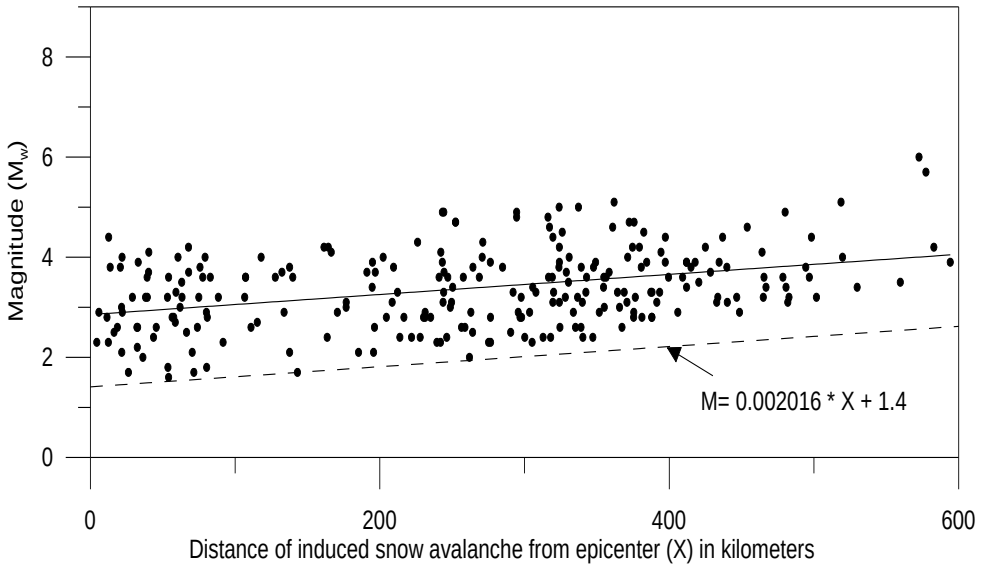

Figure 6.4: Relation between earthquake magnitude and distance of induced snow avalanche from epicenter. The dashed line is the lower bound obtained from least-squares linear regression mean.

Where, M_w and X represent the moment magnitude of earthquake and distance of induced snow avalanche from the epicenter of the earthquake, respectively. The above equation provides the threshold value of earthquake magnitude i.e. 1.4 responsible for avalanche triggering at zero distance from epicenter of earthquake.

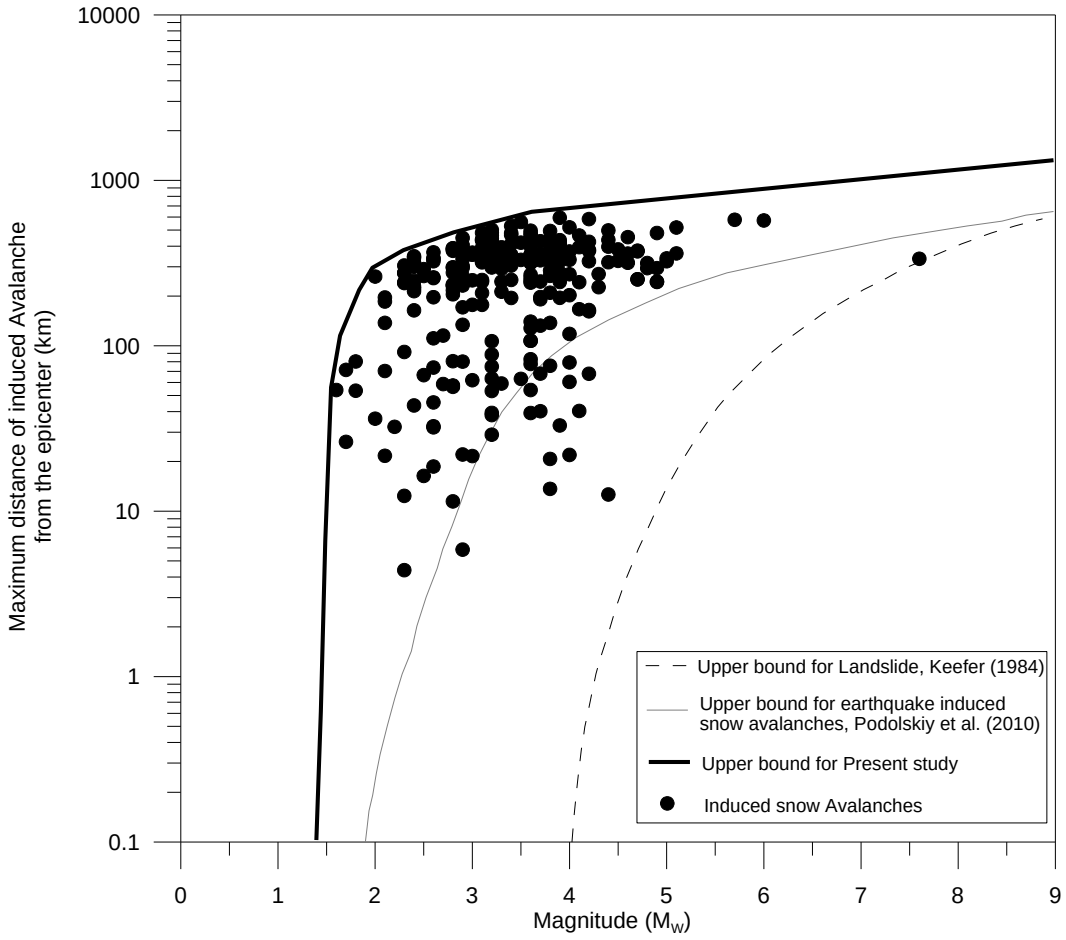

Figure 6.5: Comparison of obtained distance of induced snow avalanche from epicenter of earthquake with other studies. The solid circle shows the data of present work. The dash line, thin gray line and thick black line represent the approximate upper bound for landslides (Keefer, 1984), ice avalanches (Podolskiy et al., 2010a) and present study, respectively (modified after Podolskiy et al., 2010a).

The obtained threshold value of magnitude is comparable with earlier established magnitude i.e. 1.9 for earthquake induced snow avalanches provided by Chernous et al. (2006); Podolisky et al. (2010a). Singh and Ganju (2002) also reported lower limit value of magnitude i.e. 1.9 (see Table 1, Singh and Ganju, 2002) for the vicinity of present study region and the obtained value of magnitude for present region i.e. 1.4 is slightly smaller than reported by Singh and Ganju (2002), which may be due to the local

monitoring and recording of seismic events in this region. The distance of induced avalanches from the epicenter is plotted against the earthquake magnitude on semi log scale for comparison of this study with the other studies carried out for landslide and avalanches by Keefer (1984) and Podolskiy et al. (2010a), respectively (Figure 6.5). The maximum distance of triggered avalanche increases with the increase of earthquake magnitude. The magnitude and distance upper limit is estimated for the present study and this relation is comparable with the upper limit of earthquake induced landslide (Keefer, 1984) and avalanches (Podolskiy et al. 2010a) (Figure 6.5). Keefer (1984) proposed that an earthquake of magnitude 4.0 can trigger landslide at zero epicentral distance and Podolskiy et al. (2010a) suggested that an earthquake of magnitude 1.9 can trigger snow avalanche at zero epicentral distance and in present study it is found that an earthquake of magnitude 1.4 can trigger snow avalanche at zero epicentral distance in Nubra-Shyok region.

6.5 Conclusions

This study confirms the occurrence of earthquake induced snow avalanches in Nubra-Shyok region, India. A total of 249 earthquakes are identified for inducing snow avalanches in the Nubra-Shyok region, which cause a total of 347 seismogenic avalanches in this region. The avalanches triggered due to natural seismicity during the period of 2002-2012 are associated with the earthquakes of magnitude $1.7 \leq M_w \leq 6.0$ and source-to-site distance of range 4 - 594 km. The maximum numbers of earthquake induced avalanches correspond to magnitude range $2.0 \leq M_w \leq 4.9$, with peaks at $3.0 \leq M_w \leq 3.9$. In this study, threshold values of earthquake magnitudes which cause avalanches are established within the source-to-site distance of induced

avalanches of ~594 km. The threshold value of magnitude (M_w 1.4) is provided for earthquake induced snow avalanches as distance approaches to zero for Nubra-Shyok region of Western Himalaya, India.

CHAPTER 7

SUMMERRY AND CONCLUSIONS

7.1 Introduction

The research work presented in this thesis is about the implications of earthquake activities on avalanche occurrences in the highly galcerized Nubra-Shyok, region of India. The broadband seismic data recorded by four stations installed in the study area have been used to study the attenuation characteristics, earthquake source parameters and pattern of local seismicity. The avalanche susceptibility mapping of the study area using Landsat 8 imagery, ASTER GDEM and AHP model has been carried out. The implications of earthquake activity on avalanche occurrence and the magnitude distance relation for seismogenic avalanche in the study area have been introduced. This research work was carried out with the following five objectives and all the five objectives of this research work have been achieved.

1) To study the attenuation characteristics of seismic waves in Nubra-Shyok, region.
2) Estimation of earthquake source parameters in Nubra-Shyok region.
3) To study the pattern of local seismicity in Nubra-Shyok region.
4) Avalanche Susceptibility mapping of Nubra-Shyok, region.
5) To study the effect of local seismicity on the occurrence of snow avalanches in Nubra-Shyok, region.

7.2 Summary of results for Seismological Studies

In the present work, coda waves are utilized for estimation of attenuation characteristics because, coda have sampled a large volume of subsurface and not just a single path, hence seismic coda is an efficient tool for studying the average attenuation properties of the sub surface (Reese and Ni, 1996) and Coda waves do not involve complicated factor such as the source radiation pattern (Mayeda et al., 2007; Nakajima et al., 2013). The single backscattering method was used to estimate the coda wave quality factor (Q_c) for this virgin region to estimate seismic wave attenuation characteristics. A 30 sec window length of coda waves at different central frequencies 1.5, 3.0, 6.0, 9.0, 12.0, 18.0 and 24.0 Hz have been studied to determine Q_c at different recording stations. The frequency dependent coda wave quality factor relationships of the form $Q_c(f) = Q_o f^{n}$ have been computed at each recording stations separately as given in Table 7.1.

Table 7.1: $Q_c(f)$, relationship calculated at all four stations of Nubra-Shyok region

Sr. No.	Station Name	Station Code	Qc(f) Relationship
1	Sasoma	SASO	$Q_c(f) = (111\pm4.1)f^{(1.0\pm0.03)}$
2	Parta	PTPR	$Q_c(f) = (122\pm3.0)f^{(1.0\pm0.02)}$
3	Base	BASE	$Q_c(f) = (137 \pm 4.2)\, f^{(0.99 \pm 0.12}$
4	Chalunka	CHLK	$Q_c(f) = (116\pm3.8)f^{(1.0\pm0.05)}$

A regional Q_c relation has been developed for the Nubra-Shyok region by using the average value of Q_c at different frequencies obtained at each recording station of the form $Q_c(f) = (121\pm7.2)f^{(1.0\pm0.04)}$. The average Q_c values vary from 183 at 1.5 Hz to 3684 at 24 Hz central frequencies. The present regional relation developed for Nubra-Shyok, region indicates heterogeneous and tectonically active region.

The earthquake source parameters such as seismic moment, source radius and stress drop of 17 local events have been estimated following Brune's earthquake source model (1970). The seismic moments found between 2.1 x 10^{20} dyne-cm to 3.34 x 10^{23} dyne-cm. The source dimension in terms of the radius of circular fault varies from 532.3 m to 1.296 km. The stress drops of these earthquakes ranges between 0.1 to 61.7 bars and found in agreement with the other tectonically and seismically active regions of Himalaya. The average stress drop observed for Himalayan earthquakes is about 58 bars by Kumar et al., (2008) and about 60 bars as reported by Kumar, (2011).

The observed local seismicity from 2010 to 2012 in Nubra-Shyok, region of Jammu and Kashmir is mainly oriented along the Karakoram Fault. The moment magnitudes of these events lie between 1.3 and 4.3. Aseismic layer (17-40Km) sandwiched between two seismically active layers is detected in Nubra-Shyok region of Western, Himalaya. This aseismic layer shows the good spatial correlation with the low resistivity layer reported by Arora et al. (2007). Results of this study support the proposed 'partially melted crust for this region' by Caldwell et al., (2009) and Jain and Singh (2009). Most of the

local earthquakes in this region have been occurred at upper part of the crust**.** Such shallow seismic activity in the glacier region may affect the glaciers. This aspects need to be studied in more detail.

7.3 Summary of results for avalanche potential mapping

The avalanche susceptibility map of the region was not available and this area is very large and inaccessible. The climatic condition of the region are inhospitable and inhumane. Hence the help of remote sensing GIS technique is taken to map the avalanche potential of the area. The avalanche susceptibility map prepared using five avalanche occurrence factors such as slope, aspect, curvature, elevation and ground cover show that: - (i) Very High (ii) Moderate-to-High (iii) Moderate (iv) Low (v) Very Low, and covers 27.5% , 28.0% 19.0%, 20.0%, and 4.8%, of the total area respectively. The results of this study was verified using the ROC-AUC method. In the present study AUC value 0.9112 was obtained. The results validation process shows that 91.12% avalanche pixels were properly categorized in the avalanche susceptibility map and these results are acceptable. The geo-spatial analysis of avalanche susceptibity map of the area and locations of reported avalanche sites shows that only 1.66% of reported snow avalanches falls in very low susceptibility zone, while very high susceptible zone accounts for 32.78 %.

7.4 Summary of results for earthquake induced snow avalanches

Snow avalanche can be triggered by different mechanisms including metrological conditions, terrain, snow pack stability together with external factor such as seismic tremor, explosions etc. The snow avalanche triggered by seismic event is very important hazard phenomena in the snow covered

region. In this work, investigation of earthquake induced snow avalanches is introduced in Nubra-Shyok region of Western Himalaya, India. Compilation of seismogenic snow avalanche occurred in the Nubra-Shyok region and earthquakes happened in the region define by 29.5°N to 40.5°N and 70°E to 84°E i.e. ~600 km radius from Nubra-Shyok region during the period of a decade (i.e. year 2002-2012) is made, which reveal that out of 1448 natural avalanche, 347 avalanches was triggered in relation to the earthquake events during this period. The same date of occurrence of earthquakes and snow avalanches confirm seismogenic snow avalanche events in this region. In the present work, avalanches triggered due to natural seismicity during the period of 2002-2012 related with earthquakes of magnitude $1.7 \leq M_w \leq 6.0$ and distance of induced snow avalanche from epicenter of earthquakes lies in the range of 4-594 km. In this study, lower bound limits of earthquake magnitudes which cause avalanches are established upto the distance of 594 km. Relation between earthquake magnitude and distance of induced snow avalanche from epicenter reveal that an earthquake of magnitude 1.4 (M_w) can trigger a snow avalanche as distance approaches to zero from earthquake epicenter. The comparison of obtained relation with other similar types of studies i.e. Keefer, 1984; Podolskiy et al., 2010a confirm the reliability of present work.

7.5 Conclusions

The research work presented in this thesis revealed that Nubra-Shyok, region is tectonically seismically active and heterogeneous. The remote sensing and GIS technique and AHP method is very useful tool to map the avalanche susceptibility of large areas. It is also revealed that the earthquakes are acting as triggering factor for snow avalanches in this region. The

objective determined for this research work have been fulfilled. The major conlusions drwan from this research work are given below:

1. The attenuation relation $Q_c(f) = (121\pm7.2)f^{(1.0\pm0.04)}$ developed for the region show that region is tectonically active and heterogeneous.
2. Stress drops for the earthquakes happened in Nubra-Shyok region, ranges between 0.1 to 61.7 bars and found in agreement with the other tectonically and seismically active region of Himalaya.
3. The local seismicity observed by the Nubra seismological network is mainly upper crustal and oriented along the Karakoram fault. Aseismic layer is also found in the middle part of crust.
4. The Nubra region is highly susceptible to snow avalanches with only 4.8% of area in very low susceptible zone.
5. The avalanches triggered due to natural seismicity during the period of 2002-2012 are associated with the earthquakes of magnitude $1.7 \leq M_w \leq 6.0$ and source-to-site distance of range 4 - 594 km Lower bound limits of earthquake magnitudes which cause avalanches are established upto the distance of 594 km.
6. An earthquake of magnitude 1.4 (Mw) can trigger a snow avalanche as distance approaches to zero from earthquake epicenter in Nubra-Shyok region.

7.6 Future Scope of Research.

1. As this seismological network was deployed to monitor the seismicity of the region but many seismic signatures related to snow avalanche and other mass movements were also observed in seismograms of all four recording stations but could not be interpreted.

2. A seismic network installed near avalanche slopes may be very useful in locating, speed determination of snow avalanches.

References

1. Abercombie R., and Leary P., (1993). Source parameters of small earthquakes recorded at 2.5km depth, Cajon Pass, Southern California: Implications for earthquake scaling; Geophysical Research Letters, 20, pp. 1511-1514.
2. Agarwal V., Bolch T., Syed T.H., Pieczonka T., Strozzi T., Nagaich R., (2017). Area and mass changes of Siachen Glacier (East Karakoram), Journal of Glaciology. 63 (237), pp. 148–163.
3. Aki K., (1967). Scaling law of seismic spectrum. Journal of Geophysical Research 72 (4), pp. 1217–1231.
4. Aki K., (1969). Analysis of the seismic coda of local earthquakes as scattered waves. J Geophys Res, 74, pp. 615-631.
5. Aki K., and Chouet B., (1975). Origin of the coda waves: source attenuation and scattering effects. J Geophys Res., 80, pp. 3322-3342.
6. Ancey C., (2009). Snow avalanches. In: Delage P, Schrefler B, (editors). Wiley & Sons, New York.
7. Andrews D. J., (1986). Objective determination of source parameters and similarity of earthquakes of different size, In Earthquake Source Mechanics (ed. Das et.al) (Ewing Series, 6, AGU, Washington DC 1986), pp. 259-267.
8. Archuleta R. J., Cranswick E., Mueller C., and Spudich, P., (1982). Source parameters of the 1980 Mammoth Lakes, California, earthquake sequence. J. Geophysics Res. 87, pp. 4595-4607.
9. Arora B. R., Unsworth M. J., Rawat G., (2007). Deep Resistivity Structure of the Northwest Indian Himalaya and its Tectonic

Implications. Geophysical Research Letters 34, L04307. doi:10.1029/2006GL029165

10. Bansal B. K., (1998). Determination of source parameters for small earthquake in the Koyna region. 11th Symposium on the Earthquake engineering, Roorkee,1, pp. 57-66.

11. Bashart M., Shah H.R., Nashir (2016). Landslide susceptibility mapping using GIS and weighted overlay method: a case study from NW Himalayas, Pakistan. Arbian Journal of Geosciences. 9(4).

12. Bilham, R. and Gaur, V.K., (2000). The geodetic contribution to Indian seismotectonics, Curr. Sci., 79, pp. 1259–1269.

13. Bhutiyani M.R, Parshad R, Shekhar S, Ganju A, Snehmani (2013) Manifestations of climate change in Karakoram Himalayas: Extreme precipitation event induced earth-flow over the Siachen Glacier in Nubra Valley. Proceedings of International Symposium on Cryosphere & Climate Change -2012, pp. 69-72.

14. Bhutiyani M.R., Kale V.S. and Pawar N.J., (2010). Climate change and the precipitation variations in the northwestern Himalaya: 1866–2006. International Journal of Climatology, 30, pp. 535-548.

15. Bhutiyani, M. R., (1999). Mass-balance studies on the Siachen Glacier in the Nubra Valley, Karakoram Himalaya, India. J. Glaciol., 45, 112–118.

16. Bhutiyani M.R., (1992), The avalanche problems in Nubra and Shyok valley Karakoram Himalaya, India J. Inst. Mil. Engrs India, Vol. 3(3).

17. Brune J. N., (1970). Tectonic stress and the spectra of seismic shear waves from earthquakes, J. Geophys. Res., 75, pp. 4997-5009.

18. Brune J. N., (1971). Correction to tectonic stress and the spectra of seismic shear waves from earthquakes, J. Geophys. Res. 76, 5002.

19. Brune J. N., Fletcher J., Vernon F., Haar L., Hanks T., and Berger J., (1986). Low stress-drop earthquakes in the light of new data from the Anza, Calfornia telemetered digital array. Reprinted from Earthquake Source Mechanics, Geophysical Monograph 37 (Maurice Ewing 6) Americal Geophysical Union.

20. Caldwell W.B., Klemperer S.L., Rai S.S. and Lawrence J.F. (2007). Testing the presence of fluids/crustal melts in the India–Asia collision zone using Rayleigh wave dispersion analysis (Abstract T31B-0464), Eos Trans. AGU 88, no. 52 (Fall Meet. Suppl.), T31B-0464.

21. Caldwell W.B., Klemperer S.L., Rai S.S., and Lawrence J.F., (2009). Partial Melt in the Upper-Middle Crust Of The Northwest Himalaya Revealed by Rayleigh Wave Dispersion, Tectonophysics, 477, pp.58–65.

22. Campbell K. W., (2001). Development of semi-empirical attenuation relationships for the CEUS, U.S. Geological Survey, Award 01HQGR0011, final report.

23. Chen X., Chen H., You Y., Liu J., (2015). Susceptibility assessment of debris flows using the analytic hierarchy process method - A case study in Subao river valley. China. Journal of Rock Mechanics and Geotechnical Engineering 7 (4): pp. 404–410

24. Chen Y., Yu J., Shahbaz K., Xevi E., (2009). A GIS-Based Sensitivity Analysis of Multi-Criteria Weights. Proceedings of the

18th World IMACS Congress and MODSIM09 International Congress on Modelling and Simulation. Cairns, Australia.

25. Chen W.P., and Molnar P., (1983). Focal depths of intracontinental and intraplate earthquakes and their implications for the thermal and mechanical properties of the lithosphere, Journal of Geophysical Research., 88, pp. 4183 – 4214.

26. Chernous, P.A., Yu.V. Fedorenko Y., E., Mokrov E.., Barashev N.V., Hewsby E., Beketova E.B., (2004). Issledovanie vliyaniya seismichnosti na obrazovanie lavin [Study of seismicity effect on avalanche origin]. Mater. Glyatsiol. Issled. /Data Glaciol. Stud. 96, pp. 167–174. [In Russian with English summary.]

27. Chernous, P.A, Fedorenko Y., E. Husebye, E. Beketova (2002). Russian-Norwegian project on seismicity-induced avalanches, International Snow Science Workshop, Penticton, B.C, pp. 25-30.

28. Chernous P., Fedorenko Y, Mokrov, E., Barashev, N., (2006). Studies of seismic effects on snow stability on mountain slopes. Polar Meteorol. Glaciol, 20, pp. 62–73.

29. Ciolli M., Tabarelli S., Zatelli P., (1998). 3D Spatial Data Integration for Avalanche Risk Management. In: Fritsch D, Englich M, Sester M (editors). ISPRS Commission IV Symposium on GIS- Between Visions and Applications, pp.121–127.

30. Cooley, James W.; Tukey, John W. (1965). An algorithm for the machine calculation of complex Fourier series". Math. Comput. 19, pp. 297–301. doi:10.2307/2003354.

31. Dasgupta S., Narula P.L., Acharya S.K., Banerjee J., (2000). Seismotectonic atlas of India and its environs. Geological Survey of India, India.

32. Dave (2015). Landslides in Langtang during and after the Nepal Earthquake, The Landslide blog, AGU blogsphere.

33. Dewey, J.F. and Bird, J.M., (1970). Mountain belts and the new global tectonics: J. Geophysical Research, 75, pp. 2625-2647.

34. Dimri A. P. and Dash S. K., (2010). Winter temperature and precipitation trends in the Siachen Glacier. Current Science, 98 (12), pp.1620-1625.

35. Dortch J., Owen L.A., Haneberg W.C., Caffee M.W., Dietsch C., Kamp U., (2009), Nature and timing of mega-landslides in northern India. Quaternary Science Reviews, 28, pp. 1037-1056.

36. Dunlap W.J., Weinberg, R.F., Searle, M.P., (1998). Karakoram fault zone rocks cool in two phases. Geological Society of London, 155, pp. 903–912.

37. Fah D., Moore J.R., Burjannek J., Iosifescu I., et al. (2012). Coupled seismogenic geohazards in Alpine regions. Bollettino di Geofisica Teorica ed Applicata Vol. 53, n. 4, pp. 485-508. DOI 10.4430/bgta0048.

38. Fan G., Ni J.F. and Wallace T.C. (1994). Active tectonics of the Pamirs and Karakoram, J. Geophys. Res., 99(B4), pp. 7131–7160.

39. Fedrenko Y., Chernous P., Mokrov E., Husebye E., Beketova E., (2002). Dynamic Avalanche modeling including seismic loading in the Khibiny mountains. IPR Congress publication, 2, pp. 705-714.

40. Feng X and Guo A (1985) Earthquake landslide in China. Proceedings of the International Conference and Field Workshop on Landslides, Tokyo, pp. 339–346.

41. Fletcher J. B., (1980). Spectra from high dynamic range digital recordings of Oroville, California, aftershocks and their parameters, Bull. Seismol. Soc. Am., 70, pp. 735-755.

42. Fu R.S., Xu Y.M., Huang J.H., (2000). Numerical Simulation of the Compression Uplift of the Qinghai-Xizang Plateau, Chinese Journal of Geophysics., 43(3), pp. 346–355 (in Chinese with English Abstract).

43. Ganju A., and Dimri A.P., (2004). Prevention and mitigation of avalanche disasters in western Himalayan region. Nat Hazards, 31, pp. 357‑371.

44. Ganju A, Thakur N. K., and Rana V., (2002). Characteristics of avalanche accidents in Western Himalayan Region. Proc. of International Snow Science Workshop. 29 September–4 October 2002, Penticton, B.C., Canada. International Snow Science Workshop, pp. 200–207.

45. Gansser A., (1964). Geology of the Himalayas. Willey Interscience London.

46. Gansser A., (1980). The significance of the Himalayan suture zone. Tectonophysics, 62, pp. 37-52.

47. Geiger, L., (1912). Probability method for the determination of earthquake epicenters from the arrival time only, Bull. St. Louis Univ., 8, 60.

48. Ghosh A. (2015). We are very very lucky to be alive, Times of India, 28 April, 2015, New Delhi, India.

49. Glazoversuskaya T.G., Myagkov S.M., Troshkina E.S., Akifeva K.V., Kondakova N.L., Kravtcova V.I., (1992). Rasprostranenie irejim lavin [Avalanches spreading and regime]. In Myagkov,S.M. and L.A. Kanaev, eds. Geografiya lavin [Geography ofavalanches]. Moscow, Moscow State University Press, 43‑111.[In Russian.]

50. Giddings, J.C. and La Chapelle E. (1962), "The formation rate of depth hoar", Journal of Geophysical Research, Vol. 67, pp.2377-2383.

51. Godin L., Grujic D., Law R.D., Searle M.P. (2006). Channel flow, ductile extrusion and exhumation in continental collision zones: an introduction, Geol. Soc., London, Special Publications, 268, pp. 1–23.

52. Guangwei F., and Ni J.F., (1989). Source parameters of the 13 February 1980, Karakoram earthquake, Bulletin of Seismological Society of America, 79, pp. 945-954.

53. Guillén C. P., Tapia M., Furdada G., Suriñach E., McElwaine J.N., Steinkogler W., Hiller M., (2014). Evaluation of a snow avalanche possibly triggered by a local earthquakeat Vallée de la Sionne, Switzerland, Cold Regions Science and Technology, Vol. 108, pp. 149–162.

54. Guillén C. P., (2016). Advanced seismic methods applied to the study of snow avalanche dynamics and snow avalanche formation. Ph.D. thesis, University of Barcelona.

55. Gupta S.C., Kumar A., (2002). Seismic wave attenuation characteristics of three Indian regions: a comparative study. Curr Sci 82:407-413

56. Gupta S.C., Singh V.N., Kumar A., (1995). Attenuation of Coda Waves in the Garhwal Himalaya, India. Phys Earth Planet Interiors 87:247-253.

57. Hanks T.C. and Kanamori H., (1979). A Moment Magnitude Scale. Journal of Geophysical Research, 84 no b5.

58. Hanks T. C., and Boore, D. M., (1984). Moment-Magnitude relations in theory and practice, J. Geophysics Res., 89, pp. 6229-6235.

59. Hashim M., Pour A.B, Misabari S., (2017). Mapping land slide occurrence zones using Remote Sensing and GIS techniques in Kelantan state, Malaysia. IOP Conf. Series: Journal of Physics: Conf. Series 852 (2017) 012023.

60. Hazarika D., Paul A., Wadhawan M., Kumar Naresh, Sen K., Pant C.C., (2017). Seismotectonics of the trans-Himalaya, Eastern Ladakh, India: constraints from moment tensor solutions of local earthquake data. Tectonophysics 698, pp. 38–46.

61. Hermann R., (1980). Q Estimates Using Coda of Local Earth- quakes. Bull Seismol. Soc. Am., 70(2), pp. 447-468

62. Hewitt, K., Clague J.J., Orwin J.F., (2008). Legacies of catastrophic rock slope failures in mountain landscapes. Earth Sci. Rev., vol. 87, No. (1–2), pp. 1–38.

63. Hanley J.A., McNeil B.J., (1983). A method of comparing the areas under receiver operating characteristic curves derived from the same cases. Radiology, 148: 839–843.

64. Higashiura M., Nakamura T., Nakamura H., Abe O., (1979). An avalanche caused by an earthquake. Rep. Natl Res. Center Disaster Prev, vol. 21, pp. 103–112. [In Japanese with English summary].

65. Imsong W, Bhattacharya F., Mishra R.L., Phukan S., (2017). Geomorphic evidence of late quaternary displacement of the Karakoram fault in Nubra and Shyok valley of Ladakh Himalaya. Current Sci., 112(11), pp. 2295-2305.

66. IS (2002) IS 1893–2002 (Part L) Indian Standard Criteria for Earthquake Resistant Design of Structures, Part 1—General Provisions and buildings. Bureau of Indian Standards, New Delhi.

67. Jain A.K., and Singh S., (2009). Geology and Tectonics of Southeastern Ladakh and Karakoram. Geological Society of India, Banglore, 181 p.

68. Johnston D. H., and Toksöz M.N. (1981). Definitions and terminology, in M. N. Toksöz, and D. H. Johnston, ed., Seismic Wave Attenuation: SEG, pp. 1-5.

69. Joshi A., (2006). Use of acceleration spectra for determining the frequency dependent attenuation coefficient and source parameters. Bulletin of Seismological society of America , 96:2165-2180.

70. Kanna N., Gupta S., Prakasam K.S., (2018). Micro-seismicity and seismotectonic study in Western Himalaya–Ladakh-Karakoram using

local broadband seismic data. Tectonophysics, 726(2018), pp.100-109.

71. Kanamori H., Stewart, G. S., (1978). Seismological aspects of the Guatemala earthquake of February 4, 1976. Journal of Geophysical Research 83, pp.3427–3434.

72. Kargel J. S, Leonard G. J., Dan H. Shugar, Haritashya U. K., et al. (2015). Geomorphic and geologic controls of geohazardsinduced by Nepal's 2015 Gorkha earthquake. Interdisciplinary Arts and Sciences Publications, University of Washington Tacoma, pp.1-32.

73. Kayastha P, Dhital M.R., Smedt F.D., (2013). Application of the analytical hierarchy process (AHP) for landslide susceptibility mapping: a case study from the Tinau watershed, west Nepal. Computers and Geosciences 52, pp. 398-408.

74. Keefer D.K., (1984a). Landslides caused by earthquakes. Geol. Soc. Am. Bull., 95, pp. 406-421.

75. Keilis-Borok V.I., (1959). An Estimation of the Displacement in an Earthquake Source and of Source Dimensions. Annali di Geofisica, 12, pp. 205-214.

76. Khattri, K.N., (1999). An evaluation of earthquakes hazard and risk in northern India, Him. Geol., 20, pp. 1–46.

77. Knopoff, L., (1964): Q. Reviews of Geophysics, 2(4), pp. 625-660.

78. Komac M., (2006). A landslide susceptibility model using the analytical hierarchy process method and multivariate statistics in perialpine Slovenia. Geomorphology 74(1), pp.17-28.

79. Kumar, Arjun (2011). Study of earthquake source parameters using micro earthquakes and strong motion data. Ph.D Thesis, Indian Institute of Technology, Roorkee.

80. Kumar, A., Gupta, S. C., Kumar, A., Sen, A., Jindal, A. K., & Jain, S. (2006). Estimation of source parameters from local earthquakes in Western part of the Arunachal Lesser Himalaya. In 13th Symposium on Earthquake Engineering (pp. 9-17).

81. Kumar A., Mittal H., Sachdeva R., and Kumar A., (2012). Indian strong motion instrumentation network. Seismological Research Letters, 83(1), pp. 59-66.

82. Kumar A., Kumar A., Mittal H., (2013a). Earthquake source parameters –Review Indian context. Research and Development (IJCSEIERD), 3(1), pp. 41-52.

83. Kumar D., Sriram V., Sarkar I., Teotia S. S., (2008). An Estimate of a Scaling Law of Seismic Spectrum for Earthquakes in Himalaya. Indian Minerals 61(3-4) & 62 (1-4), pp. 83-92.

84. Kumar N., Mate S., Mukhopadhyay S. (2014). Estimation of Qp and Qs of Kinnaur-Himalaya. Journal of Seismology, 18 (1), pp. 47–59. http://dx.doi.org/10.1007/s10950-013-9399-7.

85. Kumar P., Yuan X., Kind R., Kosarev G., (2005). The lithosphere–asthenosphere boundary in the Tien Shan–Karakoram region from S receiver functions, evidence for continental subduction, Geoph. Res. Lett., 32, L07305, pp. 1–4.

86. Kumar R., Gupta S. C., Kumar A., Mittal H., (2013b). Source parameters and f max in lower Siang region of Arunachal lesser Himalaya. Arabian Journal of Geosciences, pp. 1-11.

87. Kumar A., Kumar A., Gupta S. C., Mittal H., Kumar R. (2013c). Source parameters and fmax in Kameng region of Arunachal Lesser Himalaya. Journal of Asian Earth Sciences, 70-71, pp. 35-44.

88. Kumar A., Kumar A., Gupta S. C., Jindal A. K., Ghangas, V., (2014a). Seismicity and source parameters of local earthquakes in Bilaspur region of Himachal Lesser Himalaya. Arabian Journal of Geosciences, 7(6), pp. 2257-2267.

89. Kumar R., Gupta, S. C., Kumar, A., (2014b). Attenuation characteristics of seismic body waves for the crust of Lower Siang region of Arunachal Himalaya. International Journal of Advanced Research, 2(6), pp. 742-755.

90. Kumar A., Mittal H., Kumar R., Ghangas V., (2014c). High Frequency Cut-Off of Observed Earthquake Spectrum and Source Parameters of Local Earthquakes in Himachal Himalaya. International Journal of Science and Research, 3 (7), pp. 1642-1651.

91. Kumar N., Parvez I.A., and Virk H.S., (2005). Estimation of coda wave attenuation for NW Himalayan region using local earthquakes. Physics of the Earth and Planetary Interiors, 151, pp. 243-258.

92. Kumar P., Joshi A, Kumar S., Chadha, R.K., (2015). Detailed Attenuation Study of Shear Waves in the Kumaon Himalaya, India,

Using the Inversion of Strong- Motion Data. Bulletin of Seismological society of America, 105(4), DOI: 10.1785/0120140053

93. Kumar S., Srivastva P.K., Snehmani (2016). GIS-based MCDA–AHP modelling for avalanche susceptibility mapping of Nubra valley region, Indian Himalaya. Geocarto Innternational, 32(11), pp. 1254-1267.

94. Kumar S., Srivastva P.K. and Snehmani (2018).Geospatial Modelling and Mapping of Snow Avalanche Susceptibility. Journal of Indian Society of Remote Sensing, 46(1), pp. 109-119.

95. La Chapelle, E.R., (1968). The character of snow avalanching induced by the Alaska earthquake. In The Great Alaska Earthquake of 1964. Vol. 3: Hydrology, Part A. Washington, DC, National Academy of Sciences, pp. 355–361. (NAS Publication 1603.)

96. Leech M.L., (2008). Does the Karakoram fault interrupt mid-crustal channel flow in the western Himalaya?, Earth Planetary Science Letters, 276, pp. 314–322.

97. Lienert, B.R., (1994). Hypocenter 3.2, A Computer Program for Locating Earthquakes Locally Regionally and Globally. Hawai Institute Of Geophysics And Paleontology.

98. Levin V., Roecker S., Graham P. and Hosseini, A., (2008). Seismic anisotropy indicators in Western Tibet: Shear wave splitting and receiver function analysis, Tectonophysics, 462, pp. 99–108.

99. Lou X., Cai C., Yu C., Ning J,. (2009). Intermediate-depth earthquakes beneath the Pamir-Hindu Kush Region: Evidence for

collision between two opposite subduction zones, Earthq. Sci., 22, pp. 659−665.

100. Madariaga R, and Ruiz S., (2016). Earthquake dynamics on circular faults: a review 1970-2015. Journal of Seismology, DOI 10.1007/s10950-016-9590-8.

101. Maggioni M, Gruber U (2003) The influence of topographic parameters on avalanche release dimension and frequency. Cold Regions Science and Technology 37, pp. 407– 419.

102. Maggioni M. (2004). Avalanche release areas and their influence on uncertainty in avalanche hazard mapping, Ph.D. thesis. University of Zurich, Zurich, Switzerland, 146.

103. Malczewski J., (2006). GIS-based multicriteria decision analysis: a survey of the literature. International Journal of Geographical Information Sciences 20, pp. 703–726.

104. Mandal P., Padhy, S., Rastogi B.K., Satyanarayana, V.S., Kousalya, M.,Vijayraghavan, R., and Srinvasa A., (2001). Aftershock activity and frequency dependent low coda Qc in the epicentral region of the 1999 Chamoli earthquake of Mw 6.4. Pure and Applied Geophysics, 158, pp.1719-1735.

105. Mayeda, K., Malagnini L and Walter W.R., (2007). A new spectral ratio method using narrowband coda envelopes: evidence for departure in self-similarity in the Hector Mine sequence, Geophys. Res. Lett., 34, L11303. doi:10.1029/ 2007GL030041.

106. McKenzie D. and Sclater J.G., (1971). The Evolution of the Indian Ocean since the Late Cretaceous, Geophysical Journal International, 24(5), pp.437-528.

107. McClung D., Schaerer P., (1993). The Avalanche Handbook. The Mountaineers Books, Seattle WA, U.S.A.

108. Marano K. D., Wald D. J., Allen T. I., (2010). Global earthquake causalities due to secondary effect sects: a quantitative analysis for improving rapid loss analyses. Natural Hazards, vol. 52, pp.319-328. doi 10.1007/s11069-009-9372-5.

109. Massa, M., Lovati S., D'Alema, Ferretti E., Bakavoli G., (2010). An Experimental approach for estimating seismic amplification effects at the top of a ridge, and the implication for ground-motion predictions: the case of Narni, Central Italy. Bull. Seismol. Soc. Am. 100 (6), pp. 3020–3034.

110. Marussi A., (1964). Geophysics of the Karakoram, Italian Expeditions to the Karakoram (K-2) and Hindu-Kush, Sci. Rept., 2. 1, 242 pp.

111. Mayeda K., Malagnini L., and Walter W.R., (2007). A new spectral ratio method using narrow band coda envelopes: Evidence for non-self-similarity in the Hector Mine sequence. Geopysical Research Letters, 34 (L11303), pp. 1-5. doi:10.1029/2007GL030041

112. McClung D, and Schearer, P., (2006). The Avalanche Handbook. The Mountaineers Books, Seattle WA, U.S.A. 342 pp.

113. McClung D. M., and Schaerer P., (1993). The Avalanche Handbook, 271 pp., The Mountaineers, Seattle, Wash.

114. McClung D. M., and Schweizer J., (1999). Skier triggering, snow temperatures and the stability index for dry slab avalanche initiation. Journal of Glaciology, 45(150), pp. 190–200.

115. McClung D. M., (2016). Avalanche character and fatalities in the high mountains of Asia. Annals of Glaciology, 57(71), pp. 114-118. doi: 10.3189/2016AoG71A075.

116. Mitchell B.J., (1995). Anelastic Structure and Evolution of the Continental Crust and Upper Mantle from Seismic Sur- face Wave Attenuation. Reviews of Geophysics, 33(4), pp. 441-462.

117. Mohammed A.A.A.S., Naqvi H.R., Firdouse Z., (2015). An assessment and identification of avalanche hazard sites in Uri sector and its surroundings on Himalayan mountain. Journal of Mountain Science, 12(6), pp 1499–151.

118. Molnar P. and Tapponnier P., (1975). Cenozoic tectonics of Asia: effects of continental collision, Science, 189, pp. 419-426.

119. Molnar P. and Tapponier P., (1978). Active Tectonics of Tibet, J. Geophys. Res., 88, pp. 5361-5375.

120. Molnar P., (1988). A review of geophysical constraints on the deep structure of the Tibet plateau, the Himalaya and the Karakoram and their tectonic implications, Phiols, Trans, R. Soc. London Ser., 326, pp. 33-88.

121. Molnar P. and Lyon-Caen H., (1989). Fault plane solutions of earthquakes and active tectonic of the Tibetan Plateau and its margins, Geophys. J. Int., 99, pp. 123-153.

122. Mridula, Sinhval A., Wason H.R., (2016). Identification of seismically susceptible areas in western Himalaya using pattern recognition. J. Earth Syst. Sci., 125(4), pp. 855-871. DOI 10.1007/s12040-016-0698-6

123. Mukhopadhyay S., and Sharma J., (2010). Attenuation characteristics of Garhwal-Kumaon Himalayas from analysis of coda of local earthquakes. Journal of Seismology, 14, pp. 693-713.

124. Murphy M.A., Yin A., Kapp, P., Harrison T.M., Lin D. and Jinghui G., (2000). Southward propagation of the Karakoram fault system, southwest Tibet: Timing and magnitude of slip, Geology, 28, pp. 451–454.

125. Murphy M.A., Yin, A., Kapp P., (2002). Structural evolution of the Gurla Mandatha detachment system, southwest Tibet: implications for the eastward extent of the Karakoram fault system, Geol. Soc. Am. Bull., 114, pp. 428–447.

126. Nagarajan R, Venkataraman G, Snehmani, (2014). Rule Based Classification of Potential Snow Avalanche Areas. Natural Resources and Conservation 2(2), pp. 11-24

127. Nakajima J., Hada S., Hayami E., Uchida N., Hasegawa A., Yoshioka S., Matsuzawa T., and Umino N., (2013). Seismic attenuation beneath northeastern Japan: Constraints on mantle dynamics and arc magmatism. Journal of Geophysical Research: solid Earth. 118, pp. 5838–5855. doi:10.1002/2013JB010388

128. Nefeslioglu HA, Sezer EA, Gokceoglu C, Ayas Z., (2013). A modified analytical hierarchy process (M-AHP) approach for decision

support systems in natural hazard assessments. Computers & Geosciences 59, pp. 1-8.

129. Ni, J. and Barazangi, M., (1984). Seismotectonics of the Himalayan collision zone geometry of the under thrusting Indian plate beneath the Himalaya; J. Geophys. Res. 89(B2), pp. 1147-1163.

130. O'Neill, M. E., (1984). Source dimensions and stress drops of small earthquakes near Park field, California, Bull. Seismol. Soc. Am., 71, pp. 27-40.

131. Oreshin S., Kiselev S., Vinnik L., Surya Prakasam, K., Rai S.S., Makeyeva, L., Savvin, Y., (2008). Crust and mantle beneath western Himalaya, Ladakh and western Tibet from integrated seismic data. Earth and Planetary Science Letters, 271 (1–4), pp. 75–87. doi:10.1016/j.epsl.2008.03.048

132. Paidi V., Kumar A., Gupta S. C., Kumar A., (2013). Estimation of source parameters of local earthquakes in the environs of Koldam site. Arabian Journal of Geosciences, pp.1-12.

133. Pandey, Y., Dharmaraju, R., Chauhan P. K. S., (2001). Estimation of source parameters of Chamoli Earthquake, India. Journal of Earth System Science, 110(2), 171-177

134. Pandit R, Mishra A., (2014) August 20. 18 years after he went missing, armyman's body found in Siachen. Times of India.

135. Pandit R, and Mishra A (2014) August 20. 18 years after he went missing, armyman's body found in Siachen. Times of India.

136. Pandit R (2016), February 03. 10 army soldiers are missing in siachen avalanche years after he went missing, armyman's body found in Siachen. Times of India.

137. Paul A. , Kamal, Ganju A, Rana V, Tyagi D.K., Vikas Juyal, Gosain M and Thakur N., (2011), Source Mechanism studies around Karakoram fault in Siachen region, NW Himalaya. Journal of Himalyan Geology, 32(2), pp 149-157.

138. Paul A., Gupta S.C., and Pant C.C., (2003). Coda Q estimates for Kumaon Himalaya. Proceedings Indian Academy of Sciences, 112, pp. 569-576.

139. Pedersen H., Le Brun, B., Hatzfeld, D., Campillo, M., Bard, P.-Y. (1994). Ground-motion amplitude across ridges. Bull. Seismol. Soc. Am. Vol. 84 (6), pp. 1786–1800.

140. Phillips RJ (2008) Geological Map of The Karakoram Fault Zone, Eastern Karakoram, Ladakh, NW Himalaya. Journal of Maps, pp. 21-37.

141. Podolskiy E.A., Sato A., Komori J., (2009). Avalanche issue in Western Himalaya, India. Seppyo, J. Jpn. Soc. Snow Ice, 71(6), pp. 498‑502.

142. Podolskiy E.A., Nishimura K., Abe O., Chernous P.A., (2010 a). Earthquake-induced snow avalanches: historical case studies. Journal of Glaciology, 56(197). pp.431-446.

143. Podolskiy E., Nishimura K., Abe O., Chernous, P., (2010b). Earthquake-induced snow avalanches: II. Experimental study. J. Glaciol. 56 (197), pp. 447–458.

144. Ragle R. H., Sater J. E., Field W. O., (1965). Effects of the 1964 Alaskan earthquake on glaciers and related features. Arctic Institute of North America. 18 (2), pp135-137.

145. Rai H., (1983). Geology of the nubra valley and its significance on the evolution of the ladakh Himalaya. In: Thakur, V. C., and Sharma, K. K., (eds.), Geology of Indus Suture Zone of Ladakh. Wadia Institute of Himalayan Ggeology Dehradun, p.79-97.

146. Rai S.S., K. Priestley, Suryaprakasam K., Srinagesh D., Gaur V. K., and Du Z., (2003). Crustal shear velocity structure of the south Indian shield, Journal of Geophysical Research., 108(B2). 2088. doi: IO.1029/2()02JBG01776.

147. Rai, S.S., Priestley, K. And Gaur, V.K., (2006). Configuration of The Indian Moho Beneath The NW Himalaya and Ladakh: Geophysical Research Letters, V. 33, P. L15308.

148. Rai S.S., Ashish, A., Padhi, A., Sarma, P.R., (2009). High crustal seismic attenuation in Ladakh-Karakoram. Bulletin of the Seismological Society of America 99 (1). doi:10.1785/012007261.

149. Rajinder Parshad, Snehmani, Kumar P, Srivastva P.K., Ganju A., (2017a). Attenuation of coda waves in the Nubra-Siachen region, NW Himalaya, India. Journal of Geological Society of India, 89, pp.497-502.

150. Rajinder Parshad, Srivastva P.K., Snehmani, Ganguly S., Kumra S. Ganju A., (2017b). Avalanche Susceptibility Mapping in Nubra-Shyok Basin using RS and GIS. Indian Journal of Science and Technology. 10 (31), pp.1-19.

151. Rajinder Parshad, Snehmani, Srivastva P.K., Rani R, Ganju A., (2015), Aseismic Layer Detected in the Mid-Crust of Nubra-Siachen Region, India Using Local Seismic Data, International Journal of Geosciences, Vol. 6, pp 993-1006, DOI: 10.4236/ijg.2015.69079.

152. Rautian T.G., (1976). The roles of source function and medium response in the model of formation of seismic vibrations, in Problems of Engineering Seismology, 18:3-14.

153. Rautian, T.G. and Khalturin, V.I. (1976). Spectral structure of the coda of local earthquakes as an instrument of investigation of the source radiation. Proceedings of the USSR Academy of Sciences, 226, pp. 566-569.

154. Reese C.C. and Ni J.F. (1996). Attenuation of coda waves in southern Tibet. Geophysical Research Letters, 23(21), pp. 3015-3018.

155. Robinson C.A., Yin A., Manning C.E., Harrison T.M., Zhang S.H., Wang X.F., (2004). Tectonic evolution of the northeastern Pamir: Constraints from the northern portion of the Cenozoic Kongur Shan extensional system, western China, Geol. Soc. Am. Bull., 116, pp. 953– 973.

156. Robinson A.C., Yin A., Manning C.E., Harrison T.M., Zhang S.H. and Wang X.F., (2007). Cenozoic evolution of the eastern Pamir: implications for strain-accommodation mechanisms at the western end of the Himalayan–Tibetan orogen, Geol. Soc. Amer. Bull., 7/8, pp. 882–896.

157. Rodriguez C.E., Bommer J.J., Chandler R.J., (1999). Earthquake-induced Landslides 1980-1997. Soil Dynamic and earthquake engineering, 18, pp.325-346.

158. SAC (2016). Monitoring snow and glaciers of Himalaya region, SAC, ISRO, Ahmedabad, India, 413 pages.

159. SASE, Annual Technical Report 2002-2003 (2003) (Unpublished).

160. Saaty T.L. (1980). The Analytical Hierarchy Process. McGraw-Hill, New York.

161. Saaty T.L., and Vargas L.G., (1991). Prediction, projection and forecasting. Dordrecht: Kluwer Academic Publishers; 251 pp.

162. Schaer M. (2012). Earthquake and snow avalanches. COGEAR, pp. 1-14.

163. Schweizer J, Jamieson JB, Schneebeli M., (2003). Snow avalanche formation. Reviews of Geophysics, 41, pp. 10-16.

164. Searle M.P., Dewey, J.F., Dunlap, W.J., Strachan, R.A., Weinberg, R.F., (1998). Transpressional tectonics along The Karakoram Fault Zone, Northern Ladakh; Constraints Ontibetan Extrusion. Geological Society Special Publications; Continental Transpressional and Transtensional Tectonics 135, pp. 307–326.

165. Searle, M.P. and Richard, J.P., (2007). Relationships Between Right–Lateral Shear along The Karakoram Fault and Metamorphism, Magmatism, Exhumation And Uplift: Evidence from The K2-Gasherbrum, Pangong Ranges, North Pakistan And Ladakh. Geological Society of London 164, pp. 439–450.

166. Searle M. P., 1996. Geological evidence against large-scale pre-Holocene offsets along the Karakoram fault: implications for the limited extrusion of the Tibetan Plateau, Tectonics, 15, 171-186.

167. Seeber, L. And Armbruster, J. G., (1981). Great Detachment Earthquakes Along The Himalayan Arc And Long Term Forecasting. In: Earthquake Prediction: An Int. Review, Am. Geophys. Union (Maurice Ewing Series), 4, pp. 259-277.

168. Seluck L., (2013). An avalanche hazard model for Bitlis Province, Turkey, using GIS based multi-criteria decision analysis. Turkish Journal of Earth Sciences 22, pp. 523-535.

169. Shahabi H, Khezri S, Ahmad B.B., Hashim M., (2014). Landslide susceptibility mapping at central Zab basin, Iran: a comparison between analytical hierarchy process, frequency ratio and logistic regression models. Catena 115, pp. 55-70.

170. Shahabi H, Hashim M., (2015). Landslide susceptibility mapping using GIS-based statistical models and Remote sensing data in tropical environment. Nature Scientific Reports, DOI: 10.1038/srep09899.

171. Sharma, M. L., and Wason H. R., (1995). Seismic moment magnitude relationship for the Garhwal Himalaya region; Bull. Ind. Soc. Earth Tech. 351, 32(3), pp. 85-95.

172. Sharma S.S., and Ganju A., (2000). Complexities of avalanche forecasting in Western Himalaya – an overview. Cold Regions Science and Technology, 31, pp. 95 – 102.

173. Singh A., and Ganju A., (2002). Earthquakes and avalanches in western Himalaya. Proceedings of the 12th Symposium on Earthquake Engineering. Indian institute of Technology Roorkee, India.

174. Singh C., Singh, A., Bharathi, V.K.S., Bansal A.R., and Chadha, R.K., (2012a). Frequency- dependent body wave attenuation characteristics in the Kumaun Himalaya. Tectonophysics, 524-525, pp. 37-42.

175. Singh D. D., Rastogi, B. K., Gupta, H. K., (1979). Spectral analysis of body waves for earthquakes and their source parameters in the Himalaya and nearby regions; Phys. Of Earth and Planet. Interior. 18, pp. 143-152.

176. Singh M.K., Gupta R.D., Snehmani, Bhardwaj A, Ganju A., (2016a). Effect of sensor modelling methods on computationof 3-D coordinates from Cartosat-1 stereo data. Geocarto Int, 31(5):506‑526. doi:http://dx.doi.org/10.1080/10106049.2015.1059900.

177. Singh M.K., Gupta R.D., Snehmani, Kumar S, Ganju A., (2016b). Assessment of freely available CartoDEM V1 and V1.1R1 with respect to high resolution aerial photogrammetric DEM in high mountains. Geocarto Int. 31(9):943‑955. doi: http://dx.doi.org/10.1080/10106049.2015.1094524.

178. Singh M.K., Gupta R.D., Snehmani, Bhardwaj A, Ganju A. (2016c). Scenario-based validation of moderate resolution DEMs freely available for complex Himalayan terrain. Pure Appl Geophys. 173:463‑485. doi:http://dx.doi.org/10.1007/ s00024-015-1119-5.

179. Singh V.P., Duda J. & Shanker, D., (2005). A plausible model for the present day seismicity and tectonic activity in the Hindukush complex zone, Journal of Asian Earth Sciences, 25, pp. 147–156.

180. Singh, P., Tripathi, J.N., Kumar, S., (2012b). Quality factor of seismic coda waves in Garhwal Himalayas. International journal of civil engineering and Technology, 3(2), pp. 279-291.

181. Schaer, M. (2012). Earthquake and snow avalanches, WSL Institute for Snow and Avalanche Research, SLF Davos, pp. 1-14.

182. Seeber L. and Armbruster J. G., (1981). Great detachment earthquakes along the Himalayan arc and long term forecasting. In: Earthquake Prediction: An Int. Review, Am. Geophys. Union (Maurice Ewing Series), 4, pp. 259-277.

183. Shekhar M.S., Chand H., Kumar S., Srinivasan K., Ganju A., (2012). Climate-change studies in the western Himalaya. Annals of Glaciology 51(54), pp. 105-112.

184. Smith M.J., McClung D.M., (1997). Avalanche frequency and terrain characteristics at Rogers' Pass, British Columbia, Canada. Journal of Glaciology 43(143), pp. 165-171.

185. Snehmani, Bhardwaj A, Pandit A, Ganju A., (2014). Demarcation of potential avalanche sites using remote sensing and ground observations: a case study of Gangotri glacier. Geocarto International, 29 (5), pp. 520-535.

186. Snehmani, Singh M.K., Pakrasi K, Ganju A., (2016). Monitoring the status of Siachen glacier using the multi temporal remote sensing

approach. In N.J. Raju (Ed) Geostatistical and Geospatial approaches for the characterization of natural resources in the environment.

187. Stocklin J., (1977). Structure correlation of the Alpine range between Iran and central Asia, Mem. H. Ser. Soc. Geol., France, 8, pp. 333-353.

188. Tiwari V.M., Rajasekhar R.P., Mishra D.C., (2009). Gravity anomaly, lithospheric structure and seismicity of Western Himalayan Syntaxis, J. Seismol., 13, pp. 363–370.

189. Tucker B. E. and Brune J. N., (1977). Source mechanism and m-M analysis of aftershocks of the San Fernando Earthquake, Geophysics J., 49, pp. 371-426.

190. Valdiya, K. S., (1980). Geology of Kumaun Lesser Himalaya, Wadia Institute of Himalayan Geology, Dehradun, p 291

191. Valdiya K. S., (1980a). The Two Intracrustal Boundary Thrusts of The Himalaya. Tectnophysics,66, pp. 323-48.

192. Valli F., Arnaud N., Leloup P.H., Sobel E.R., Mahéo G., Lacassin R., Guillot S., Li H., Tapponnier P. and Xu Z., (2007). Twenty million years of continuous deformation along the Karakoram fault, western Tibet: a thermochronological analysis, Tectonics, 26, doi: 10.1029/2005TC001913.

193. Wang, Q. et al. (2001). Present Day Crustal Motion In China Constrained By Global Positioning System Measurements, Science (294).

194. Wang, Q., Zhang, P.Z., Freymueller, J.T., Bilham, R., Larson, K.M., Lai X., You, X., Niu, Z., Wu, J., Li, Y., Liu, J., Yang, Z.,

and Chen, Q., (2001). Present day crustal motion in China constrained by global positioning system Measurements. Science, 294, pp. 574- 577.

195. Wason H. R. and Sharma, M. L., (2000), Source parameters study of local earthquakes in the Garhwal Himalaya Region based on the digital broadband data. 12 WCCE.

196. Wason, H. R., Sharma, M. L., Khan, P. K., Kapoor, K., Nandini, D., Kara V., (1999). Preliminary analysis of broadband seismic data of the Chamoli earthquake of March 29, 1999 and its aftershock sequence. In Proc. of the workshop on Chamoli Earthquake and its Impact WIHG, Dehradun, India.

197. Wittlinger G., Vergne J., Tapponnier P., Farra V., Poupinct, G., Su M.J.H., Herquel, G. and Paul, A., (2004). Teleseismic imaging of subducting lithosphere and Moho offsets beneath western Tibet, Earth Planet. Sci. Lett., 221, pp. 117–130.

198. Woerd J., Owen L. A., Tapponnier P., Xiwei X., Kervyn F., Finkel R. C., Barnard P. L., (2004). Giant, ~M8 earthquake-triggered ice avalanches in the eastern Kunlun Shan, northern Tibet: Characteristics, nature and dynamics. Bulletin of Geological Society of America, 116(3/4), pp. 394–406.

199. Yang QL, Gao JR, Wang Y, Qian B.T., (2011). Debris flows characteristics and risk degree assessment in Changyuan Gully, Huairou District, Beijing. Procedia of Earth and Planetary Science 2, pp. 262-271.

200. Yilmaz B., (2016). Application of GIS-Based Fuzzy Logic and Analytical Hierarchy Process (AHP) to Snow Avalanche Susceptibility Mapping, North San Juan, Colorado. Thesis, University of Colorado, Boulder, p 94.

201. Yin, A., and Harrison, T.M., (2000). Geologic Evolution of Himalayan-Tibet Orogen. Annual Review of Earth and Planetary Science, 28 (1), pp. 211-280.

202. Yin J.X., and Bian Q.T., (1995). Geological Map of the Karakoram Mountain-West Kunlun Mountain and Adjacent Areas (in Chinese), Beijing, Science Press.

203. Yin, A., Rumelhart, P.E., Butler, R., Cowgill, E., Harrison, T.M., Foster, D.A., Ingersoll, R.V., Qing, Z., Xian-Qiang, Z., Xiao-Feng,W., Hanson, A. & Raza, A., (2002). Tectonic history of the Altyn Tagh fault system in northern Tibet inferred from Cenozoic sedimentation, Geol. Soc. Amer. Bull., 114, 1257–1295.

204. Zeng Z.S., Ding Z.F., Wu Q.J., et al., (2000). Seismological Evidence for Multiple Incomplete Crustal Subductions in the Himalayas and Southern Tibet, China. Chinese Journal of Geophysics, 43(6), pp. 780–797 (in Chinese with English Abstract).

205. Zobin V. M., and Hasakov J., (1995). Source spectral properties of small earthquakes in the northern North Sea. Tectonophysics. 248, pp. 207-218

206. Zweig M.H., Campbell G., (1993). Receiver-operating characteristic (ROC) plots: a fundamental evaluation tool in clinical medicine. Clin. Chem., 39(4), pp. 561-577.

APPENDIC-1: BIO-DATA OF THE AUTHOR

RAJINDER PARSHAD

Ph.D. (pursuing), M. Tech. (Applied Geophysics)

Email: sharma.dab@gmail.com

Mob: +91-9467682466

Educational Profile

- **Ph.D. Earth sciences (Geophysics),** (pursuing) from University of Petroleum & Energy Studies, Dehradun (India).
- **M.Tech. Applied Geophysics** from Department of Geophysics Kurukshetra University, Kurukshetra with 74.48% marks in July, 2009.
- **B.Sc.** from Kurukshetra University, Kurukshetra with Physics, Geology and Mathematics with 71.00% marks in June, 2006.

Research Papers In Referred Journals

- **Rajinder Parshad,** Parveen Kumar, Snehmani and P.K.Srivastva (2018) "Seismically Induced Snow Avalanches at Nubra- Shyok region of Western Himalaya, India", Natural Hazards (communicated).
- **Rajinder Parshad,** Snehmani, Parveen Kumar, Reeta Rani, P.K.Srivastva and A.Ganju (2017a) "Attenuation of coda waves in the Nubra-Siachen region, NW Himalaya, India", Journal of Geological Society of India. 89, pp.497-502.
- **Rajinder Parshad,** P.K.Srivastva, Snehmani, S.Ganguly and A.Ganju (2017b) ," Avalanche Susceptibility Mapping in Nubra-Shyok Basin using RS and GIS ", Indian Journal of Science and Technology Vol. 10, Issue 31, pp.1-19.
- **Rajinder Parshad,** Snehmani, P K Srivastva, Reeta Rani, A. Ganju (2015), "Aseismic layer detected in the mid-crust of Nubra-Siachen region, India using local seismic data**..**" International Journal of Geo sciences, 6, pp. 993-1006.
- **Rajinder Parshad,** Snehmai, Reeta Rani, V. Ghanghas, A. Kumar, V.Rana, P. Joshi, P.K. Shrivastva, A. Ganju (2014), "Source Parameters of Local Eartquakes in Nubra Region, NW Himalaya". Intl

Journal of Advanced Research , Vol 2, Issue 8, pp 151-158.

Research Papers in Conferences

- Bhutiyani, M.R, Ravikant and **Rajinder Parshad** (2015**),** "Mass movement events in upper Karakoram Himalayas: Implication of climate change", Journal of Engineering Geology, Vol. XL No1, pp 7-20.
- Bhutiyani, M.R, Ravikant and **Rajinder Parshad** (2014), "Glacier surface velocity: Spatio-Temporal monitoring of Landslide Debris" in National Conference of Himalayan Glaciology-2014 at Shimla, HP (India).
- Bhutiyani, M.R, **Rajinder Parshad,** Sudhanshu Shekhar, A.Ganju**,** Snehmani (2013) "Manifestations of climate change in Karakoram Himalayas: Extreme precipitation event induced earth-flow over the Siachen Glacier in Nubra Valley" proceedings of International Symposium on Cryosphere & Climate Change(ISCCC-2012).
- **Rajinder Parshad,** Snehmai, Vikas Rana, N K Thakur, Bhutiyani M.R, (2012) "Seismogenic Avalanches in Siachen region India: A case study" in International Symposium on Cryosphere & Climate Change(ISCCC-2012), April 2012 at Manali, India.
- **Rajinder Parshad,** Snehmai, A.Ganju, Vikas Rana (2011) "Mid-Crustal aseismic layer beneath seismically active brittle layer in Siachen region, India as revealed by the focal depth of local earthquake events in the region" in International conference on Indian monsoon & Himalayan Geodynamics (IMHG-2011), Nov. 2011 held at WIHG, Dehradun, India.

Specialised Training/Workshop Attended

- Two weeks **TiP & TPE Science & Technology training** on **"Glaciers and Glaciations in the context of climate change" at** Grindelwald **Switzerland** and Tubingen **Germany** in August, 2013 .
- 4th **Third Pole Environment (TPE)** workshop at WIHG, Dehradun, India during 02-04, April, 2013.

- One week training on installation of seismic instruments in glaciated regions, at RMPL, Chennai (India)
- One week training on seismic data processing of glaciated regions at **IMD, Delhi** (India)
- Five weeks **Summer Training** on **"Seismology with special emphasis on earthquake location"** at **National Geophysical Research Institute (NGRI)**, Hyderabad in June, 2007.

Experience

- Currently working at **National Center of Excellence in Geosciences Research, Geological Survey of India (GSI)**, Faridabad.
- Worked as SRF in MoES sponsored project entitled **"Seismicity monitoring around Karakoram fault through Seismic netwotk in Siachen region"** from 03 May, 2011 to 24 Feb. 2012 at **Snow and Avalanche Study Estt. (SASE)-RDC,** Chandigarh.
- Worked as JRF in DST sponsored project entitled **"Study of Atmospheric and Avalanche parameters affecting Gangotri Glacier"** from 14 Oct. 2010 to 02 May 2011 at **Snow and Avalanche Study Estt. (SASE)-RDC,** Chandigarh.
- Worked as Teaching Associate from 09 Sept., 2009 to 15 May, 2010 at **Department of Geophysics**, Kurukshetra University, Kurukshetra (India)**.**

Professional Memberships

- Society of Cryospheric Science **(SCS)**, Chandigarh, India
- Indian Society of Remote Sensing **(ISRS)**, Dehradun, India
- Society of Exploration Geophysicists **(SEG),** Tulsa, OK (USA).
- Society of Petroleum Geophysicists **(SPG),** ONGC, India.
- European Association of Geoscientists and Engineers **(EAGE**)

APPENDIC-2: REPRINT OF PUBLISHED RESEARCH PAPERS

PAPER 1:

Rajinder Parshad, Snehmani, Parveen Kumar, Reeta Rani, P.K.Srivastva and A.Ganju (2017) "Attenuation of coda waves in the Nubra-Siachen region, NW Himalaya, India", Journal of Geological Society of India.

JOURNAL GEOLOGICAL SOCIETY OF INDIA
Vol.89, May 2017, pp.497-502

Attenuation of Coda Waves in the Nubra-Siachen Region, Himalaya, India

Rajinder Parshad[1*], Snehmani[2], Parveen Kumar[3], P. K. Srivastva[4] and A. Ganju[2!]

[1] Geological Survey of India, NH-5P, NIT, Faridabad - 121 001, India
[2] SASE-RDC, DRDO, Plot No.1, Sector-37, Chandigarh - 160 036, India
[3] Wadia Institute of Himalayan Geology, 33, GMS Road, Dehradun - 248 001, India
[4] University of Petroleum & Energy Studies (UPES, Bidholi Campus, Dehradun - 248 007, India
E-mail: sharma.dab@gmail.com*; snehmani@sase.drdo.in[2]; sainiparveen.saini@gmail.com[3]; pksrivastava@ddn.upes.ac.in[4]; a.ganju@sase.drdo.in[!]

ABSTRACT

The attenuation properties have been estimated in the Nubra-Siachen region situated in the highly mountainous region of Himalayan belt. Coda wave quality factor (Q_c) has been determined for this virgin region by using the single backscattering method. A total of thirty earthquakes recorded in this region, which fall in the epicentral distance range of 3 to 115km have been used for the present work. A 30 sec window length of coda waves at different central frequencies 1.5, 3.0, 6.0, 9.0, 12.0, 18.0 and 24.0 Hz have been studied to determine Q_c at different recording stations. The frequency dependent coda wave quality factor relationships of the form $Q_c(f) = Q_o f^n$, have been computed at each recording stations separately: BASE: $Q_c(f) = (137 \pm 4.2)\ f^{(0.99 \pm 0.12)}$, CHALUNKA: $Q_c(f) = (116\pm3.8)f^{(1.0\pm0.05)}$, PARTA: $Q_c(f) = (122\pm3.0)f^{(1.0\pm0.02)}$, and SASOMA: $Q_c(f) = (111\pm4.1)f^{(1.0\pm0.03)}$. A regional Q_c relation has been developed for the Nubra-Siachen region by using the average value of Q_c at different frequencies obtained at each recording station of the form $Q_c(f) = (121\pm7.2)f^{(1.0\pm0.04)}$. The average Q_c values vary from 183 at 1.5 Hz to 3684 at 24 Hz central frequencies. The present regional relation developed for Nubra-Siachen region indicates heterogeneous and tectonically active region.

INTRODUCTION

The Eurasian plate and the Indian plate started colliding about 55 Ma ago (Yin and Harrison, 2000) and is still continuing at the present time (Wang et al., 2001). This successive collision forms the Himalaya. The collision has also resulted into large scale thrusting and the same has progressed southward forming the Main Central Thrust (MCT) and Main Boundary Thrust (MBT). The Indus-Tsangpo Suture (ITSZ) located about 250 km, north of MCT marks the pre-collision boundary along which the Indian plate subducted below the Eurasian plate and the subduction ended in Eocene times (Gansser, 1964). Along the MCT, the higher Himalaya overthrusted the lesser Himalaya and along MBT, the lesser Himalaya thrusted over the Siwaliks. The Nubra-Siachen region is situated in the highly mountainous terrain of higher Himalaya. This region is of strategic importance for the countries sharing their borders in the region. This region is considered as virgin region as, till now no study has been made regarding the attenuation characteristics of this area. Attenuation characteristics of medium decide the decay of the amplitude of ground motion at various sites. The attenuation characteristics of a region can provide essential information, regarding earthquake hazard of that region. Various techniques have been developed to study the attenuation characteristic of seismic waves using different parts of the seismogram (e.g., Aki, 1969; Aki and Chouet, 1975; Hermann, 1980; Mitchell, 1995). Quantitatively attenuation characteristics have been studied by using a factor named as quality factor. The quality factor 'Q' is defined as the fractional loss of energy per cycle (Knopoff, 1964). In the present work, single back scattering method proposed by Aki and Chouet (1975) has been used to determine the coda wave quality factor (Q_c) for Nubra-Siachen region, India. In this method coda waves have been utilized to estimate the quality factor.

Ground motion in the vicinity of earthquakes often dies away slowly leaving a coda wave following the direct body waves and surface waves because of inhomogeneities in the earth. These seismic coda waves are backscattered waves from numerous randomly distributed heterogeneities in the earth (Aki, 1969; Aki and Chouet, 1975; Rautian, 1976; Rautian and Khalturin, 1976). The single backscattering model proposed by Aki and Chouet (1975) suggests that coda waves are interpreted as backscattered body waves generated by the numerous heterogeneities present in the Earth's crust and upper mantle. It implies that scattering is a weak process and outgoing waves are scattered only once before reaching the receiver. Under this assumption the coda amplitudes for a central frequency is related to the source function, lapse time and quality factor. In the present work, coda waves of 30 sec window length, filtered at six frequency bands centered at 1.5, 3, 6, 9, 12, 18 and 24 Hz, have been used to study the attenuation characteristics of Nubra-Siachen region, India.

TECTONIC SETTING AND DATA

Nubra region is tectonically disturbed (Rai, 1983). The prominent tectonic feature of this region is, approximately 800 km, dextral strike slip Karakoram fault. The Karakoram fault separates rocks of the Karakoram and Ladakh terrains. The Karakorum fault runs almost parallel to the main body of Siachen glacier. The other major tectonic features of this region are Karakoram shear zone, Shyok suture zone and Khalsar thrust. The intervention of strongly mylonitized granite gneiss, volcanic, conglomerate, slate, phyllite-limestone intercalations, amphibolites and serpentinite in the Shyok suture zone and the frontal Asian plate margin along the Nubra–Shyok valleys forms the Karakoram shear zone (KSZ) (Jain and Singh, 2009). This is very narrow in width (1-5Km) and extends for nearly 200 km in Nubra valley, Shyok suture zone (SSZ) is an association of dismembered ultramafics, gabbro, basalt and sediments having chert, shale and Orbitolina-bearing limestone (Jain and Singh, 2009). Karakoram batholith complex (KBC) comprises of various lithology such as biotite granite, leucogranite, metamorphics. Monotonous vertical cliffs of biotite-muscovite granite in upper parts of Nubra valley beyond Panamik constitute the main body of the Karakoram batholith (Jain and Singh, 2009).

The data of local seismological network comprising of four broad band recording station installed in Nubra region, Jammu & Kashmir has been used in the present work. Geographical coordinates of stations are given in Table 1. This network is situated in the highly mountainous

0016-7622/2017-89-5-497/$ 1.00

Table 1. Geographical coordinates of stations used in the present work

Sr. No.	Station Name	Station Code	Latitude (Degree)	Longitude (Degree)	Elevation (m) MSL
1	Sasoma	SASO	77.49 E	34.92 N	3430
2	Parta	PTPR	77.41 E	34.61 N	3180
3	Base	BASE	77.20 E	35.18 N	3455
4	Chalunka	CHLK	77.12 E	34.82 N	3180

terrain of Ladakh Himalaya, where elevations of recording stations from mean sea level lie between 3180 to 3455 m. The four recording station used the same type of instrumentation i.e. the Trillium 120P broadband seismometer and Taurus 24 bit data acquisition system. These instruments are operational in continuous mode. Sampling interval of digital data is kept at 0.01 sec. A total of thirty earthquakes recorded at this network have been used in the present study. The location of earthquakes and recording stations is shown in Fig. 1. The parameters of the events used in the present work are given in Table 2. An example of the seismograms recorded at all the four stations is shown in Fig. 2.

METHODOLOGY

In the present work, single backscattering model proposed by Aki and Chouet (1975) has been used to estimate coda wave quality factor. According to this model the coda waves are interpreted as back-scattered body waves generated by the numerous heterogeneities present in the Earth's crust and upper mantle. Under this assumption the coda amplitude, A(f, t) in a seismogram can be expressed for a central frequency 'f' over a narrow bandwidth signal, as a function of the lapse time 't', measured from the origin time of the seismic event, as

$$A(f, t) = S(f)\, t^{-a} \exp(-\pi f t/Q_c) \quad (1)$$

where S(f) represents the source function at frequency 'f', and is considered a constant as it is independent of time and radiation pattern, and therefore, not a function of factors influencing energy loss in the medium; 'a' is the geometrical spreading factor, and taken as 1 for body waves, and Q_c is the quality factor of coda waves representing attenuation in a medium. By taking logarithm of equation (1), it is linearized as given below:

$$\ln [A(f,t)] = \ln S(f) - \ln(t) - (\pi f t/Q_c) \quad (2)$$

$$\ln[A(f, t)\, t] = C - b\, t \quad (3)$$

where in equation (3), the term 'b' and 'C' represent $\pi f/Q_c$ and ln S(f), respectively. Equation (3) is an equation of straight line. Hence, Q_c can be obtained from the slope of the ln[A(f, t) t] versus 't' curve.

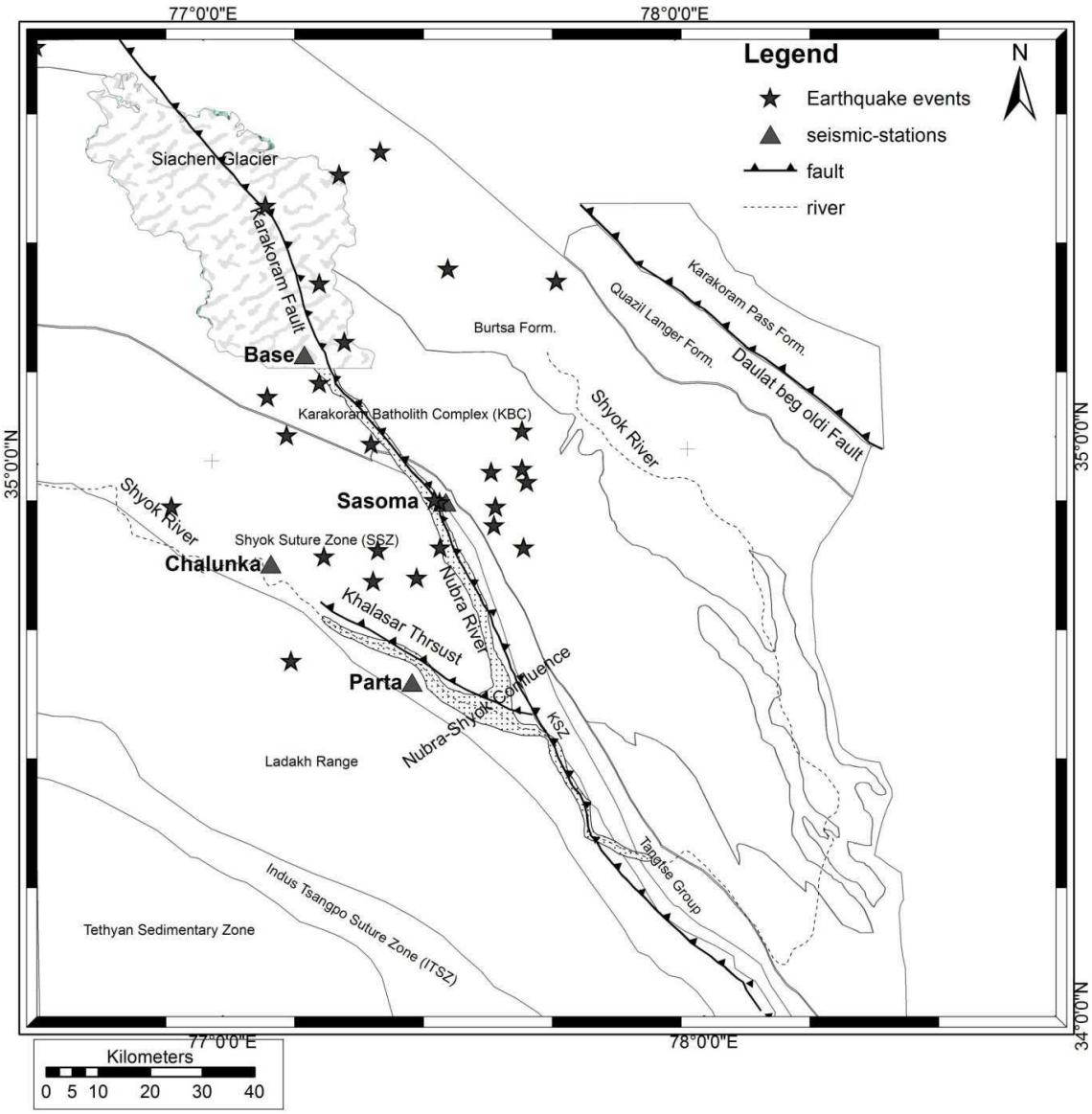

Fig. 1 The location of recording stations and epicenters of the events used in the present study along with the tectonic map of the region.

Table 2. The parameters of the events used in present work

Sr. No.	Hypocentral Parameters						Waveform used for the stations (Station code)
	dd-mm-year	Origin Time Hr:Min:Sec	Long (degree)	Lat (degree)	Depth (km)	Mw	
1	01-01-2010	10:19:13	77.370	35.528	10	2.5	PTPR, BASE, CHLK
2	08-01-2010	13:24:10	77.230	35.131	10	3.7	PTPR
3	14-01-2010	08:32:51	77.425	34.791	10	3.8	SASO, PTPR
4	17-01-2010	07:09:52	77.232	34.831	10.3	2	SASO, PTPR
5	22-01-2010	02:51:07	77.466	34.924	3.2	2.6	PTPR
6	08-02-2010	04:14:22	77.477	34.920	10	4.2	SASO
7	10-02-2010	03:19:14	77.159	35.042	56.2	1.7	BASE
8	11-02-2010	01:42:44	77.507	35.323	10	1.8	SASO
9	11-02-2010	11:51:19	77.590	34.878	9	1	SASO, BASE
10	14-02-2010	06:09:34	77.651	34.838	80.6	1.7	BASE
11	23-04-2010	00:02:05	77.735	35.297	10	1.8	SASO, BASE
12	29-04-2010	12:28:33	77.654	35.040	12	2.6	SASO,BASE
13	14-05-2010	02:27:26	76.644	35.721	16.8	3.7	BASE
14	11-07-2010	13:40:10	77.125	35.439	120	2.1	BASE
15	16-07-2010	21:51:17	77.336	35.024	9.5	1.8	BASE
16	12-08-2010	03:06:03	77.594	34.910	14.2	2.5	PTPR, CHLK
17	16-08-2010	00:30:59	77.652	34.974	12.8	3.2	CHLK
18	24-08-2010	11:21:14	77.282	35.490	10.9	3.2	BASE
19	02-09-2010	03:04:03	77.476	34.842	45.7	4.4	BASE, CHLK
20	05-09-2010	04:15:02	77.587	34.970	8.7	2.7	PTPR, CHLK
21	06-09-2010	23:30:15	77.334	34.787	6.5	3.6	PTPR, CHLK
22	09-09-2010	16:13:12	77.345	34.840	12.3	4.5	PTPR, CHLK
23	11-09-2010	05:11:53	77.661	34.951	47.6	2.8	SASO, BASE
24	17-09-2010	14:11:16	77.661	35.926	13.2	4.1	SASO, PTPR, CHLK
25	19-09-2010	03:12:18	77.235	35.303	0.1	3.6	CHLK
26	01-10-2010	02:00:27	77.158	34.652	10.7	3	PTPR, CHLK
27	15-10-2010	01:34:38	77.158	34.652	46	2.6	SASO
28	28-10-2010	10:43:14	77.285	35.201	10	4	SASO, PTPR, BASE, CHLK
29	02-12-2010	12:21:24	76.914	34.923	10	3	BASE,CHLK
30	19-12-2010	11:18:21	77.120	35.109	10	3.4	BASE,CHLK

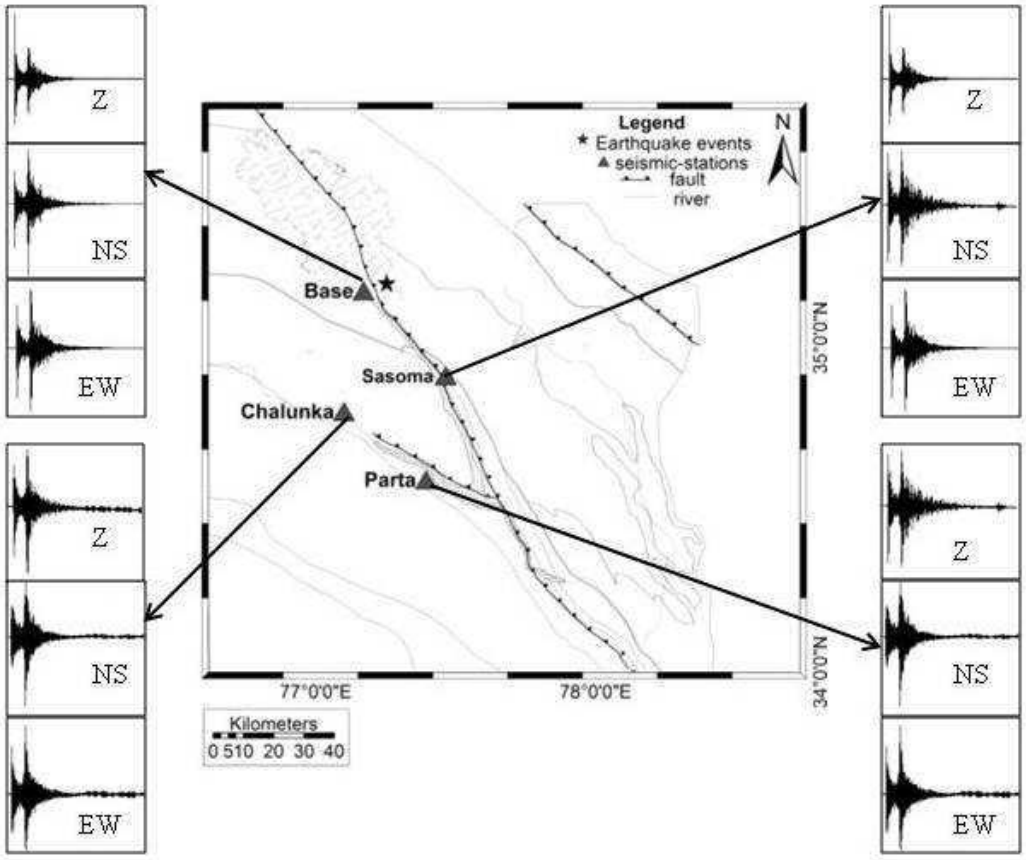

Fig. 2 Three component of seismogram of the event occurred on 28.10.2010 at all the four stations. The epicenter of the event and recording stations are denoted by star and triangle, respectively.

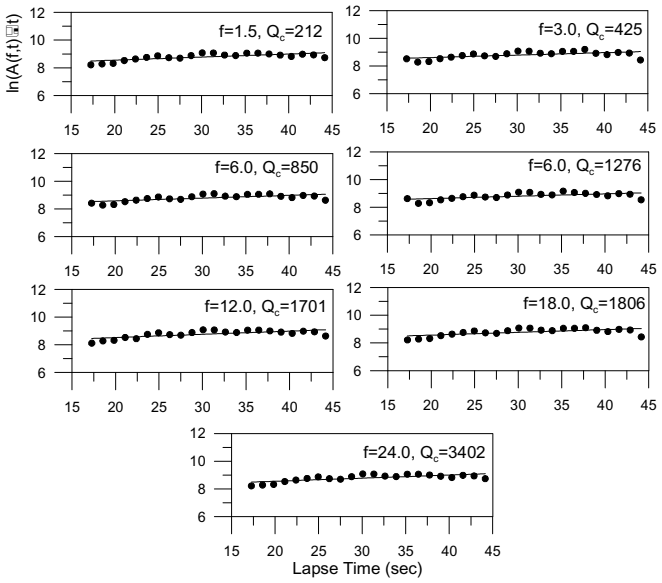

Fig. 3. Plot between logarithmic coda amplitudes and lapse time for difference central frequencies at Base station for the events occurred on 16-07-2010.

Table 3. Obtained Q_c relation at each recording station.

Sr. No.	Station Name	Station Code	Obtained Q_c Relation
1	BASE	BASE	$(137\pm4.2)f^{(0.99\pm0.12)}$
2	CHALUNKA	CHLK	$(116\pm3.8)f^{(1.0\pm0.05)}$
3	PARTA	PTPR	$(122\pm3.0)f^{(1.0\pm0.02)}$
4	SASOMA	SASO	$(111\pm4.1)f^{(1.0\pm0.03)}$

Table 4. Q(f) Relationship for Himalaya region, India.

Attenuation relation	Region	Reference
$Q(f) = 126f^{0.95}$	Garhwal Himalaya	Gupta et al. (1995)
$Q(f) = 30f^{1.21}$	Garhwal	Mandal et al. (2001)
$Q(f) = 86f^{1.02}$	NE Himalaya	Gupta and Kumar (2002)
$Q(f) = 92f^{1.07}$	Kumaon Himalaya	Paul et al. (2003)
$Q(f) = 158f^{1.05}$	NW Himalaya	Kumar et al. (2005)
$Q(f) = 112f^{0.97}$	Garhwal Himalaya	Joshi (2006)
$Q(f) = 87f^{0.71}$	Garhwal region	Sharma et al.(2009)
$Q(f) = 104f^{1.3}$	Kumaon Himalaya	Singh et al. (2012a)
$Q(f) = 61.8f^{0.992}$	Garhwal Himalaya	Singh et al. (2012b)
$Q(f) = 119f^{0.99}$	Garhwal-Kumaon Himalaya	Mukhopadhyay and Sharma (2010)
$Q(f) = 28f^{1.2}$	Kumaon Himalaya	Parveen Kumar et al. (2015)

The coda waves of 30 sec duration, observed on all the event-station pairs, have been analysed in the present work. The starting time of this 30 sec window is considered by using the S-wave travel time (t_s) and it is taken as twice the t_s in the present work (Rautian and Khalturin 1978). At these window lengths all the seismograms are band pass filtered at central frequencies of 1.5, 3.0, 6.0, 9.0, 12.0, 18.0 and 24.0 Hz. The Q_c values corresponding to different central frequencies are used to calculate the frequency dependent coda-Q relation.

RESULTS AND DISCUSSION

Coda waves of 30 sec window length, at different central frequency of 1.5, 3, 6, 9, 12, 18 and 24 Hz, have been analyzed to estimate Q_c relation for the Nubra-Siachen region. In the present work, Q_c relation of form $Q_o f^n$ has been determined at four stations and the Q_c value obtained at each station is further used to determine regional Q_c relation for Nubra-Siachen region, NW Himalaya. The Q_c relation is estimated for all the three component i.e. North-South (NS), East-West (EW) and vertical (Z). The average value of Q_c from these three component provide us the final Q_c relation at a station as given in Table 3. The number of events used at BASE, SASOMA, CHALUNKA and PARTA stations are 15, 11, 13 and 12, respectively. The slope of linear equation (3) between logarithmic coda amplitudes and lapse time gives the Q_c values at different central frequencies and is shown in Fig. 3 at base station for the event occurred on 16-07-2010. Figure 3 shows value of Q_c obtained at different central frequencies for a particular event. Thus several values of Q_c are obtained at each central frequency

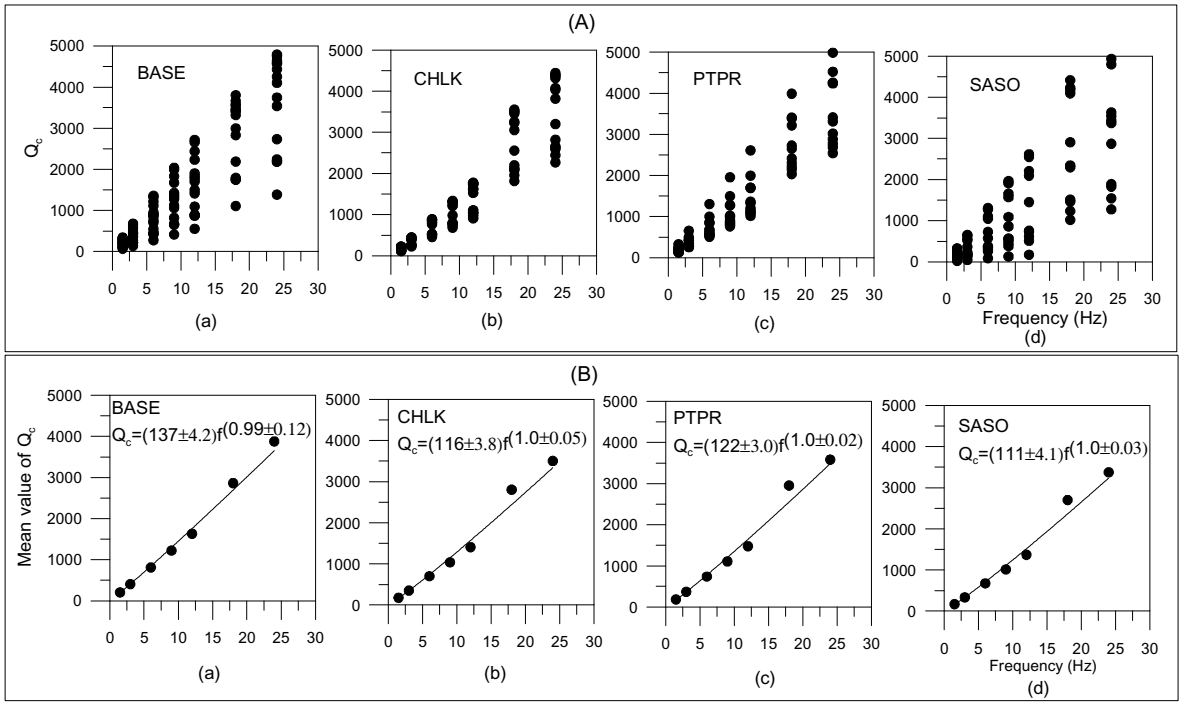

Fig. 4 (A) Plot of obtained Q_c values as a function of frequency and **(B)** Mean values of Q_c as a function of frequency at **(a)** BASE, **(b)** CHALUNKA, **(c)** PARTA and **(d)** SASOMA station, respectively.

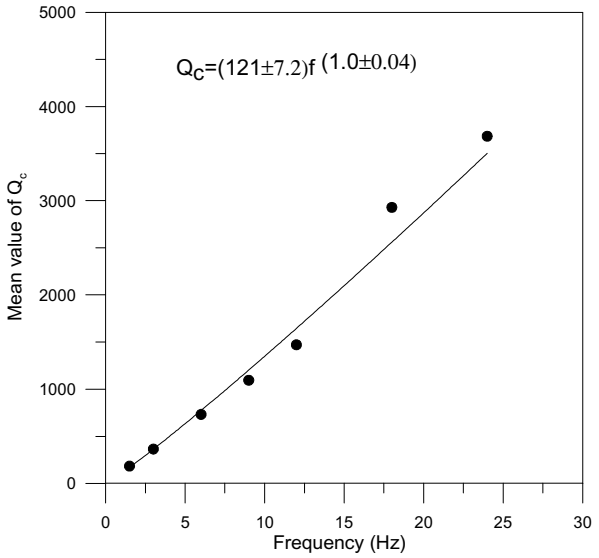

Fig.5. Regional $Q_c(f)$ relationship for Nubra-Siachen region based on the obtained value of Q_c at different stations.

corresponding to several number of events i.e. Q_c values vary from 69 to 339 at 1.5 Hz and 1385 to 4789 at 24 Hz at BASE station; 113 to 222 at 1.5 Hz and 2269 to 4442 at 24 Hz at CHALUNKA station; 21 to 327 at 1.5 Hz and 1274 to 4934 at 24 Hz at SASOMA station; 127 to 326 at 1.5 Hz and 2540 to 4984 at 24 Hz at PARTA station as shown in Fig. 4(A). The mean value of Q_c is calculated at each frequency and it is further used to develop Q_c relation of form $Q_o f^n$ at each recording station as shown in Fig. 4(B). The Q_c relation computed

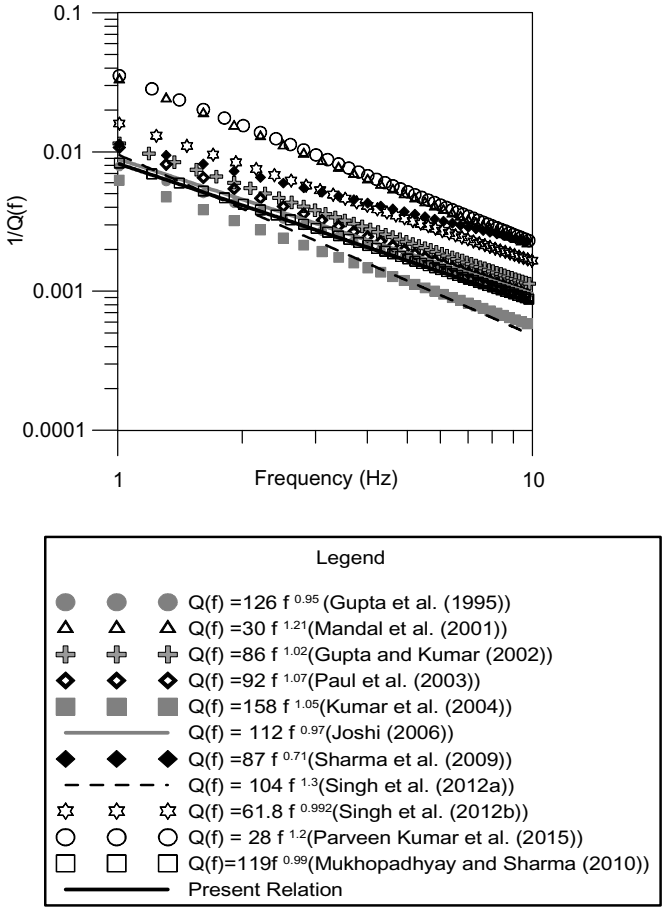

Fig.6. Comparison of $Q_c(f)$ relation obtained in present work with the available relation of Himalaya region.

at each station is given in Table 3. The final values of Q_c obtained at each station is further used to calculate regional Q_c relation for Nubra-Siachen region and is plotted in Fig. 5. The best fit line gives $(121\pm7.2)f^{(1.0\pm0.04)}$, which represent regional attenuation characteristics of the Nubra-Siachen region of Himalaya. The $Q_o f^n$ relation is used for separating different regions into active and stable groups. The parameter 'Q_o' and 'n' in this relation represent heterogeneities and level of tectonic activity of the region, respectively. This relation propose low values of Q_o (<200) for tectonically and seismically active regions and high Q_o (>600) for seismically stable region and intermediate values for moderate regions (Kumar et al., 2005). Regions with higher 'n' (>0.8) value manifest local heterogeneities. It is seen that the calculated value of Q_o varies in between 121±7.2 and 'n' varies in between 1.0±0.04 indicating tectonically active and highly heterogeneous region.

A comparison of Q_c obtained in the present work has been made with available Q relations in Himalaya region. It is seen from Table 4 that for Himalayan region, 'Q_o' and 'n' varies from 28 to 158 and 0.71 to 1.3, respectively and the obtained relation for Nubra-Siachen region lies within this range. The relation provided by Mukhopadhyay and Sharma (2010) for Garhwal-Kumaon Himalaya i.e. $Q(f) = 119f^{0.99}$ as tabulated in Table 4, gives the closest resemblance with the obtained Q_c relation for Nubra-Siachen region. As Mukhopadhyay and Sharma (2010) has also used the same method with similar lapse time ($2t_s$) and coda length (30s) and their study region is also not very far from present study area and these factors may be responsible for this resemblance. Comparison of present relation with available relations of Himalaya region is shown in Fig. 6 and it revealed that the relation obtained in present work falls within the range of values that are justified for tectonically active Himalaya regions.

CONCLUSIONS

In the present work, attenuation characteristics have been determined for Nubra-Siachen region, Himalaya, India as it is a virgin area regarding the attenuation studies. In this paper single back scattering method has been used to obtain regional Q_c relation for Nubra-Siachen region, Himalaya, India. Data of thirty events recorded at four stations in Nubra-Siachen region have been used in this study. In this work Q_c relation at each station is obtained individually. The values of Q_c obtained at four different stations further used to obtain a regional regression relation of form $Q_c(f) = (121\pm7.2)f^{(1.0\pm0.04)}$, which represent the attenuating property of rocks in the Nubra-Siachen region. Low value of Q_o and high value of 'n' obtained in the present $Q_c(f)$ relation shows that the region is seismically active and characterized by local heterogeneities.

Acknowledgements: The research was funded by the Ministry of Earth Sciences, Government of India; grant no. MoES/P.O(Seismo)/1(83)/2010, dated 10/08/2010 and grant no. MoES/P.O(Seismo)/1(267)/2016, dated 12/01/2016. The authors extend their thanks to the SASE personnel's for field data collection. Author Parveen Kumar sincerely acknowledges Director, Wadia Institute of Himalayan Geology, Dehradun.

References

Aki, K. (1969) Analysis of the seismic coda of local earthquakes as scattered waves. Jour.f Geophys. Res., v.74, pp.615-631.

Aki, K. and Chouet, B. (1975) Origin of the coda waves: source attenuation and scattering effects. Jour. Geophys. Res., v.80, pp.3322-3342.

Gansser, A. (1964) Geology of the Himalayas. Willey Interscience, London, 289p.

Gupta, S.C. and Kumar, A. (2002) Seismic wave attenuation characteristics of three Indian regions: a comparative study. Curr. Sci., v.82, pp.407-413.

Gupta, S.C., Singh, V.N., and Kumar A. (1995) Attenuation of Coda Waves in the Garhwal Himalaya, India. Physics Earth Planet. Inter., v.87, pp.247-253.

Hermann, R. (1980) Q estimates using Coda of local earthquakes. Bull. Seismol. Soc. Amer., v.70(2), pp.447-468.

Jain, A.K. and Singh, S. (2009) Geology and Tectonics of Southeastern Ladakh and Karakoram. Geol. Soc. India, Banglore, 181p.

Joshi, A. (2006) Use of acceleration spectra for determining the frequency dependent attenuation coefficient and source parameters. Bull. Seismol. Soc. Amer., v.96, pp.2165-2180.

Knopoff, L. (1964) Q. Rev. Geophys., v.2(4), pp.625-660.

Kumar, N., Parvez, I.A., and Virk, H.S. (2005) Estimation of coda wave attenuation for NW Himalayan region using local earthquakes. Phys. Earth Planet. Inter., v.151, pp.243-258

Kumar, P., Joshi, A., Sandeep, Kumar, A. and Chadha, R.K. (2015) Detailed Attenuation Study of Shear Waves in the Kumaon Himalaya, India, Using the Inversion of Strong-Motion Data. Bull. Seismol. Soc. Amer., v.105(4), DOI:10.1785/0120140053

Mandal, P., Padhy, S., Rastogi, B.K., Satyanarayana, V.S., Kousalya, M., Vijay-raghavan, R. and Srinvasa, A. (2001) Aftershock activity and frequency dependent low coda Qc in the epicentral region of the 1999 Chamoli earthquake of Mw 6.4. Pure Appld. Geophys., v.158, pp.1719-1735.

Mitchell, B.J. (1995) Anelastic Structure and Evolution of the Continental Crust and Upper Mantle from Seismic Surface Wave Attenuation. Rev. Geophys., v.33(4), pp.441-462.

Mukhopadhyay, S. and Sharma, J. (2010) Attenuation characteristics of Garhwal-Kumaon Himalayas from analysis of coda of local earthquakes. Jour. Seismol., v.14, pp.693-713.

Paul, A., Gupta, S.C., and Pant, C.C. (2003) Coda Q estimates for Kumaon Himalaya. Proc. Indian Acad. Sci., v.112, pp.569-576.

Rai, H. (1983) Geology of the nubra valley and its significance on the evolution of the ladakh Himalaya. *In:* Thakur, V. C. and Sharma, K.K., (Eds.), Geology of Indus Suture Zone of Ladakh. Wadia Institute of Himalayan Ggeology Dehradun, pp.79-97.

Rautian, T.G. (1976) The roles of source function and medium response in the model of formation of seismic vibrations, in Problems of Engineering Seismology, v.18, pp.3-14.

Rautian, T.G. and Khalturin, V.I. 1976: Spectral structure of the coda of local earthquakes as an instrument of investigation of the source radiation. Proc. USSR Acad. Sci., v.226, pp.566-569.

Rautian, T.G. and Khalturin, V.I. (1978) The use of the coda for the determination of the earthquake source spectrum. Bull. Seismol. Soc. Amer., v.68, pp.923–948.

Sharma, B., Teotia, S.S., Kumar, D., and Raju, P.S. (2009) Attenuation of P- and S-waves in the Chamoli Region, Himalaya, India. Pure Appld. Geophys., v.166, pp.1949-1966.

Singh, C., Singh, A., Bharathi, V.K.S., Bansal A.R., and Chadha, R.K. (2012a) Frequency- dependent body wave attenuation characteristics in the Kumaun Himalaya. Tectonophysics, v.524-525, pp.37-42.

Singh, P., Tripathi, J.N., Kumar, S. (2012b) Quality factor of seismic coda waves in Garhwal Himalayas. Internat. Jour. Civil Engg. Tech., v.3(2), pp.279-291.

Wang, Q., Zhang, P.Z., Freymueller, J.T., Bilham, R., Larson, K.M., Lai X., You, X., Niu, Z., Wu, J., Li, Y., Liu, J., Yang, Z., and Chen, Q., 2001: Present day crustal motion in China constrained by global positioning system Measurements. Science, v.294, pp.574-577.

Yin, A. and Harrison, T.M. (2000) Geologic Evolution of Himalayan-Tibet Orogen. Annual Rev. Earth Planet. Sci., v.28(1), pp.211-280.

(Received: 17 August 2016; Revised form accepted: 24 August 2016)

PAPER 2:

Rajinder Parshad, P.K.Srivastva, Snehmani, S.Ganguly and A.Ganju (2017) ," Avalanche Susceptibility Mapping in Nubra-Shyok Basin using RS and GIS ", Indian Journal of Science and Technology. Vol. 10, Issue 31, pp.1-19.

ISSN (Print) : 0974-6846
ISSN (Online) : 0974-5645
Indian Journal of Science and Technology, *Vol 10(31), DOI: 10.17485/ijst/2017/v10i31/105647, August 2017*

Snow Avalanche Susceptibility Mapping using Remote Sensing and GIS in Nubra-Shyok Basin, Himalaya, India

Rajinder Parshad[1,2]*, P. K. Srivastva[1] Snehmani[3], S. Ganguly[4], S. Kumar[3] and A. Ganju[3]

[1]Department of Petroleum Engineering and Earth Sciences, University of Petroleum and Energy Studies, Bidholi Campus, Dehradun – 248007, Uttarakhand, India; sharma.dab@gmail.com, pksrivastava@ddn.upes.ac.in
[2]Geological Survey of India, National Centre of Excellence in Geosciences Research, NH-5P, NIT, Faridabad-121001, India
[3]Snow and Avalanche Study Establishment, Research and Development Centre, Sector 37A, Chandigarh - 160036, India; snehmani@gmail.com, satish498@gmail.com, a.ganju@gmail.com
[4]National Disaster Management New Delhi – 110029, India; suryaganguly@rediffmail.com

Abstract

Objectives: To produce an avalanche susceptibility map using static terrain factor accountable for avalanche occurrence in Nubra-Shyok basin, Himalaya, India. **Methods/Statistical Analysis:** Expert judgements based Analytical hierarchy process model was applied in the present study. The weight values for each avalanche contributory factor (aspect, elevation, slope, curvature and ground cover), was assigned by comparing possible pairs in a matrix. Receiver operator characteristics- Area under the Curve technique was used to validate the results. **Findings**: The calculated weight values of the slope factor is 0.47, which is found most significant, while the weight value of elevation factor is 0.25, were also found to be significant factor. The weight value of Ground cover was 0.05 and creates a least importance. The curvature and aspect weight values were 0.12 and 0.11 respectively, and produce intermediate degree of importance. The avalanche susceptibility map of the Nubra-Shyok basin was divided into five zones: - (I) Very High (II) Moderate-to-High (III) Moderate (IV) Low (V) Very Low, and covers 27.5% , 28.0% 19.0%, 20.0%, and 4.8%, of the total area respectively. ROC-AUC method was applied to verify the study results. The value of Area under the curve (0.9112) shows that results of the present study are acceptable and 91.12% avalanche pixels are properly categorized. **Application/Improvements:** This study will help in safe movement across the Nubra-Shyok basin, India.

Keywords: Nubra, Remote Sensing, Snow Avalanche, Shyok, GIS

1. Introduction

Snow avalanches are major natural hazard in the snow covered mountain region, and posed a major threat to man and the materials in higher Himalaya. Snow avalanches have engulfed thousands of human life in western Himalaya region and these deaths are termed as 'white death'[1]. Harsh climatic condition and snow avalanches are responsible for around 75% of the deaths in the Nubra-Shyok basin[2]. The casualties on the Pakistan side are even

*Author for correspondence

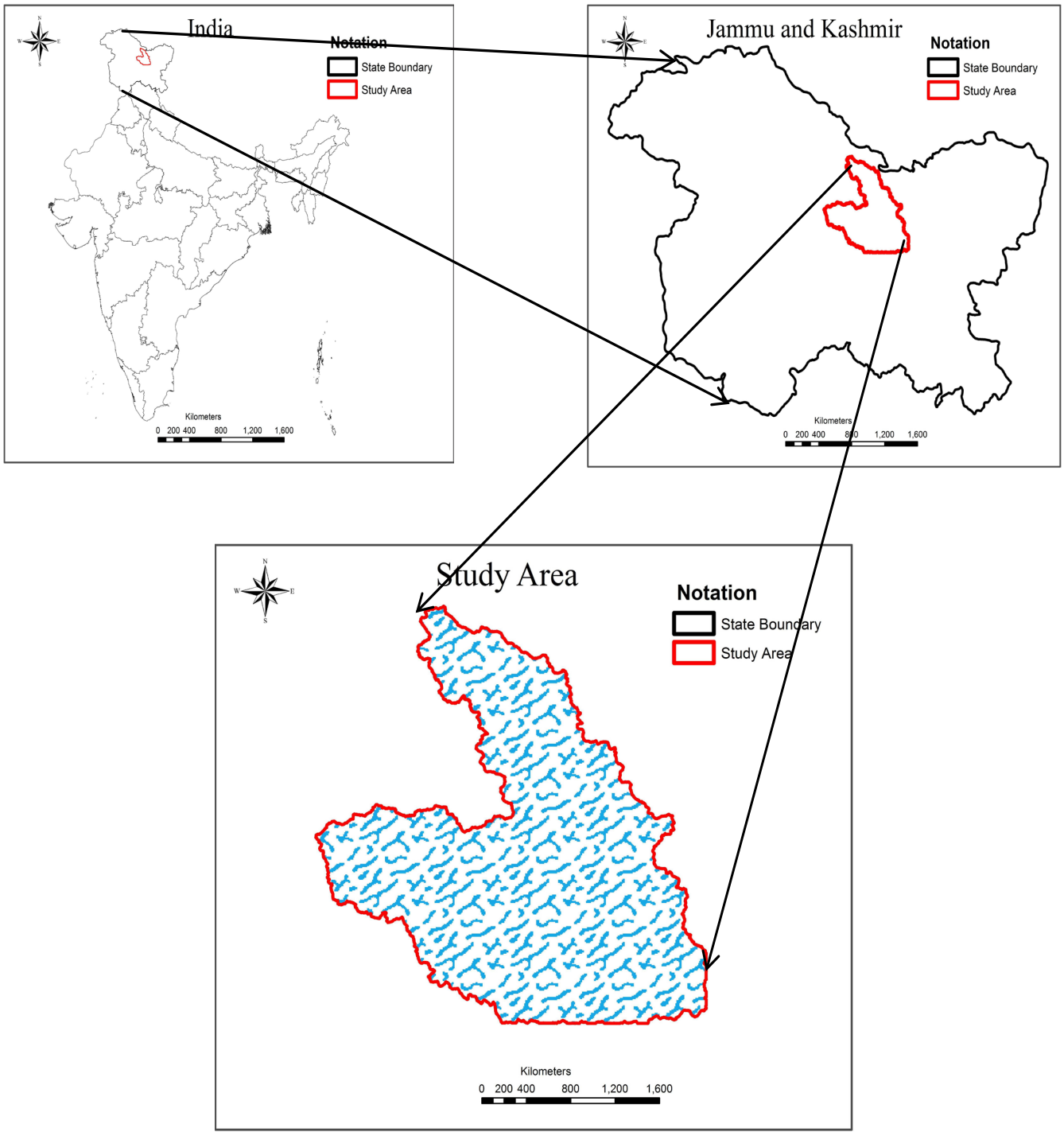

Figure 1. Location map of study area-Nubra –Shyok basin, India.

more[2]. Ten army personnel's buried alive under snow avalanche on February 3, 2016. On April 7, 2012 more than 140 personnel were killed by a deadly avalanche in Siachen Glacier, Pakistan. In 2010, an avalanche killed some 24 Pakistani troops[3]. Six persons were buried in an avalanche and one was missing in the Siachen glacier[4]. The snow avalanches cannot be predicted accurately in space and time window, as the avalanche prediction is a very complex process and includes dynamic meteorological factors i.e., temperature, snowfall, wind speed, precipitation and its intensity and static terrain factors[5] (curvature, slope, aspect, elevation, and ground cover). An avalanche susceptibility map proves very useful for the evaluation of danger and planning for safe travel activities in snow covered regions. Geographical Information System (GIS) has proved its usage in the assessment of natural hazards. The major advantage of GIS in natural hazard evaluation is its capability of integration of large heterogeneous datasets, their management and analysis.

A significant reason while applying the AHP model is that this model provides a strong capability for complex decision problems[6]. The AHP model has been successfully used for assessment of natural hazard problems[7], it is also an important tool for delineation of avalanche prone areas[8,9]. The study area is situated in highly mountainous region of Western Himalaya, India. This region is heavily glacerized, approximately 37% area of Nubra basin and 20% of Shyok basin are glacerized. Approximately 74 km long Siachen glacier is the major glacier in the region, this glacier is second largest glacier system outside the polar region. North Terong, South Terong, Termashehr, Gyongla and Lolofond are the other major glaciers of the region. The SE flowing Nubra river is the major river in the region and after flowing around 76 km it meets Shyok river at Nubra Shyok confluence near. The climatic conditions of the Nubra-Shyok region are so harsh that it is considered closed to continental snow conditions[10]. The Nubra-Shyok basin is characterized by cold temperatures. The precipitation in the region is mainly in the form of snow fall, however in lower reaches slight liquid precipitation occurs in summer season. Owing to high relief and steep valley slopes, this region has experienced large number of slope failure of huge magnitude[11]. Changing climatic condition in the last three decades in the NW Himalayas has increased the incidences of cloud bursts, floods, avalanches and landslides[12].

2. The Dataset Used

The remote sensing data of spatial resolution 30×30 m was used to generate the five static terrain factors. The Landsat 8 OLI imagery and ASTER GDEM, with spatial

Table 1. Various data layers and avalanche occurrence factors used in the study

Sr. No.	Layer	GIS data type	Scale
1	Slope	GRID	30 m × 30 m
2	Aspect	GRID	30 m × 30 m
3	Curvature	GRID	30 m × 30 m
4	Elevation	GRID	30 m × 30 m
5	Ground Cover	GRID	30 m × 30 m

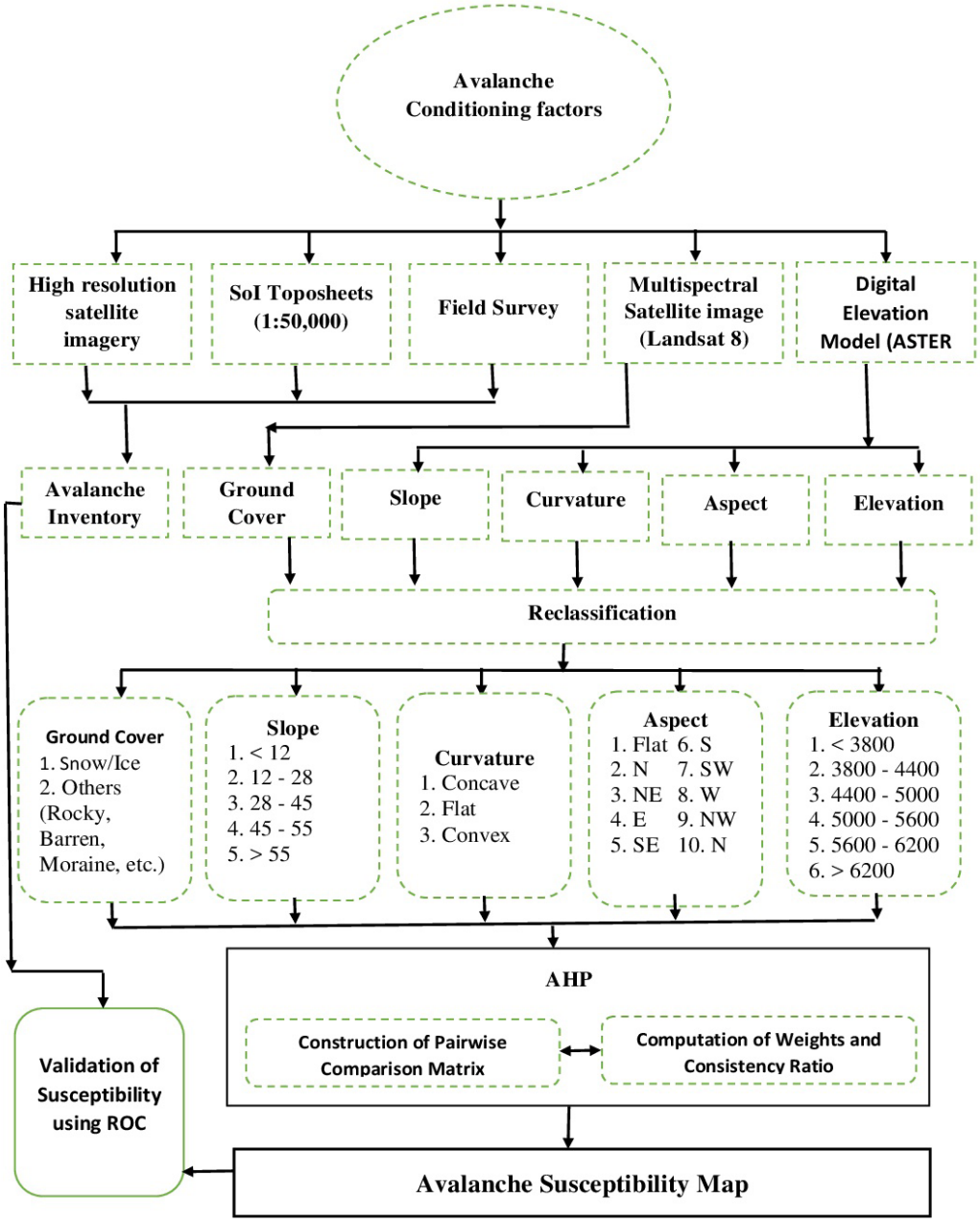

Figure 2. Methodology.

resolution 30×30 m was used to generate five static terrain factors. Elevation, aspect, slope and curvature were derived from ASTER GDEM while the ground cover for the Nubra-Shyok basin was derived from Landsat imagery dated 10-February-2015. The ground cover map was classified into two classes one is others that includes rocky, moraines, barren, etc. and another is snow/ice. The Nubra-Shyok region is a cold desert and devoid of vegetation and hence vegetation classes were not considered for image classification values. The various static terrain factors produced using Landsat 8 image and the ASTER GDEM are presented in Table 1.

2.1 Avalanche Inventory Map

The avalanche inventory map is a useful tool to know the active and potentially hazardous avalanche sites. Using the mapsheets (1:50,000 scale), satellite imagery and data of field investigation, an avalanche inventory map was prepared for Nubra-Shyok basin.

2.2 Generation of Thematic Layers and Analysis of Avalanche Occurrence Factors

Snow avalanche is a natural geophysical phenomenon in the snow covered mountains. The assessment of avalanche susceptibility is a tedious job, as it involves two types of factors one is static terrain factors and another is dynamic metrological factors. The different metrological condition leads to different type of bonding in snowpack as the snowpack develops from successive addition of layer on a slope under varying meteorological conditions[13]. The main reason behind occurrence of snow avalanches is additional stresses produced in the snowpack by natural phenomena such as addition of fresh snow and external triggering factors such as shaking produced by earthquake and/or anthropogenic activity. The avalanche occurs as and when the additional stresses produced by natural phenomena or manmade activity surpass the snowpack strength. The frequency of avalanches triggered naturally is more sturdily related to terrain parameters than climatic parameters[14]. Snowpack stability also depends upon the dynamic metrological parameters and these metrological parameters are governed by changing weather conditions. However, ground cover, aspect, altitude slope and curvature are static in nature. As sufficient knowledge about metrological parameters of Nubra-Shyok basin is not available and these are valid for short-term, hence, this study is carried using terrain parameters.

2.2.1 Slope

The ASTER GDEM data was used to derive the slope map for Nubra-Shyok basin Figure 3 and slope map is further categorized into five classes. Slope is considered essential static terrain factor for assessment of avalanche danger in the snow covered mountainous region. Rare snow avalanches occurs on mountain slopes below 25^0 [15] , however most of the hazardous snow avalanches is reported on snow covered mountains with slope greater than 30^0 but less than 45^0. Small avalanches is observed on a mountain slope less than 25^0, as shear stress on such gentle slopes is so small to start the avalanche process . The steeper slopes (45^0 -55^0) does not support the snow accumulation, which results in frequent small avalanching, hence less amount of snow is available for avalanching, on such steep slopes. The slope values were divided into five classes Table 2. The slope class (28^0-45^0) is most vulnerable for avalanche occurrence, hence assigned maximum weightage, while slope class $<12^0$ is least vulnerable to avalanche occurrence and hence assigned minimum weightage, Table 3.

2.2.2 Elevation

The snow avalanche occurrence is not directly related to the elevation factor; however metrological parameters governing snowpack stability such as intensity and type of precipitation, temperature and wind speed, changes with elevation, so elevation is also considered important terrain

Table 2. Slope classes considered for avalanche susceptibility mapping

Class	Explanation
<12	practically no avalanche observed
12-28	Considerable numbers of Hazardous avalanches occurs in this zone
28-45	Majority of dangerous avalanches
45-55	small avalanches
>55	slope is very steep and the avalanche frequency is very high, due to the steepness of the slope snow keeps on sliding under the influence of gravity and hence the snow masses available for avalanching is very less

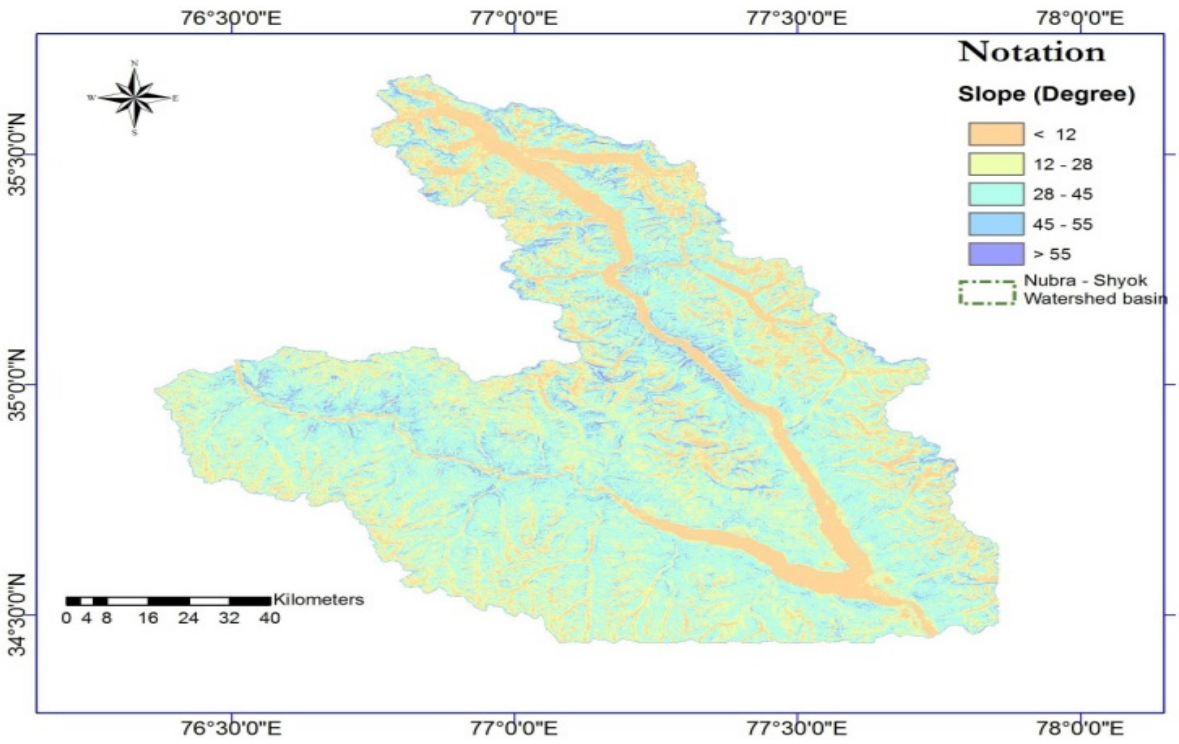

Figure 3. GIS layer of slope prepared for avalanche susceptibility mapping.

factor in avalanche susceptibility mapping. Generally, with the increase of elevation the wind speed also increases, which in turn increase the amount of wind-transported snow. The air temperature decrease with increase in elevation, hence at higher reaches snow remains available for avalanching for longer duration, however at lower elevation snow starts melting with increase in temperature. The snow avalanches are reported mainly between 2700 m to 6000m in Western part of Indian Himalaya[16] and the dangerous avalanches are reported mainly between 5000 m to 5600m altitude range in the upper Himalaya zone[10].

The elevation varies from 2468m to 7709 m in Nubra-Shyok basin. The zone of origin for all dangerous avalanches in the Nubra-Shyok area lies above 5000m[10]. The elevation class values were divided into six groups Figure 4. The elevation class 5000 m to 5600m is most vulnerable for avalanche occurrence, hence assigned maximum importance while elevation class > 6200m is least vulnerable for avalanche occurrence and hence given minimum importance and other classes were assigned intermediary importance. (Table 3).

Table 3. Assignment of ratings for each thematic layer

Thematic Layer	Class	Ratings
Slope	$<12^0$	1
	12^0-28^0	4
	28^0-45^0	9
	45^0-55^0	5
	$> 55^0$	3
Elevation	< 3800	1
	3800-4400	3
	4400-5000	4
	5000-5600	9
	5600-6200	5
	> 6200	2

Table 3 Continued

Aspect	Flat	1
	North	9
	North-East	9
	East	3
	South-East	5
	South	3
	South-West	1
	West	1
	North-West	7
Curvature	Concave	1
	Flat	4
	Convex	9
Ground Cover	Snow/Ice	9
	Others (Rocky, Barren, Moraines)	4

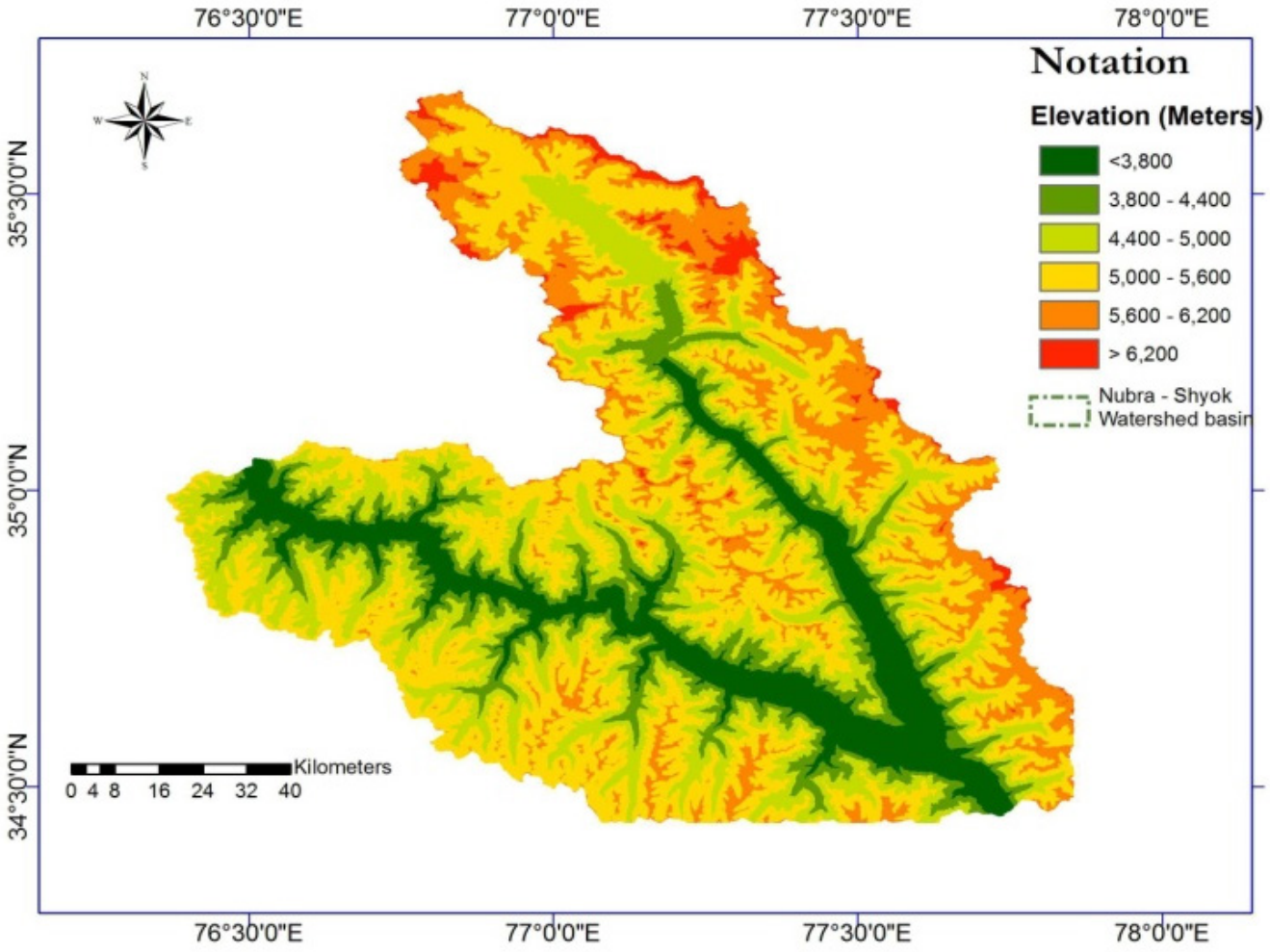

Figure 4. GIS layer of elevation prepared for avalanche susceptibility mapping.

2.2.3 Aspect

The orientation of snow covered slope with respect to the sun has a direct bearing on the snowpack stability. The shaded slopes stay unstable for longer times while the sun facing slope stabilize more quickly in comparison to the shady slopes. The wind keeps on drifting the snow from the wind facing slopes and accumulating the drifted snow on leeward slopes, hence leeward slope are more treacherous in comparison to wind facing slopes. ASTER GDEM was used to produce aspect map for Nubra-Shyok basin, and aspect map was further divided into nine classes as presented in Figure 5. Most of the avalanche slopes in Nubra-Shyok basin are in northern aspect and these poses danger of snow avalanche throughout the year[10]. Hence North-East and North aspect class are more vulnerable to avalanche occurrence, hence these were considered the important aspect classes.

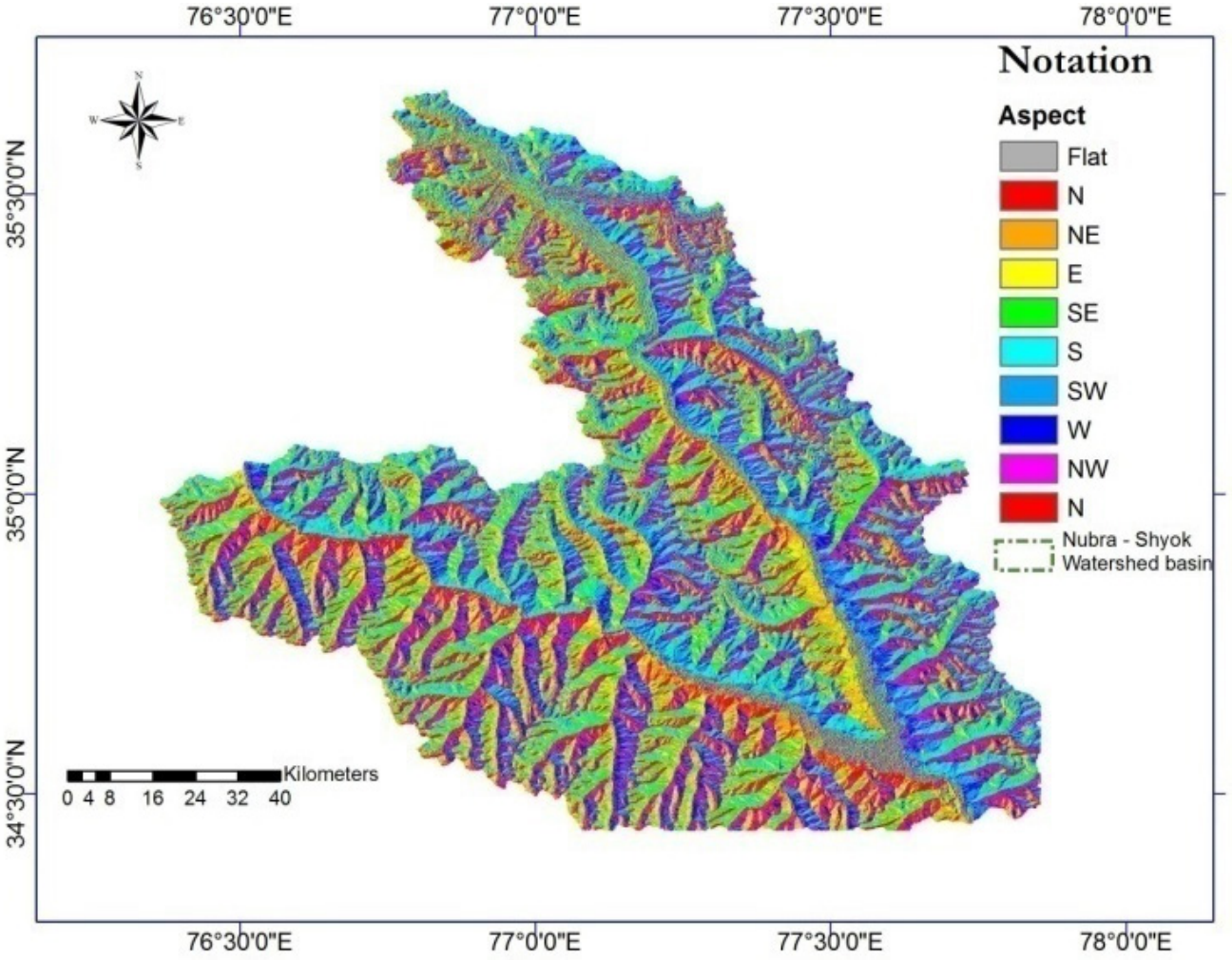

Figure 5. GIS layer of aspect prepared for avalanche susceptibility mapping.

2.2.4 Curvature

Curvature is also considered as the significant factor in evaluation of avalanche susceptibility[17]. As concave surface can hold large snow amount, hence snowpack on concave surfaces are more stable than on convex surfaces. Concave surface upkeep the stabilization of snowpack while the snow cover on convex surfaces is more unstable[18]. The ASTER GDEM was used to produce the curvature map and curvature map was divided into three different classes: Concave, flat and Convex Figure 6. The convex curvature is more venerable to avalanche initiation in comparison to concave surfaces, hence convex curvature class given more weightage than the concave. While the flat curvature class was assigned intermediate importance.

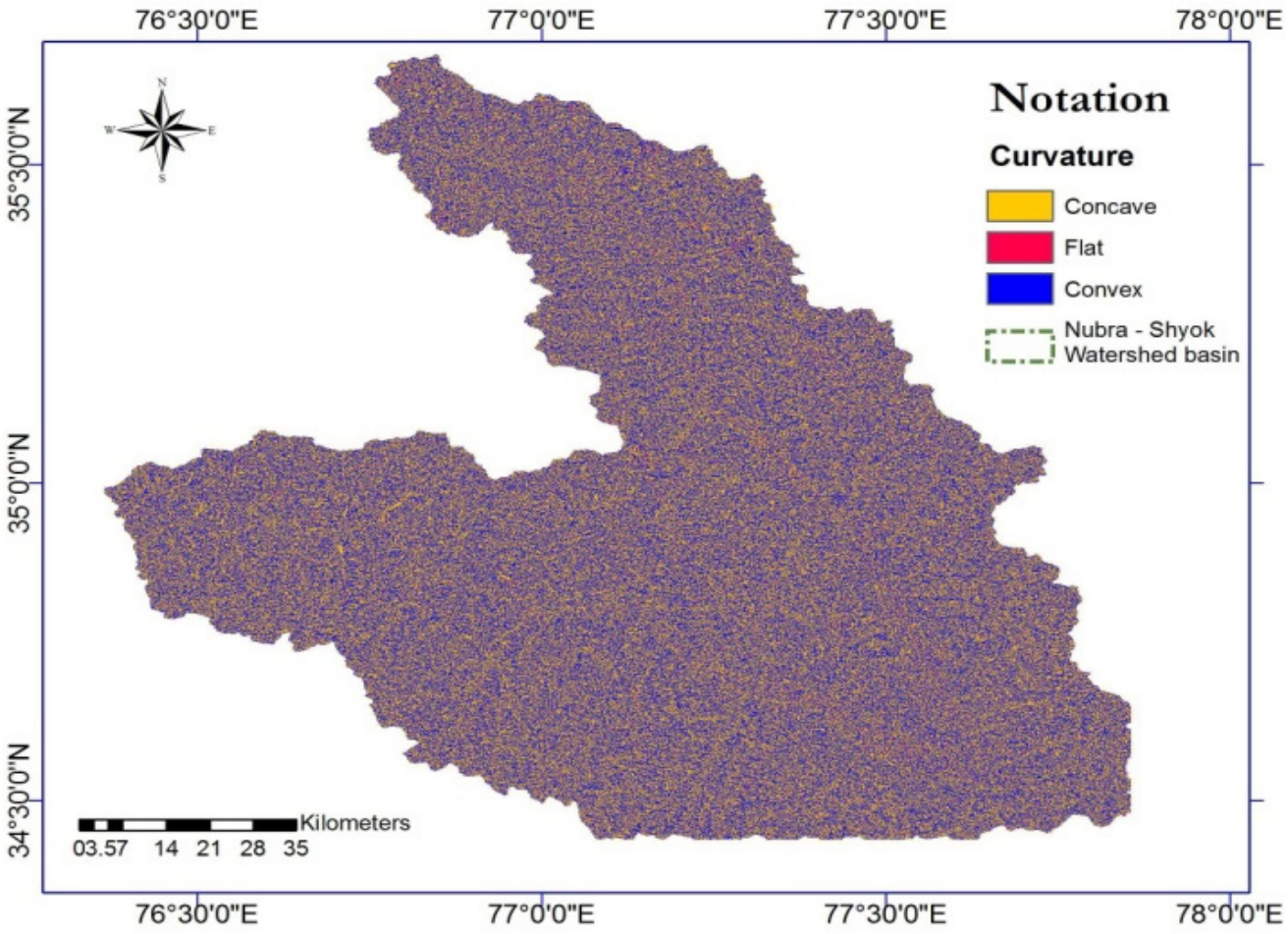

Figure 6. GIS layer of curvature prepared for avalanche susceptibility mapping.

2.2.5 Ground Cover

Ground cover was recognized as one of the important factor among the static terrain factors[16]. Good vegetation coverage may anchor the snow on slopes, hence in such areas less amount of snow that would be available for avalanching. Avalanches can be anchored by dense forest area[19]. As the upper Himalaya zone are devoid of vegetation and hence ground conditions are not supporting to snow avalanches anchorage[10]. During field visits it is observed that there is no such vegetation in the Nubra-Shyok region that can anchor the avalanches, most of the ground cover is either snow/ice covered or barren, hence the values of ground cover are divided into two classes Snow/Ice and Non-snow including barren, rocky, moraines, etc. (Figure 7). The Snow/Ice class is assigned the maximum weightage.

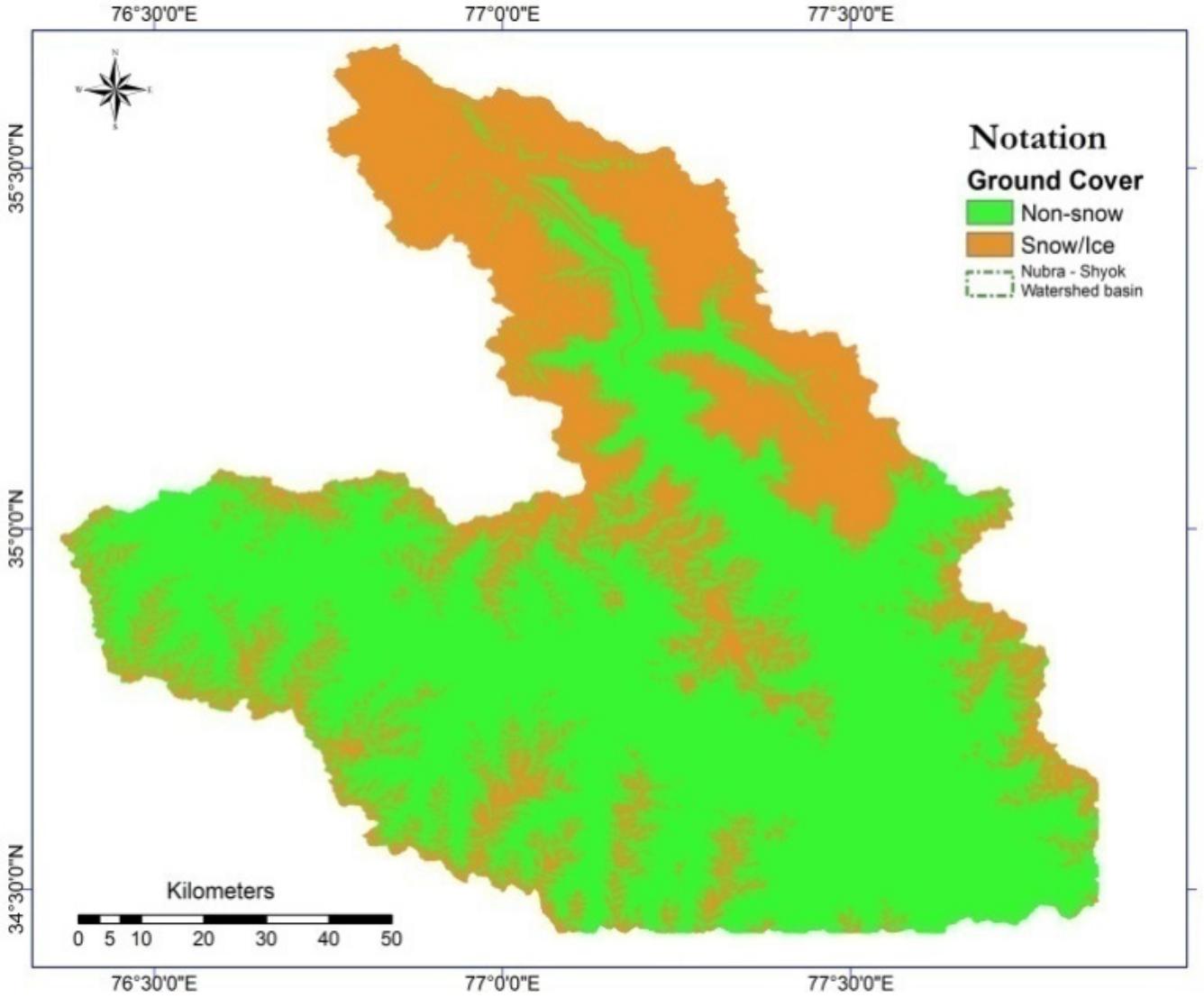

Figure 7. GIS layer of Ground Cover prepared for avalanche susceptibility mapping.

2.3 AHP Model for Avalanche Susceptibility Mapping

The Analytical Hierarchy process (AHP) is a mathematical tool of analyzing complex decisions problem with multiple criteria. It was introduced by Satty in 1970's and the introduction was published in 1980[20]. AHP was used for studies of various kind of natural hazard problems such as snow avalanches[7–9] landslide susceptibility evaluation and mapping[21–24] debris risk mapping[25] and susceptibility assessment of debris flow[26].

AHP is a qualitative method and it produces a hierarchy for the decision parameters. AHP model does not

Table 4. The importance value scale (Satty, 1980)

Importance value	Definition	Explanation
1	Equal importance	Contribution to objective is equal
3	Moderate importance	Attribute is slightly favoured over another
5	Strong importance	Attribute is strongly favoured over another
7	Very strong importance	Attribute is very strongly favoured over another
9	Extreme importance	Evidence favouring one attribute is of the highest possible order of affirmation
2,4,6,8	Intermediate values	When compromise is needed

require the dataset for training of model. AHP model works on the basis of expert knowledge and judgements. The prime goal of the study was delineation of avalanche susceptibility zones of the Nubra-Shyok basin, this was achieved by making use of fundamental evaluation factors such as aspect, elevation, curvature, slope and vegetation cover (described in Section 2.2). The characteristics of every class of all five layers and judgement of expert were used to assess and give the internal weight/rating. The weight was assigned to each class of five factors in consonance with the importance scale specified by Saaty (1980). (Table 4). The possible pairs in a matrix are compared so that a weight and consistency ratio can be assigned to each class. (Table 5). In pairwise comparison matrix, preferences of each factor were evaluated[27]. The Consistency Ratio (CR) was also calculated in the AHP model. The consistency ratio defines satisfaction level of consistency for factor weights in pairwise comparison**.** The CR was calculated using the formula as given in Equation (1)[20].

$$CR = \frac{CI}{RI} \qquad (1)$$

RI represents the average value of the CI produced using a random matrix that depends on the matrix order. The principal Eigenvalue, λmax was used to check the consistency of a matrix. The upper bound of the Eigenvalue is the same size as the element in the matrix. A Consistency Index (CI) was used to define the degree of consistency. Higher the value of CI lowers the degree of consistency of matrix.

Table 5. Pairwise comparison matrix and weight values in each layer using AHP

Layer	Ground cover	Curvature	Slope	Aspect	Elevation	Weight value
Ground cover	1	2	7	2	5	0.05
Curvature	1/2	1	4	1	2	0.12
Slope	1/7	1/4	1	1/5	1/2	0.47
Aspect	1/2	1	5	1	2	0.11
Elevation	1/5	1/2	2	1/2	1	0.25

$$CI = \frac{y_{max-n}}{n-1} \quad (2)$$

A CR value greater than 0.1 needs reassessment of the judgments in the original matrix of pairwise comparisons, because the decision marker is less consistent. In

Table 6. Zone wise distribution of produced avalanche susceptibility map

Avalanche Susceptibility	Area (Km^2)	%
Very low	461.70	4.8
Low	1923.76	20
Moderate	1827.57	19
Moderate-to-high	2693.26	28
Very high	2645.17	27.5

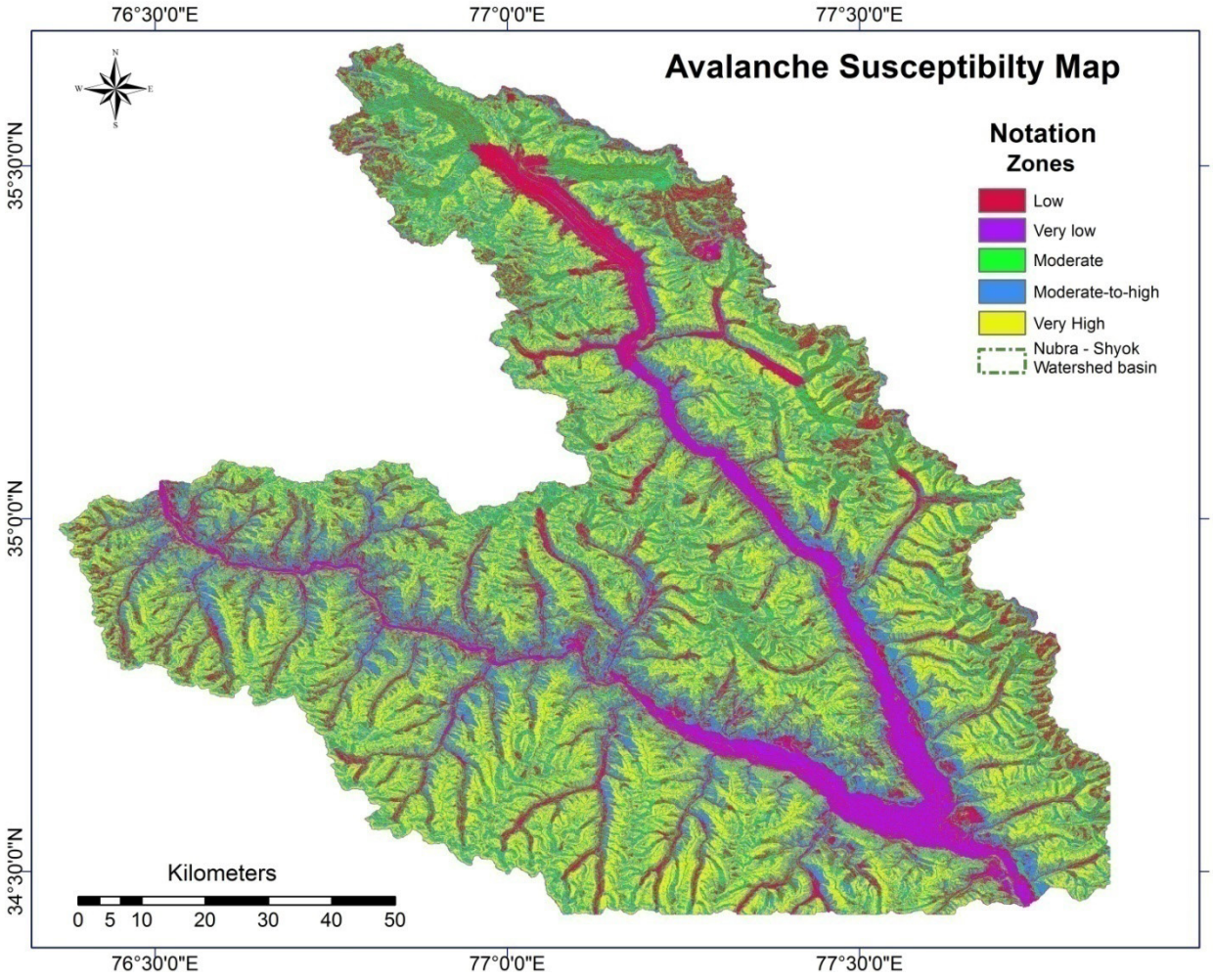

Figure 8. Avalanche susceptibility map using AHP model.

this study, CR value less than 0.10 was obtained for estimated class weights. The avalanche susceptibility map for Nubra-Shyok basin was produced by incorporating the weight values of the every avalanche occurrence factors in Equation (3).

$$\mathbf{ASI} = \sum_{i=1}^{n} (\mathbf{R_i} \times \mathbf{W_i}) \qquad (3)$$

Where ASI, stands for avalanche susceptibility index map, represents the ratings of each class of the factors, and is used for representing the weight values for each avalanche occurrence factors. The avalanche susceptibility index map was divided into five susceptible zones. These five avalanche susceptible zones for Nubra-Shyok basin are tabulated in Table 6 and avalanche susceptibility map is presented in Figure 8.

3. Results and Discussion

The calculated weight value of the slope factor was 0.47, which is found most significant factor for avalanche occurrence. The other major significant avalanche occurence were found elevation with weight value 0.25. The weight value of ground cover factor was found 0.05, which receives the least importance. The weight values of aspect and curvature were 0.11 and 0.12, respectively and both these factors received approximately equal and intermediary degree of importance. The weight values for each factor and the pairwise comparison matrix are presented in Table 5.

The ground cover is the least significant factor while slope is the most significant terrain factor for avalanche occurrence, in Nubra-Shyok basin. Hence, least weight-

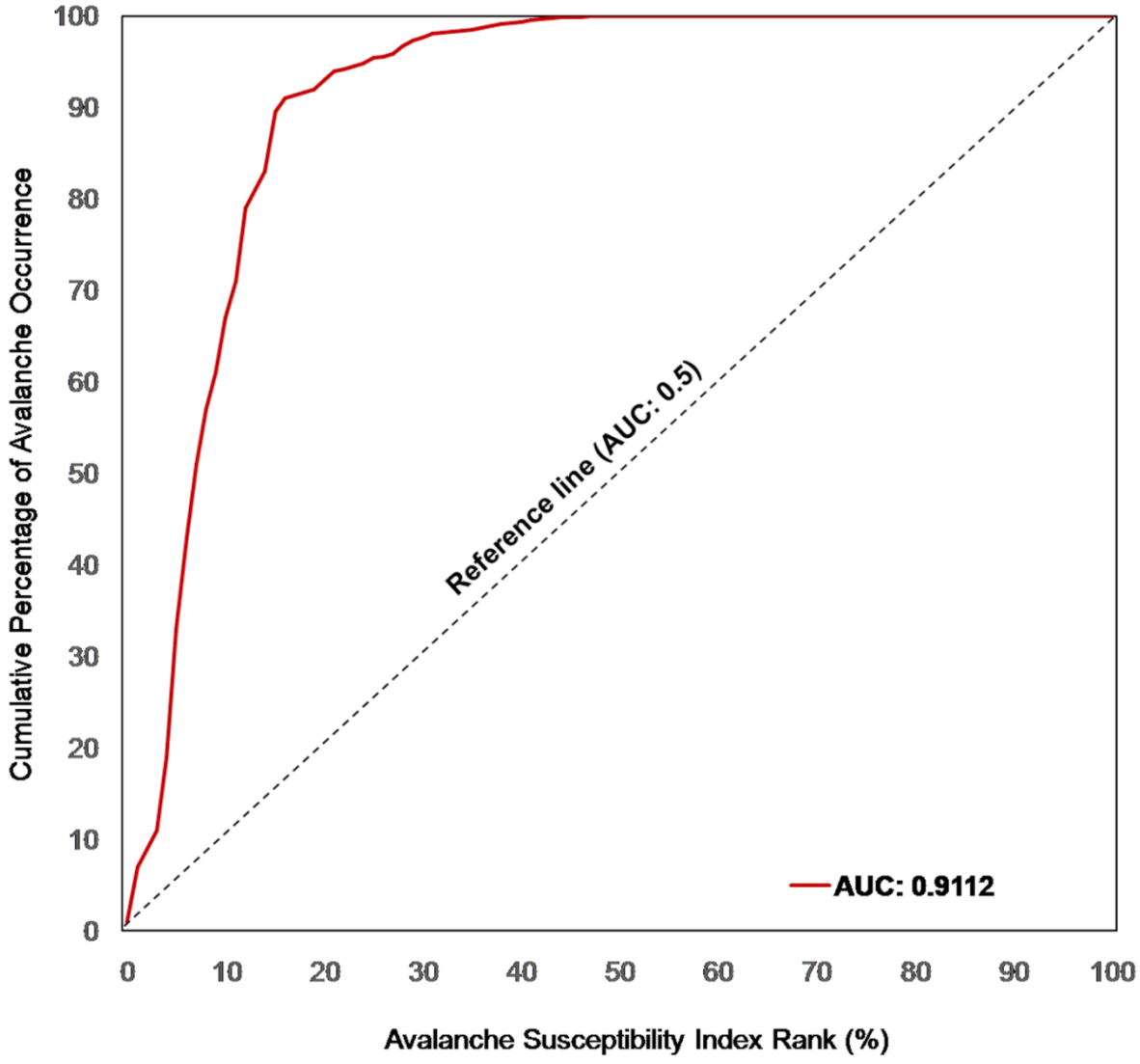

Figure 9. Validation of avalanche susceptibility map using ROC-AUC technique.

age were assigned to the ground cover factor and highest weightage was assigned to slope factor. The slope class 28^0-45^0 Table 4 is most venerable to avalanche initiation in the study region and highest rating was assigned to this slope class. The snow/ice ground cover class assigned the highest value of rating while other class which includes moraines, rocky, barren, etc. assigned the least rating. The second dominate terrain factor for avalanche occurrence in Nubra-Shyok basin considered Elevation. The maximum occurrence of avalanches was observed in the elevation range of 5000 m to 5600 m[10], hence highest rating was given to this elevation class. Curvature and aspect contributing more or less equally to the avalanche phenomena in the Nubra-Shyok basin. The concave surfaces retard the avalanche initiations while convex surfaces help in avalanche formation. Hence, concave curvature class were given least rating while the convex curvature class given highest rating. Northeast and North slopes are more vulnerable to avalanches in the Nubra-Shyok basin, hence highest rating was assigned.

Nubra-Shyok basin avalanche susceptibility map was divided into five zones: - (I) Very High (II) Moderate-to-High (III) Moderate (IV) Low (V) Very Low. The spatial coverage of these five avalanche susceptible zones are 4.8%, 20.0%, 19.0%, 28.0% and 27.5% , respectively. The zonal distribution of the final map is shown in Table 6.

The results of this study were verified using the ROC-AUC method. It is very popular statistical assessment methods, especially for natural mass movements such as landslides. The ROC-AUC is plot of the possibility of true positive versus false positive observed avalanche susceptibility. The value of ROC-AUC in the range 0.5-1 is for good acceptance, and value below 0.5 shows a random acceptance[28]. AUC value 0.9112 was obtained Figure 9. The results validation process shows that 91.12% avalanche pixels were properly categorized in the avalanche susceptibility map and these results are acceptable.

4. Conclusion

The Nubra-Shyok basin is highly complex mountainous region and climatic condition of this region is also very inhumane. The avalanche susceptibility mapping of such region is very tedious task. The AHP model incorporated in GIS environment is used to generate the avalanche susceptibility for Nubra-Shyok basin. To produce an avalanche susceptibility map of the study area AHP model was favoured. AHP model is being widely used for natural hazard problems. This model can integrate large dataset volumes and easily obtain the weight values of several numbers of criteria. In this study avalanche inventory map was prepared, creation of avalanche occurrence static terrain factors and their analysis, development of pairwise comparison matrix, weight values estimation for each factor, susceptibility mapping, and confirmation of results. Five numbers of static terrain factors responsible for avalanche occurrences, such as curvature, elevation aspect, ground cover and slope, were used as an input data generation of avalanche susceptibility map for Nubra-Shyok basin. Depending upon the significance and availability these terrain factors were analysed very judiciously. The avalanche susceptibility map of Nubra-Shyok basin demonstrate that 27.5% of total area is in very high susceptibility zone and only 4.8% of the total areais in very low susceptibility zone. In the validation process ROC-AUC value was found 0.9112 and hence, this means avalanche susceptibility map of Nubra-Shyok basin produced in this study is 91.12% accurate. The results of this study confirm that GIS-based AHP method is appropriate to identify and locate the avalanche prone areas. This

avalanche susceptibility map may be used by the policy makers for better planning of infrastructure growth in the region and safe movement across the region.

5. Acknowledgement

The research was funded by the Ministry of Earth Sciences, Government of India; grant no. MoES/P.O(Seismo)/1(83)/2010, dated 10/08/2010 and MoES/P.O(Seismo)/1(267)/2016, dated 12/01/2016. The authors extend their thanks to the SASE personnel's for field data collection.

6. References

1. Singh A, Ganju A. Earthquakes and avalanches in western Himalaya. Proceedings of the 12th Symposium on Earthquake Engineering; India: Indian institute of Technology Roorkee. 2002. p. 1–8.
2. Pandit R, Mishra A. 18 years after he went missing armyman's body found in Siachen; 2014.
3. Pakistan weather portal 2012 Avalanche in Pakistan- Tragedy at Himalayas. Available from: http://pakistanweatherportal.com/2012/04/08/avalanche-in-pakistan-tragedy-at-himalayas
4. India Today online. Indian Express (Internet). Available from: http://indiatoday.intoday.in/story/siachen-glacier-avalanche-burries-army-posts-in-turtuk-area-6-soldiers-killed/1/238179.html
5. McClung D, Schaerer P. The Avalanche Handbook. Seattle, WA, USA: The Mountaineers Books; 1993.
6. Malczewski J. GIS-based multicriteria decision analysis a survey of the literature. International Journal of Geographical Information Sciences. 2006; 20(7):703–26. Crossref.
7. Nefeslioglu HA, Sezer EA, Gokceoglu C, Ayas Z. A modified analytical hierarchy process (M-AHP) approach for decision support systems in natural hazard assessments. Computers and Geosciences. 2013 May; 59(2013):1–8.
8. Seluck L. An avalanche hazard model for Bitlis Province Turkey, using GIS based multi-criteria decision analysis. Turkish Journal of Earth Sciences. 2013 Jun; 22(4):523–35.
9. Snehmani, Bhardwaj A, Pandit A, Ganju A. Demarcation of potential avalanche sites using remote sensing and ground observations a case study of Gangotri glacier. Geocarto International. 2013 Jun; 29(5):520–35. Crossref.
10. Sharma SS, Ganju A. Complexities of avalanche forecasting in Western Himalaya- An overview. Cold Regions Science and Technology. 2000 Jul; 31(2):95–102. Crossref.
11. Dortch J, Owen LA, Haneberg WC, Caffee MW, Dietsch C, Kamp U. Nature and timing of mega-landslides in northern India. Quaternary Science Reviews. 2009 Jun; 28(11-12):1037–56. Crossref.
12. Baeseman J. International Symposium on Cryosphere and Climate Change India; 2017.
13. Schweizer J, Jamieson JB, Schneebeli M. Snow avalanche formation. Reviews of Geophysics. 2003 Dec; 4(4):10–6. Crossref.
14. Smith MJ, McClung DM. Avalanche frequency and terrain characteristics at Rogers' Pass British Columbia Canada. Journal of Glaciology. 1997 Jan; 43(143):165–71. Crossref.
15. Ancey C. Snow avalanches. New York: Wiley & Sons; 2009. PMid:18936996
16. Ganju A, Thakur NK, Rana V. Characteristics of avalanche accidents in Western Himalayan Region. Proceedings of International Snow Science Workshop; Canada. 2002. p. 200–7.
17. Maggioni M, Gruber U. The influence of topographic parameters on avalanche release dimension and frequency. Cold Regions Science and Technology. 2003 Nov; 37(3):407– 19. Crossref.
18. Nagarajan R, Venkataraman G, Snehmani. Rule based classification of potential snow avalanche areas. Natural Resources and Conservation. 2014 Feb; 2(2):11–24.
19. Ciolli M, Tabarelli S, Zatelli P. 3D spatial data integration for avalanche risk management. ISPRS Commission 4th Symposium on GIS- Between Visions and Applications; Germany. 1998. p. 121–7.
20. Saaty TL. The analytical hierarchy process. New York: McGraw-Hill; 1980.
21. Komac M. A landslide susceptibility model using the analytical hierarchy process method and multivariate statistics in perialpine Slovenia. Geomorphology. 2006 Mar; 74(1-4):17–28. Crossref.
22. Kayastha P, Dhital MR, Smedt FD. Application of the Analytical Hierarchy Process (AHP) for landslide susceptibility mapping a case study from the Tinau watershed west

Nepal. Computers and Geosciences. 2013 Mar; 52:398–408. Crossref.

23. Shahabi H, Khezri S, Ahmad BB, Hashim M. Landslide susceptibility mapping at central Zab basin Iran a comparison between analytical hierarchy process frequency ratio and logistic regression models. Catena. 2014 Apr; 115:55–70. Crossref.
24. Shahabi H, Hashim M. Landslide susceptibility mapping using GIS-based statistical models and Remote sensing data in tropical environment. Nature Scientific Reports. 2015 Apr; 5(9899):1–15. Crossref.
25. Yang QL, Gao JR, Wang Y, Qian BT. Debris flows characteristics and risk degree assessment in Changyuan Gully Huairou District Beijing. Procedia Earth and Planetary Science. 2011 Oct; 2:262–71. Crossref.
26. Chen X, Chen H, You Y, Liu J. Susceptibility assessment of debris flows using the analytic hierarchy process method- A case study in Subao river valley. Journal of Rock Mechanics and Geotechnical Engineering. 2015 Aug; 7(4):404–10. Crossref.
27. Chen Y, Yu J, Shahbaz K, Xevi E. A GIS-based sensitivity analysis of multi-criteria weights. Proceedings of the 18th World IMACS Congress and MODSIM09 International Congress on Modelling and Simulation; 2009. p. 3137–43. PMid:19547914
28. Hanley JA, McNeil BJ. A method of comparing the areas under receiver operating characteristic curves derived from the same cases. Radiology. 1983 Sep; 148(3):839–43. Crossref. PMid:6878708